Aerial view of cuspate spit at low tide, south side of the east entrance to the Strait of Magellan, Chile (Punta Catalina). The beach ridges are composed of gravel and are built by waves generated by strong westerly winds. The spit is approximately one kilometre wide.

(Used with permission, courtesy of Miles O. Hayes, Research Planning Institute Inc., Columbia, South Carolina, U.S.A., cover A.A.P.G. Bull., September 1981).

DEPOSITIONAL ENVIRONMENT, PETROLOGY, DIAGENESIS AND RESERVOIR ASPECTS OF THE NOTIKEWIN MEMBER, FORT ST. JOHN GROUP, WEST-CENTRAL ALBERTA.

DEPOSITIONAL ENVIRONMENT, PETROLOGY, DIAGENESIS AND RESERVOIR ASPECTS OF THE NOTIKEWIN MEMBER, FORT ST. JOHN GROUP, WEST-CENTRAL ALBERTA.

by

SCOTT GARDINER

A Thesis
Submitted to the Department of Geology
in Partial Fulfilment of the Requirements
for the Degree
Honours Bachelor of Science

McMaster University

April, 1982

Honours Bachelor of Science
(Geology)

McMaster University
Hamilton, Ontario

TITLE: Depositional Environment, Petrology, Diagenesis and Reservoir Aspects of the Notikewin Member, Fort St. John Group, West-Central Alberta.

AUTHOR: Scott Gardiner

SUPERVISOR: Dr. Gerard V. Middleton

NUMBER OF PAGES: xii, 128

ABSTRACT

Thirty-three cores of the Notikewin Member of the Lower Cretaceous Fort St. John Group in the area of the Kaybob Field were examined and sampled.

The gas-bearing sandstones and conglomerates were deposited in distributary mouth bars in a wave-dominated deltaic environment. Subsequently, these sediment depocentres are modified by wave energy and littoral currents to form beaches within or adjacent to the delta.

Petrographic studies of the chert litharenites to sublitharenites indicate two provenances; medium to high grade metamorphic terrain and a sedimentary source, both of which are in the Cordilleran highlands.

The potential of the Notikewin Member as a reservoir is controlled primarily by the presence of sand matrix in conglomerates. In sandstones, scanning electron microscopy indicates that the progressive assemblage of carbonate cement, quartz overgrowths, kaolinite and chlorite partially occlude porosity. The transformation of allogenic illite has no effect on reservoir potential.

ACKNOWLEDGEMENTS

Sincere thanks are extended to Dr. G.V. Middleton for his comments and criticism in supervision of this work. The intricacies of B. M. and M. will long be remembered.

Financial support for sample transport and thin sectioning and information supplied from Esso Resources Canada Ltd. was very much appreciated. Special thanks to Dave James whose help in the core research centre and witty use of the English language were invaluable in the early stages of this thesis.

Helpful advice and technical assistance from grad students Dale Leckie and Dan Thompson is great appreciated. Thanks also to my buddy Dan Potocki for his inspiring discussions in the beginning.

I would like to thank Jack Whorwood for his photographic expertise (real pictures from underexposed negs!) and Linda Hillier for patiently typing the manuscript.

Finally, I am indebted to my close friends, all of whom shared discussions, good times and laughter to make this an excellent year.

to my mother

TABLE OF CONTENTS

LIST OF FIGURES

LIST OF PLATES

LIST OF TABLES

1. INTRODUCTION

Unit and Area of Study

The Notikewin Member of the Lower Cretaceous Fort St. John Group is a prolific natural gas producer in the area of the Kaybob Field which is located in Townships 62 to 64, Range 19 west of the fifth meridian. The Kaybob Field produces oil from the Devonian Swan Hills/Beaverhill Lake Formations. However, within the oil producing field and extending into the outlying areas there are many Notikewin gas shows.

The area of study (figure 1.1) is located 140 miles (225 Km.) northwest of Edmonton and encompasses 42 square miles (109 sq. Km.). The study area is comprised of Townships 62 to 67, Ranges 16 to 22 W5, which includes the Kaybob Field and part of the Fox Creek Field.

Statement of Problem and Objectives

Upon examining the Notikewin Member in the area of the Kaybob Field it was observed that many of the thickest sands produced relatively low volume rates of natural gas when tested even though these wells were updip from good gas shows (>1MMcf/d). This observation indicated the need for a study of potential reservoir problems due to clay mineralogy or other diagenetic effects reducing porosity and permeability

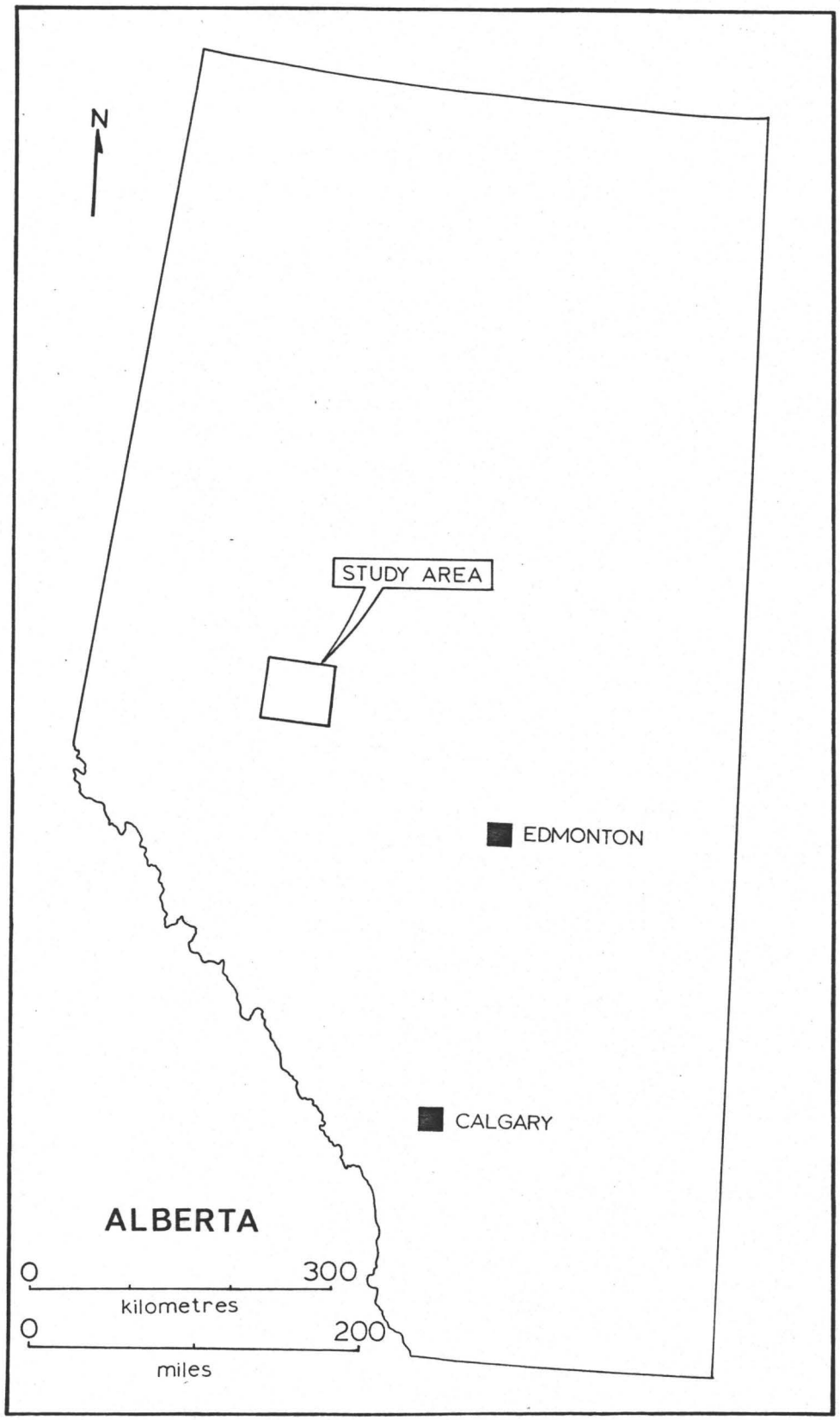
N
STUDY AREA
EDMONTON
CALGARY
ALBERTA
0
300
kilometres
0
200
miles

Figure 1.1

in sands of the Notikewin Member. These potential reservoir problems combined with the complex sedimentology of the Notikewin Member prompted the following objectives of this study:

i) determine the depositional environment of the Notikewin Member;

ii) determine detrital constituents and provenance by petrographic means;

iii) document the diagenetic history (including clay mineralogy) and its consequences for the Notikewin Member as a potential gas reservoir.

Methodology

The evidence used to determine the depositional environment includes information from examination of 33 cores which penetrated the Notikewin Member.

All 33 cores were logged and interpreted but only nine were sampled and used for the purpose and scope of this thesis. The cores were sampled for petrographic analysis, scanning electron microscopy and for X-ray identification of clays. At the time of writing, 33 cores is the total number of wells with suitable depth intervals cored in the study area. In addition to studying core, examination of radioactivity and acoustic velocity/sonic logs aided in determining depositional environment.

2. GEOLOGICAL SETTING AND DEPOSITIONAL FRAMEWORK

General Stratigraphy

The Lower Cretaceous clastic sediments of the Western Canada Sedimentary Basin are largely fluvial, deltaic or shallow marine in origin (McCrossan and Glaister, 1964; Nelson, S.J., 1970).

Lower Cretaceous strata in the area of study consist of both the Bullhead and Fort St. John Groups. Together they thin eastward and northeastward toward the plains (Stott, 1968).

Dawson (1881) originally defined the Fort St. John Group as marine sediments in the area of Peace River. This name now applies to equivalent deposits in northeast B.C. and northern Alberta.

The Bullhead Group contains coal-bearing sediments and massive conglomerates reflecting fluvial conditions (Stott, 1968). Marine sediments with tongues of carbonaceous, sandy sediments of the Fort St. John Group record the varying marine, transitional and flood plain environments along the coastline of the Early Cretaceous epicontinental sea.

The Spirit River Formation of the Fort St. John

Group is briefly defined by Badgley (1952) and more completely by the Alberta Study Group (1954) as being composed of the Wilrich, Falher and Notikewin Members. The Notikewin Member is of Middle Albian to Late Albian age based on evidence from flora (Singh, 1971).

These Lower Cretaceous strata truncate the underlying Jurassic sediments forming a regional erosional unconformity. The Notikewin Member is abruptly overlain by the Harmon Member of the Peace River Formation or the Joli Fou Formation of the Colorado Group which are equivalent names.

Correlation of Lower Cretaceous sediments in various parts of Alberta and British Columbia have been proposed by Glaister (1959), Williams (1963) and Stott (1968). Figure 2.1 indicates correlations in areas immediately adjacent to the study area. Ambiguities in the use of nomenclature for the Lower Cretaceous in the study area arise because of its location. In some contexts the Notikewin is considered to be a formation of the top of the Mannville Group. This practise is increasingly more common in subsurface studies in the northwest plains.

Study Area Stratigraphy

In the area of this study the Notikewin Member is difficult to define in the stratigraphic column because there is no distinct boundary between it and the underlying Falher Member due to vertical and lateral facies changes in the Notikewin sediments. For the purpose of this study the Notikewin

Figure 2.1 Lower Cretaceous stratigraphy of study area and adjacent parts of British Columbia and Alberta (after Glaister (1959), Williams (1963)).

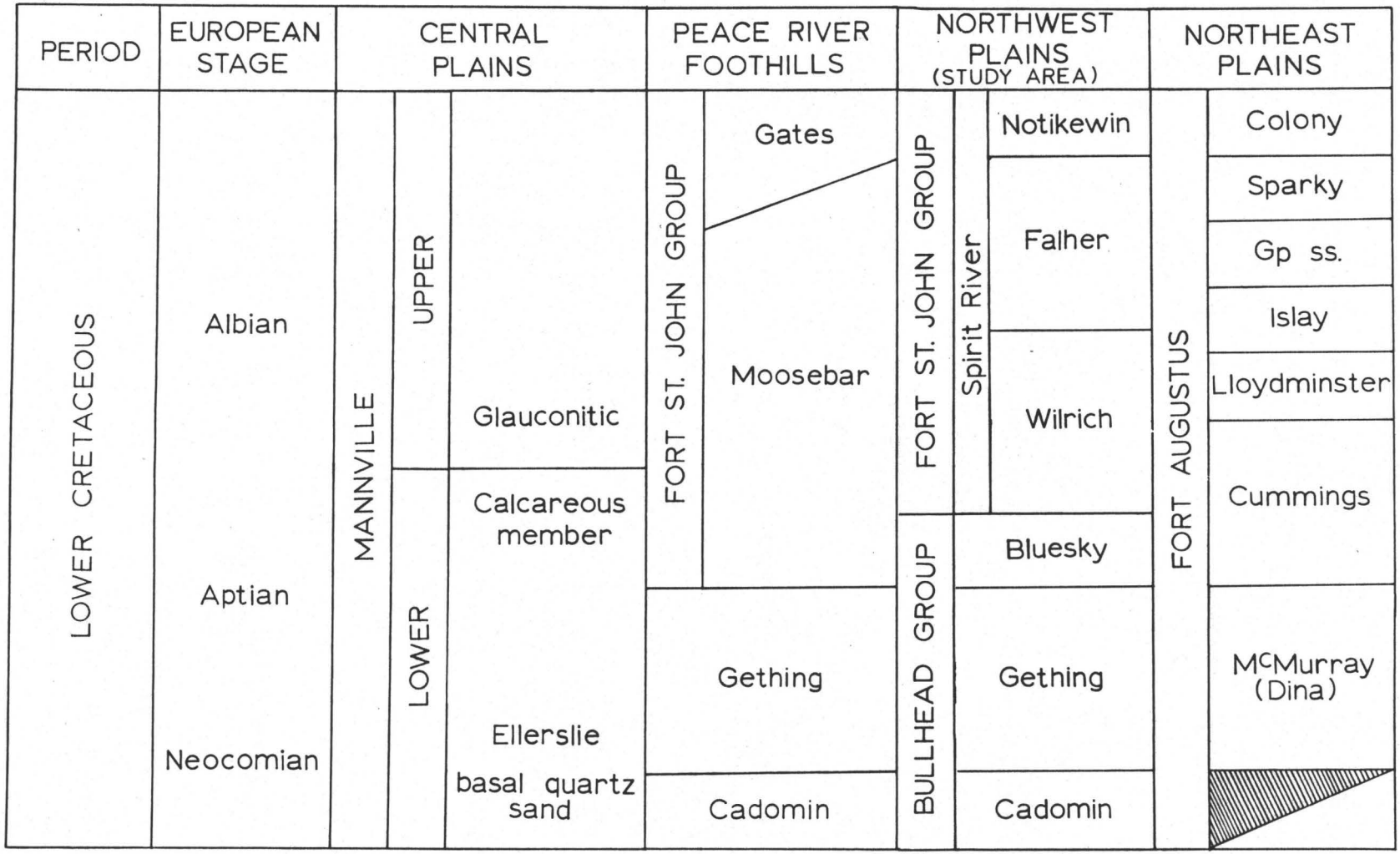
PERIOD
EUROPEAN STAGE
CENTRAL PLAINS
PEACE RIVER FOOTHILLS
NORTHWEST PLAINS (STUDY AREA)
NORTHEAST PLAINS
LOWER CRETACEOUS
Albian
Aptian
Neocomian
MANNVILLE
UPPER
LOWER
Glauconitic
Calcareous member
Ellerslie
basal quartz sand
FORT ST. JOHN GROUP
Gates
Moosebar
Gething
Cadomin
BULLHEAD GROUP
FORT ST. JOHN GROUP
Spirit River
Notikewin
Falher
Wilrich
Bluesky
Gething
Cadomin
FORT AUGUSTUS
Colony
Sparky
Gp ss.
Islay
Lloydminster
Cummings
McMurray (Dina)

Member is considered by the writer to be the interval from the lower contact of the Harmon Member (Joli Fou Formation) to the uppermost coal seam which defines the top of the Falher Member of the Spirit River Formation of the Fort St. John Group. The upper contact is sharp and easily recognized in the study area but variations in continuity of the coal seam make the bottom contact subjective.

The Notikewin sand is considered to be the uppermost sand or conglomerate encountered below the lower contact of the Harmon Member (Joli Fou Formation). Typically this sand occurs at the top of the Spirit River Formation. It can also be considered to be at the top of the Mannville Group. However, it may occur as much as 50 to 100 feet (15 to 30 metres) below the base of the Harmon shale (Joli Fou Formation) making it indistinguishable from the underlying Falher Member.

The lateral facies changes cause acute problems in correlating the Notikewin Member regionally and in detailed studies.

Regional Depositional Framework

Uplift in the Late Jurassic in western Canada was accompanied by emplacement of the Nelson and Cassiar-Omineca batholiths of the Cordillera. Denudation of the Precambrian Canadian Shield to the northeast was occurring concurrently. Dominantly fluvial sediments derived from these westerly and northeasterly sources infilled lows of the irregular pre-

Cretaceous topography (Williams, 1963). Northwest-southeast trending, topographic ridges composed of Mississippian to Devonian rocks caused thinning of the overlying Mannville sediments (Jardine, 1974). As a result, the Lower Mannville sediments vary greatly in lateral continuity.

At the end of Lower Mannville time, a short marine transgression reworked basal sands to form widespread distribution of the Bluesky Formation. Increased subsidence in Upper Mannville time caused southward transgression of the Arctic (Clearwater) sea into northeastern British Columbia and northern Alberta.

Toward the end of the Lower Cretaceous, volcanism occurred to produce the Crowsnest volcanics. Although the Crowsnest volcanics are small in areal extent, Glaister (1959) postulates similar volcanic areas elsewhere in the Cordilleran orogenic belt, which could have provided a source of volcanic detritus.

In Upper Albian time, due to further subsidence, the Gulfian Sea transgressed from the south, coalescing with the northern Arctic (Clearwater) sea which finally inundated the area allowing deposition of the Joli Fou (Harmon) marine shales.

Local Depositional Framework

Underlying the Notikewin Member throughout the study area the Wilrich and Falher Members consist of fining and coarsening upward sand sequences interbedded with shale and coal. These observations are in accord with the regional

fluvio-deltaic depositional environment proposed for Mannville sediments by Glaister (1959), Williams (1963) and McCrossan and Glaister (1964).

By Notikewin time the pre-Cretaceous topography had been compensated for by the underlying Falher, Wilrich and Bluesky sediments. Therefore, lateral thinning and discontinuity of Notikewin sands is inherent in the depositional environment, not a result of paleotopography.

The Notikewin Member ranges from 40 - 70 feet thick. It contains two sand horizons denoted A and B sands by this author. The first sand encountered down from the contact with the Joli Fou Formation is the A sand, which ranges from 3 - 30 feet in thickness. The B sand is 20 - 70 feet thick and lies below the A sand. The B sand is very discontinuous over the study area.

Due to uncertainty in the facies boundary between the Notikewin Member and the underlying Falher Member an isopach map could not be constructed. Instead an isolith map of the A sand was produced (see back cover pocket).

3. FACIES DESCRIPTION AND DEPOSITIONAL ENVIRONMENT

Introduction

A total of 33 cores were studied and logged as part of summer employment at Esso Resources Canada Ltd. Of these, 30 are in the defined study area and eight of these were sampled. The ninth sampled well is one of three wells which lie immediately adjacent to the study area. Figure 3.1 indicates locations of the nine cores sampled. The majority of core available is in the Kaybob Field. Both the metric and British system of measurement are used in this thesis.

The environmental interpretation is based on data from all 33 cores, not exclusively from the nine sampled wells. In addition, an isolith map produced from study area wells in the summer work term was an aid to determining depositional environment.

Notikewin gas in the study area is not in production. Therefore, only DST (drill stem test) data on Notikewin intervals are known (table 3.1).

From this point onward well locations will be referenced by the first two digits of their location numbers. For example 10-24-64-20 W5 becomes 10-24.

The Notikewin consists of four major facies (A, B,

WELL LOCATIONS

1. 6-36-64-20 W5
2. 10-24-64-20 W5
3. 10- 1-65-18 W5
4. 10-31-64-17 W5
5. 12-10-64-19 W5
6. 10-27-63-19 W5
7. 12-15-63-19 W5
8. 7-13-63-19 W5
9. 6-18-59-14 W5

Figure 3.1 Location of cores sampled within study area. Townships 62 - 67. Ranges 16 - 22 west of fifth meridian. Core 9 is just south of this area in 6-18-59-14 W5.

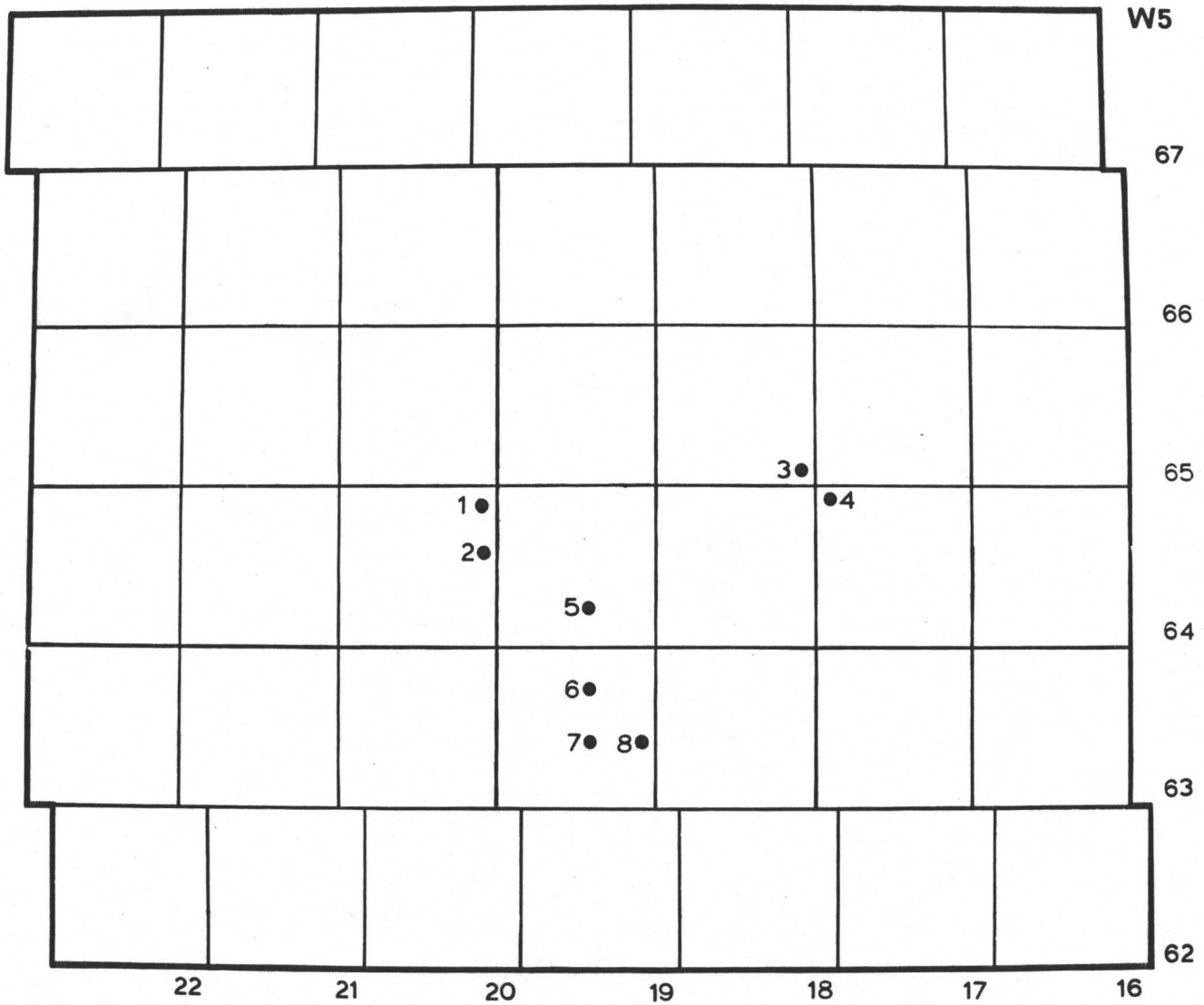
W5
67
66
65
64
63
62
1
2
3
4
5
6
7
8
22
21
20
19
18
17
16

Table 3.1 Drill stem test results for Notikewin A and/or B sand in the nine studied wells

	WELL LOCATION	DRILL STEM TEST interval tested (feet/meters)	RESULT
1.	6-36-64-20 W5	4748.0-4780.0 ft 1447.2-1456.9 m	1.19 MMcf/day 33722.9 m^3/day
2.	10-24-64-20 W5	4880.0-4918.0 ft 1487.4-1499.0 m	2.06 MMcf/day 58377.5 m^3/day
3.	10- 1-65-18 W5	4550.0-4585.0 ft 1386.8-1397.5 m	3.20 MMcf/day 90683.5 m^3/day
4.	10-31-64-17 W5	4607.0-4641.0 ft 1404.2-1414.6 m	1410 Mcf/day 39957 m^3/day
5.	12-10-64-19 W5	no tests run ---	no tests run ---
6.	10-27-63-19 W5	5016.4-5057.7 ft 1529.0-1541.6 m	1.99 MMcf/day 56619 m^3/day
7.	12-15-63-19 W5	no tests run ---	no tests run ---
8.	7-13-63-19 W5	no tests run ---	shut-in Notikewin gas ---
9.	6-18-59-14 W5	5723.4-5815.3 ft 1744.5-1772.0 m	6.5 MMcf/day 206.7 ft freshwater 184490 m^3/day 63 m freshwater

C, D) and one minor facies (E) which have been recognized and defined by the writer. The criteria used to define each facies are lithology, grain size and sedimentary structures (including bioturbation). The legend used to denote characteristics of the core is shown in Appendix I. Not all of the four major facies are necessarily present in a given core. This can be attributed by genuine absence of a given facies or due to an insufficient cored interval to expose all facies. The fifth facies (E) is labelled "minor" in this study because it is only recognized in two of the 33 cores examined.

The four major facies can be related to response on gamma-ray/sonic (acoustic velocity) logs. Figure 3.2 is a "type log" which indicates a simple sequence of the four facies and their associated log response. It is based on observations from one of the 33 unsampled cores. Refer to plates 3-1 to 3-9 for photographs of each facies. Appendix I contains stratigraphic sections representative of the nine cores studied and sampled.

FACIES A: Coarse grained sandstone/fine grained congl.

The division between coarse grained sandstone and fine grained conglomerate is made at a 2 mm. grain size. This facies, when present, most frequently occurs at the top of the Notikewin. In well 12-10, 10 inches (25.5 cm.) of conglomerate lies below the fine grained sandstone facies. The conglomerate is best developed in 10-1 where it is 14

Figure 3.2 This type log relates gamma ray-sonic (acoustic velocity) to the corresponding facies observed in core. Depth in feet.

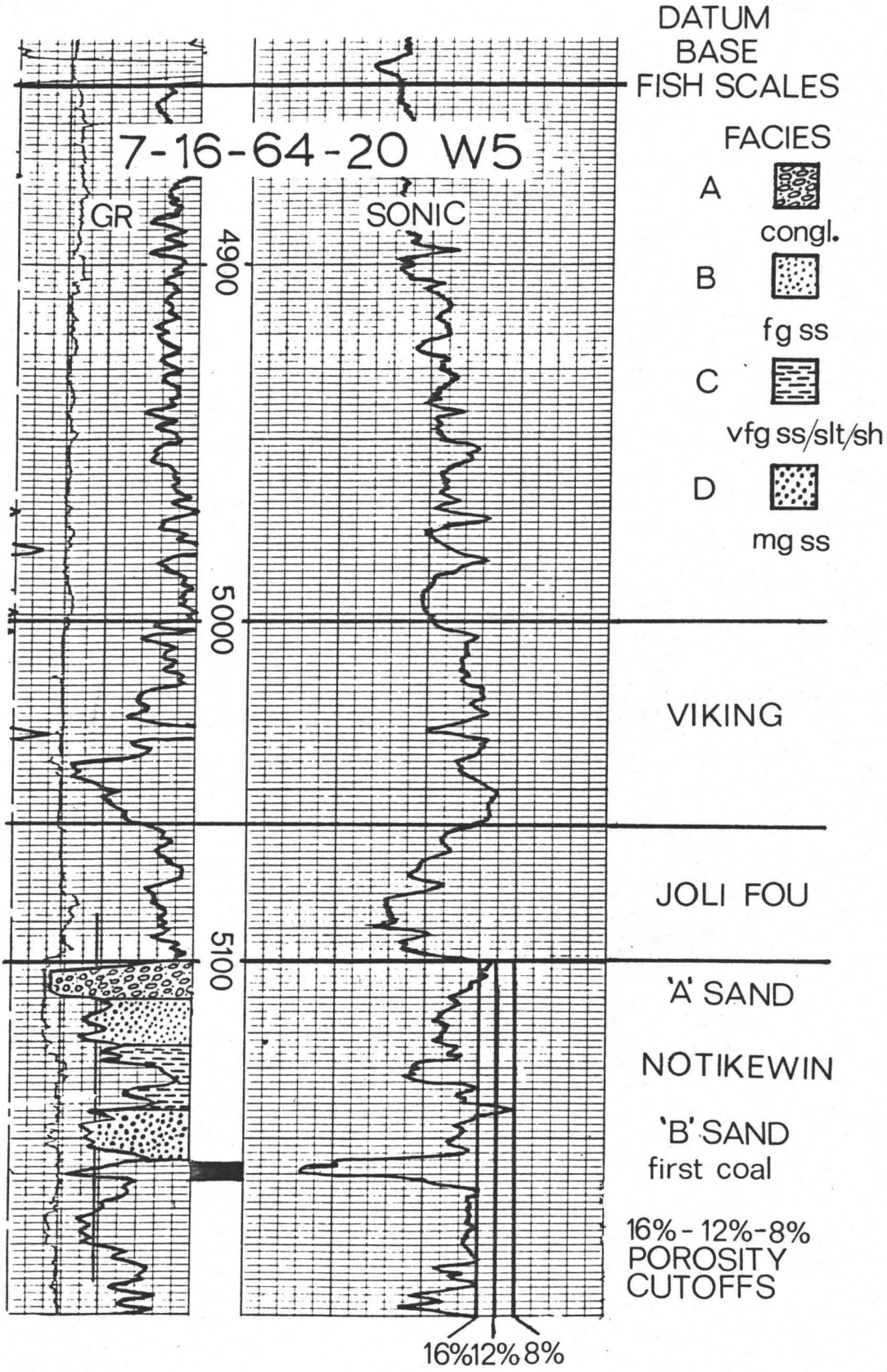
DATUM
BASE
FISH SCALES
7-16-64-20 W5
GR
SONIC
4900
5000
5100
FACIES
A
congl.
B
fg ss
C
vfg ss/slt/sh
D
mg ss
VIKING
JOLI FOU
'A' SAND
NOTIKEWIN
'B' SAND
first coal
16% - 12% - 8%
POROSITY
CUTOFFS
16%
12%
8%

feet (4.3 m.) thick.

The chert and quartz pebbles are typically very well rounded and moderately to well sorted. They vary in size from 0.5 cm. to rare 2.5 cm. pebbles. Variations of grain size occur on a centimetre scale (plate 3-1) with bands of coarse material grading into finer and vice-versa throughout the facies.

In the coarse sand fraction low angle (10°) and less frequent high angle (20° - 30°) cross-stratification is present. No truncation of cross-stratification is observed. This facies is commonly homogeneous, exhibiting no sedimentary structures. In some cores the larger pebbles are imbricated at angles up to 10°-15° to the horizontal (plate 3-2).

The conglomerate may be clast supported, resulting in extremely high porosities, or a finer grained sand matrix may be present. The porosities are commonly up to 20%-25% with correpsonding permeabilities of 0.1 md to extremes of greater than 1000 md (1 darcy) according to core plug analyses.

Accessory constituents include kaolinite, glauconite traces, carbonaceous fragments and laminae and rare woody or coaly fragments.

The pebbles of this facies are easily distinguishable from those in the overlying Joli Fou Formation. In the Joli Fou the pebbles form a lag, which represents a reworked, transgressional surface. The contact between Facies A and

Plate 3-1 Facies A. High angle (30°) cross-stratification in fine grained conglomerate/coarse grained sandstone. Grain size varies on a centimetre scale. Note carbonaceous laminae in centre of core and interstitial kaolinite clay (white). Scale in centimetres. Location: 10-7-64-18 W5.

Plate 3-2 Facies A. Imbrication of quartz and chert pebbles. The angle of imbrication is exaggerated by approximately 20° due to directional drilling of the well. Scale in centimetres. Location: 10-30-63-19 W5.

Plate 3-1

Plate 3-2

underlying facies is sharp.

FACIES B: Fine grained sandstone

This facies is characterised by very fine to fine grained, massive, well sorted, salt and pepper, quartz-rich sandstone. Intercalations of silt and silty shale occur periodically. This facies is present in many wells but may be difficult to distinguish from Facies C depending on the amount of silt and shale present and the degree of bioturbation. It varies in thickness from 26 feet (8 metres) in 10-24 where best developed, to three feet (0.94 metres).

Sedimentary structures include low angle (10°) and high angle (20° - 30°) cross-stratification and parallel laminae (plates 3-3 and 3-4). This facies is extremely homogeneous in many cores. Rare, convolute, non-parallel laminae are evidence of penecontemporaneous, soft-sediment deformation. Dominantly horizontal, sand filled burrows (Planolites?) and vertical burrows occur in the silty shale portions of this facies quite commonly.

Abundant glauconite, kaolinite, carbonaceous fragments and laminae are common accessory constituents. Wood fragments are rare. Fossil shells, both preserved and dissolved to form cavities are also rare.

The porosities determined from core plug analyses vary from 14%-23% with permeabilities of 0.1 md to 30 md. The porosity and permeability vary greatly from core to core and vertically within a given core exhibiting this facies.

Plate 3-3 Facies B. Homogeneous, fine grained, well sorted, salt and pepper, quartz-rich sandstone. Scale in centimetres. Location: 10-24-64-20 W5.

Plate 3-4 Facies B. Low angle (10°) cross-stratification in fine grained sandstone. Location: 10-24-64-20 W5.

Plate 3-3

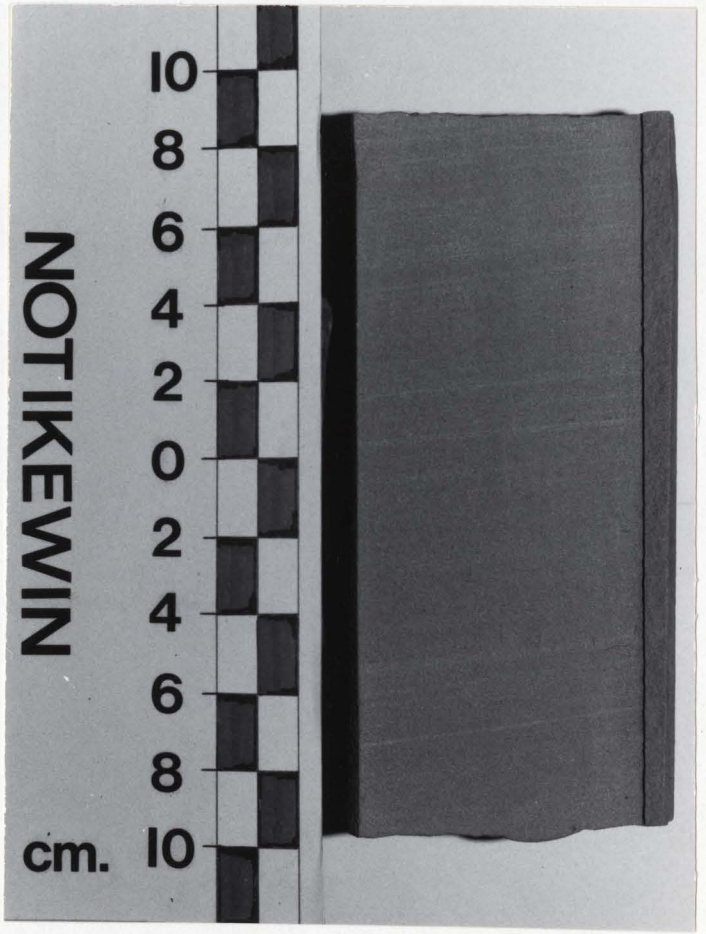

Plate 3-4

Facies A and B comprise the Notikewin A sand as defined by the writer (see figure 3.2).

FACIES C: Bioturbated, interbedded very fine grained sandstone/siltstone/shale

This facies typically consists of silt, shale and very fine grained sand interbedded on a centimetre to millimetre scale. The ratio of sand (and silt) to shale is variable but the facies is still easily recognized by the sedimentary structures present.

Convolute, non-parallel laminae and microfaulting are syngenetic sedimentary structures observed in 10-1. Scour and fill structures are rare. Parallel laminae and low angle (10°) cross-stratification are present. Silty, shaley portions form lenticular, discontinuous beds (plate 3-5). Sand filled horizontal and vertical burrows are common, producing extensive bioturbation and churning (plate 3-6).

Diagenetic ironstone concretions are common in shales of this facies.

Accessory constituents include glauconite and less extensively, kaolinite and pyrite. In 6-36 glauconite is concentrated to form a rare 4" (10 cm.) very glauconite rich band. The porosities and permeabilities of this facies are very low.

FACIES D: Medium grained sandstone

This facies is characterised by white to cream coloured medium grained quartz sandstone. The sand grains are

Plate 3-5 Facies C. Bioturbated and churned very fine grained sand, silt and shale producing convolute parallel and non-parallel laminae. Scale in centimetres. Location: 11-9-65-18 W5.

Plate 3-6 Facies C. Interbedded sandstone and silt. Both vertical and horizontal sand-filled burrows are present. Scale in centimetres. Location: Unknown.

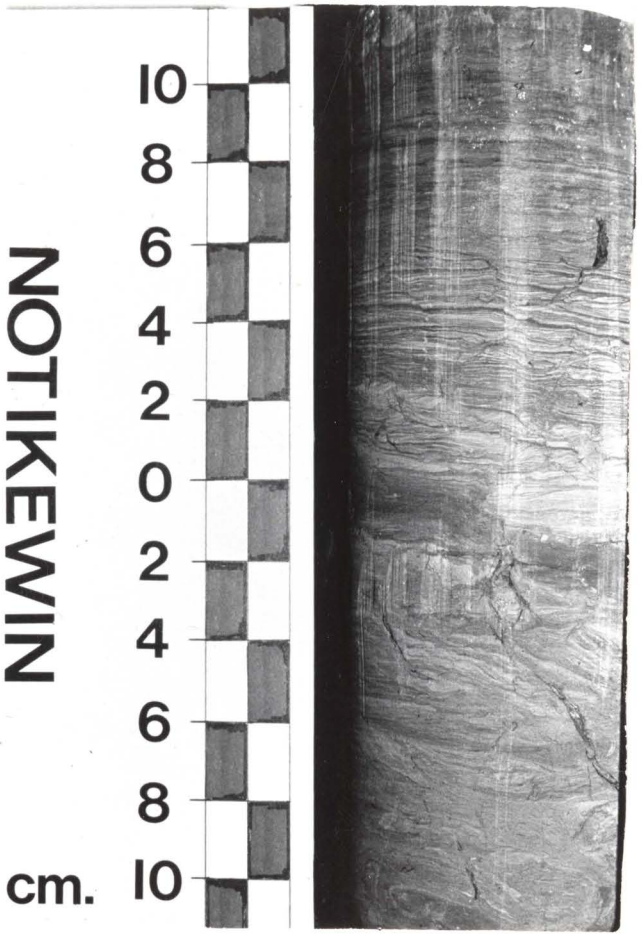

Plate 3-5

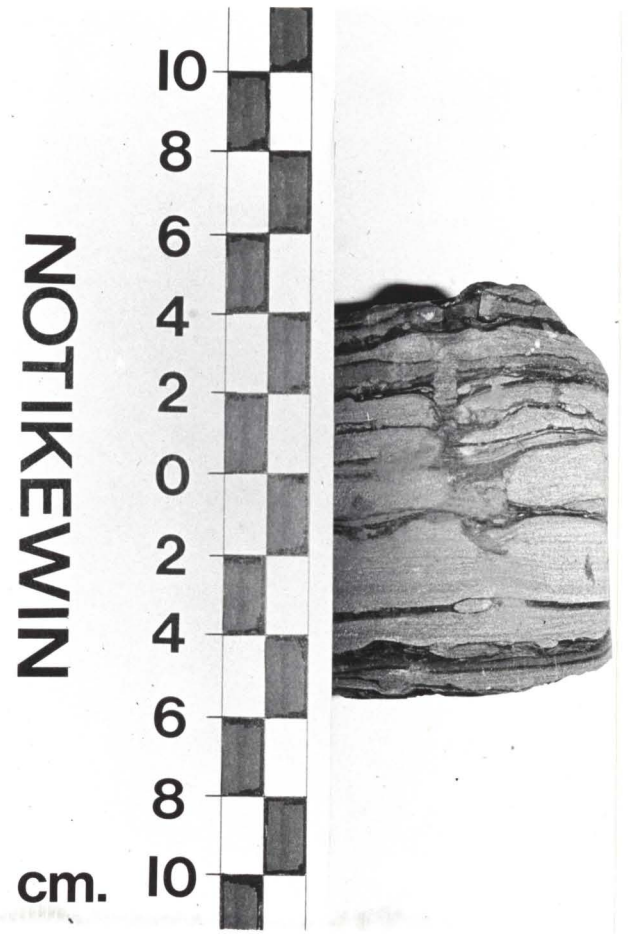

Plate 3-6

well sorted and subangular to subrounded.

High angle (30°) cross-stratification is most common (plate 3-7). Homogeneous sand is also observed. The cross-stratification is accentuated by a brown, carbonate matrix (siderite?) in the laminae (plate 3-8). Traces of vertical burrows are evident.

Accessory constituents include kaolinite, carbonaceous fragments, woody, coaly pieces, carbonaceous laminae and minor rootlets.

Porosities vary from 4%-12% with permeabilities of 0.01 md to 0.22 md based on core plug analyses.

The thickness of this facies is not easily determined due to an insufficient cored interval.

Facies D comprises the Notikewin B sand as defined by the writer.

FACIES E: Carbonaceous siltstone and shale

Siltstone, shale and minor fine grained sandstone comprise this facies. It is best developed and recognized in 10-31.

Sedimentary structures in the minor sand rich fraction include parallel convolute laminae, horizontal parallel laminae and low angle (10°) cross-stratification. Traces of bioturbation are present in finer grained material.

Other constituents include minor coal, woody, coaly pieces and traces of rootlets (plate 3-9).

Diagenetic ironstone concretions are present.

Plates 3-7 and 3-8: Facies D. High angle (30°) cross-stratification in medium grained sandstone. Cross-stratification is emphasized by brown, carbonate matrix. Scale in centimetres. Location: 11-9-65-18 W5.

Plate 3-8

Plate 3-7

Plate 3-9 Facies E. Carbonaceous rootlets in silty shale. Scale in centimetres. Location: 11-7-62-17 W5.

This facies is easily confused with Facies C. The major difference is the presence of carbonaceous and coaly material associated with this facies.

Interpretation and Depositional Environment

Criteria used to determine the depositional environment are: gamma ray/sonic (acoustic velocity) logs, facies descriptions, and an isolith map of the Notikewin A sand. Each facies will be analysed and evaluated in ascending order beginning with Facies D and E.

Facies D is thought to represent channel sand. This is substantiated by the fining-upward character of the gamma-sonic log (figure 3.2) and the abundance of carbonaceous material and woody, coaly fragments. Furthermore, the occurrence of this sand is very sporadic from well to well as observed from study of gamma-sonic logs throughout the study area. This feature is characteristic of fluvial channels encountered in the subsurface.

Overbank mud, adjacent to channel sands forms Facies E. In addition, the prominence of coal, carbonaceous fragments, carbonaceous laminae and rootlets suggests a continental setting for deposition of these associated facies.

There are two possible interpretations of Facies C both of which have implications on the environment of Facies A and B.

Facies C can be interpreted as representing a delta front environment based on the interbedded silt (or shale).

very fine grained sand and ubiquitous bioturbation. In particular it may represent the distal bar of subaqueous topset deposits. This environment is characterised by laminated silts and clays, cross bedding, scour and fill structures, and bioturbation (Reineck and Singh, 1980).

Alternatively, Facies C may be interpreted as representing deposits of the lower shoreface to slightly offshore areas of a beach environment. The laminated silts and clays and sedimentary structures are also characteristic of this environment (Reineck and Singh, 1980).

The sedimentary structures of Facies A and B combined with the isolith geometry suggest deposition which produced distributary mouth bars fed by fluvial conglomeritic channels. Therefore, matrix-supported conglomerates exhibiting high angle cross-stratification, imbrication and carbonaceour laminae may be true fluvial conglomerates. In addition, clast supported, homogeneous conglomerates may represent distributary mouth bars affected by varying degrees of wave energy in a deltaic environment. If wave energy was dominant, one would expect the development of beaches adjacent to the distributary mouth bars as sediment is redistributed by longshore drift (Leckie, D.A., 1981; Dupré and Clifton, 1979). Therefore, the degree of development of beaches from reworked distributary mouth bars would depend on the effects of waves and littoral currents. Figure 3.3 illustrates the probable sand geometries under various conditions of wave energy and

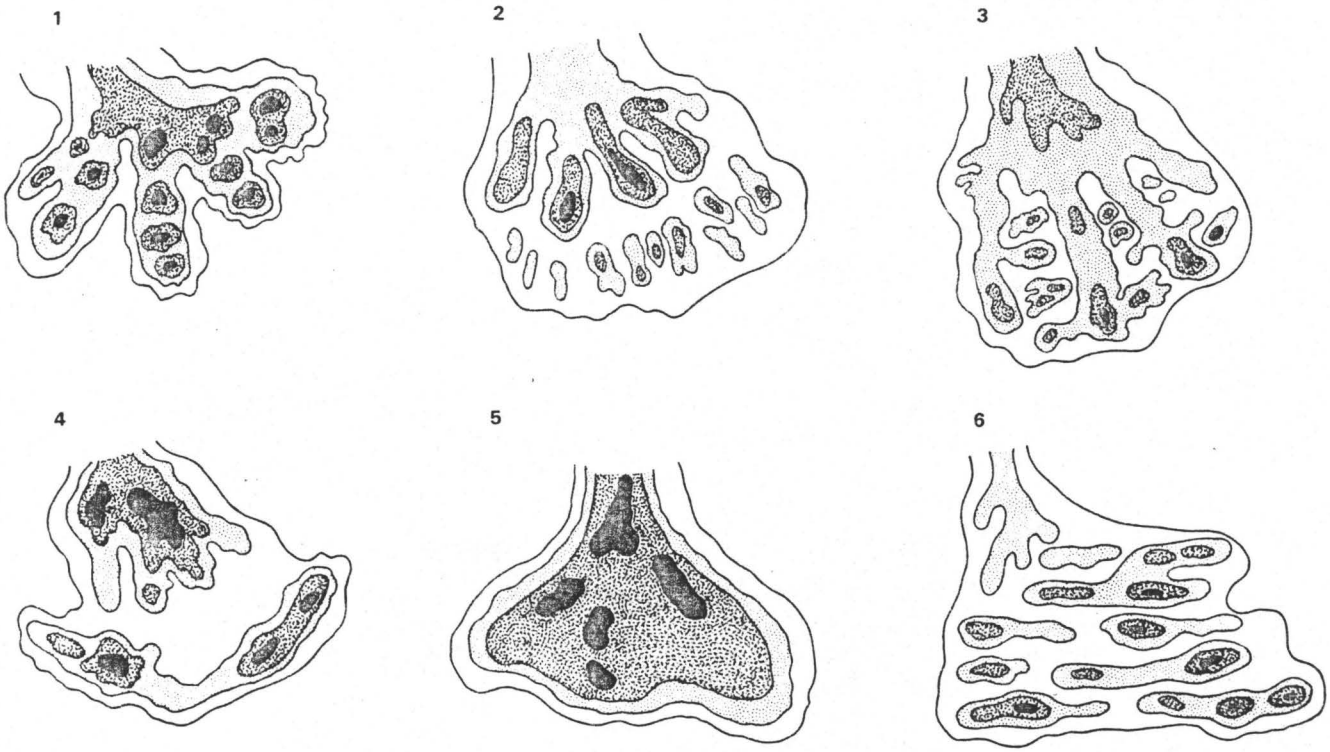

TYPE 1
Conditions: low wave energy, tidal range, and littoral drift, low offshore slope, fine-grained sediment load.
Characteristics: widespread, finger-like channel sands normal to the shoreline.
Example: modern Mississippi delta.

TYPE 2
Conditions: low wave energy, high tidal range, normally low littoral drift, narrow basin.
Characteristics: finger-like channel sands passing offshore into elongate, tidal current ridge sands.
Examples: Ord, Indus, Colorado, Ganges-Brahmaputra deltas.

TYPE 3
Conditions: intermediate wave energy, high tides, low littoral drift, shallow stable basin.
Characteristics: channel sands normal to shoreline, connected laterally by barrier–beach sands.
Examples: Burdekin, Irrawaddy and Mekong deltas.

TYPE 4
Conditions: intermediate wave energy, low offshore slope, low sediment yield.
Characteristics: coalesced channel and mouth bar sands fronted by offshore barrier islands.
Examples: Apalachicola and Brazos deltas.

TYPE 5
Conditions: high, persistent wave energy, low littoral drift, steep offshore slope.
Characteristics: sheet-like, laterally persistent barrier-beach sands with up-dip channel sands.
Examples: São Francisco and Grijalva deltas.

TYPE 6
Conditions: high wave energy, strong littoral drift, steep offshore slope.
Characteristics: multiple elongate barrier-beach sands aligned parallel to the shoreline with subdued channel sands.
Example: Senegal delta.

Figure 3.3 The morphologies of type 3 and type 4 deltas most closely resemble the isolith geometry of the Notikewin A sand (after Coleman and Wright, 1975).

currents.

Further evidence in favour of wave effected distributary mouth bars in a delta would be the presence of stacked beach ridges (Miall, 1979). These are difficult to recognize in core. Well 10-24 shows two coarsening upward cycles originally thought to represent large ridges. However, they may reflect minor progradation with introduction of fines at the base or potassium feldspar which would cause a misleading deflection in the gamma-ray curve.

Collectively, Facies C, B and A represent an overall coarsening upward sequence which is characteristic of both deltaic and beach environments (Reineck and Singh, 1980).

A distinction between these two possibilities can be made on the basis of isolith geometry if core control is sufficient. The author believes the environment of deposition of the Notikewin Member covers a range of possibilities between those cited above depending on the wave energy and littoral drift affecting the sediments.

4. PETROLOGY

Method

Twenty-one thin sections were prepared from thirty-six core samples collected (see Appendix I for thin section sample depth locations). Seven of the thin-sectioned samples are from Facies A, nine from Facies B and five are from Facies D. All thin sections were cut perpendicular to the bedding direction and impregnated with blue epoxy to indicate porosity.

Point counting was completed in four steps:

i) 21 thin sections point counted for Q-R-F classification;

ii) 10 thin sections point counted for types of rock fragments;

iii) 10 thin sections point counted for particular types of sedimentary rock fragments;

iv) 10 thin sections point counted to determine abundance of four possible quartz types (Basu et al., 1975)

1. monocrystalline quartz with less than 5° undulosity;
2. monocrystalline quartz with greater than 5° undulosity;

3. polycrystalline quartz with 2-3 crystals per grain; ≥75% of total polycrystalline quartz;
4. polycrystalline quartz with >3 crystals per grain; >25% of total polycrystalline quartz.

Steps i) to iii) are for classification of the sandstone according to Folk (1974). Step iv) is to determine quartz types as an indicator of provenance (Basu et al., 1975). For step i), 300 point counts per slide were performed while 100 counts per slide were completed for steps ii) to iv) inclusive.

Results

Minerals and constituents found in the Notikewin A and B sandstones are: quartz, chert, plagioclase, carbonate, rock fragments, detrital and authigenic clay (identified by XRD and SEM), mica, glauconite, opaques and bitumen. Tables 4.1 to 4.5 indicate point count results for classification of the sandstone (figure 4.1). All samples are classified, in general, as sublitharenites to litharenites. In particular they are named chert arenites and shale arenites (plates 4-1 and 4-2).

Quartz

Undulose and non-undulose monocrystalline quartz grains are most abundant. Approximately 70% of the grains are non-undulose and 30% are undulose. Syntaxial overgrowths of silica cement are common on these grains. Excel-

Table 4.1 Point count results, per cent minerals

FACIES	SAMPLE NO.	QUARTZ	CHERT & ROCK FRAGMENTS	CLAY & GLAUCONITE	FELDSPAR	CARBONATE	OPAQUES & HEAVIES	POROSITY ϕ	TOTAL PER CENT
	8	33.7	31.7	30.7	1.3	-	0.7	2.3	100.4
	17	14.3	60.0	6.3	0.7	-	2.7	16.0	100.0
	18	3.0	72.3	4.0	-	-	0.3	20.3	99.9
A	23	28.0	54.3	5.7	-	-	2.3	9.7	100.0
	25	15.0	62.7	2.7	-	-	1.7	18.0	100.1
	28	10.0	65.0	-	0.3	24.3	0.3	-	99.9
	29	20.7	60.0	11.7	1.7	-	2.7	3.7	100.5

n = 300 point counts per slide
mean grain size: -1ϕ (2.0 mm.) to larger than -2ϕ (5.0 mm.)

Table 4.2 Point count results, per cent minerals

FACIES	SAMPLE NO.	QUARTZ	CHERT & ROCK FRAGMENTS	CLAY & GLAUCONITE	FELDSPAR	CARBONATE	OPAQUES & HEAVIES	POROSITY ϕ	TOTAL PER CENT
	1	51.0	16.7	27.0	-	-	3.7	1.7	100.1
	4	61.0	11.7	19.7	-	3.7	3.7	0.3	100.1
	5	51.3	4.3	36.0	-	4.7	1.7	1.7	99.7
	6	58.0	13.0	15.7	-	3.3	0.3	9.7	100.0
B	9	53.7	11.7	28.3	-	-	1.3	4.7	99.7
	14	49.7	10.0	27.7	-	7.7	0.3	3.0	98.4
	15	47.3	11.7	29.0	-	5.3	2.0	4.7	100.0
	21	38.7	8.3	30.7	-	21.7	0.3	0.3	100.0
	24	57.3	10.7	29.0	-	-	1.7	1.3	100.0

n = point counts per slide
mean grain size: 0ϕ (1.0 mm.) - 1ϕ (0.5 mm.)

Table 4.3 Point count results, per cent minerals

FACIES	SAMPLE NO.	QUARTZ	CHERT & ROCK FRAGMENTS	CLAY & GLAUCONITE	FLEDSPAR	CARBONATE	OPAQUES & HEAVIES	POROSITY ϕ	TOTAL PER CENT
	12	26.3	11.7	17.0	4.0	39.3	1.3	0.3	99.9
	16	42.7	8.7	20.3	0.7	26.7	0.3	0.7	100.1
D	33	29.0	10.7	15.7	5.3	37.0	0.3	2.3	100.3
	34	48.0	13.3	29.7	4.0	-	1.0	4.0	100.0
	35	52.0	9.3	31.3	5.3	0.3	1.0	0.7	99.9

n = 300 point counts per slide
mean grain size: 2ϕ (0.25 mm.)

Table 4.4 Q-F-R values

FACIES	SAMPLE NO.	QUARTZ Q	FELDSPAR F	ROCK FRAGMENTS R
	8	51.0	2.0	48.0
	17	19.0	1.0	80.0
	18	4.0	-	96.0
A	23	34.0	-	66.0
	25	19.0	-	81.0
	28	13.0	-	87.0
	29	25.0	2.0	73.0
	1	75.0	-	25.0
	4	84.0	-	16.0
	5	92.0	-	8.0
	6	82.0	-	18.0
B	9	82.0	-	18.0
	14	83.0	-	17.0
	15	80.0	-	20.0
	21	82.0	-	18.0
	24	84.0	-	16.0
	12	63.0	9.0	28.0
	16	82.0	1.0	17.0
D	33	64.0	12.0	24.0
	34	74.0	6.0	20.0
	35	78.0	8.0	14.0

Table 4.5 Point count results

		Rock Fragment Types			Components of SRF		
FACIES	SAMPLE NO.	SRF	MRF	VRF	CHERT	CARBON-ATE	SANDSTONE SILTSTONE
A	23	96.0	4.0	-	100.0	-	-
	29	100.0	-		98.0	-	2.0
B	4	71.0	29.0	-	16.0	5.0	79.0
	6	67.0	33.0	-	34.0	1.0	65.0
	9	77.0	23.0	-	65.0	1.0	34.0
	15	78.0	22.0	-	54.0	10.0	36.0
	24	83.0	17.0	-	86.0	2.0	12.0
D	12	78.0	22.0	-	52.0	34.0	14.0
	16	89.0	11.0	-	69.0	7.0	24.0
	33	88.0	12.0	-	54.0	31.0	15.0

n = 100 point counts per slide

Figure 4.1 Classification of the Notikewin Member sandstones (after Folk, 1974). The samples are sublitharenites to litharenites with abundant chert rock fragments.

LEGEND

1. Quartzarenite
2. Subarkose
3. Sublitharenite
4. Arkose
5. Lithic arkose
6. Feldspathic litharenite
7. Litharenite
8. Volcanic-arenite
9. Phyllarenite
10. Sedarenite
11. Calclithite
12. Chert arenite
13. Sandstone arenite-Shale arenite

Q = quartz
R = rock fragments
F = feldspar

VRF = volcanic rock fragments
MRF = metamorphic rock fragments
SRF = sedimentary rock fragments
CRF = carbonate rock fragments

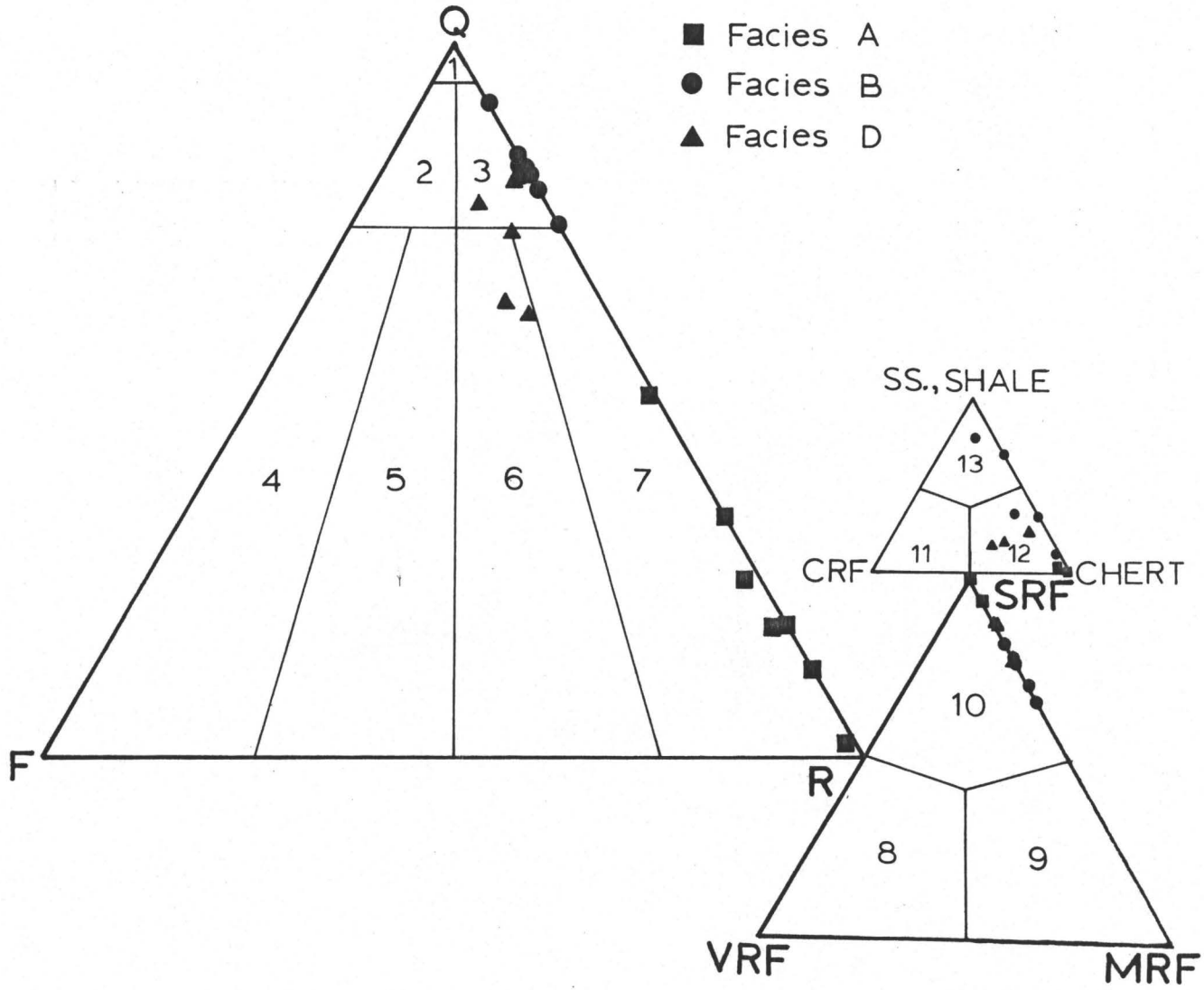
Q
Facies A
Facies B
Facies D
1
2
3
4
5
6
7
F
R
SS., SHALE
13
11
12
CRF
CHERT
SRF
10
8
9
VRF
MRF

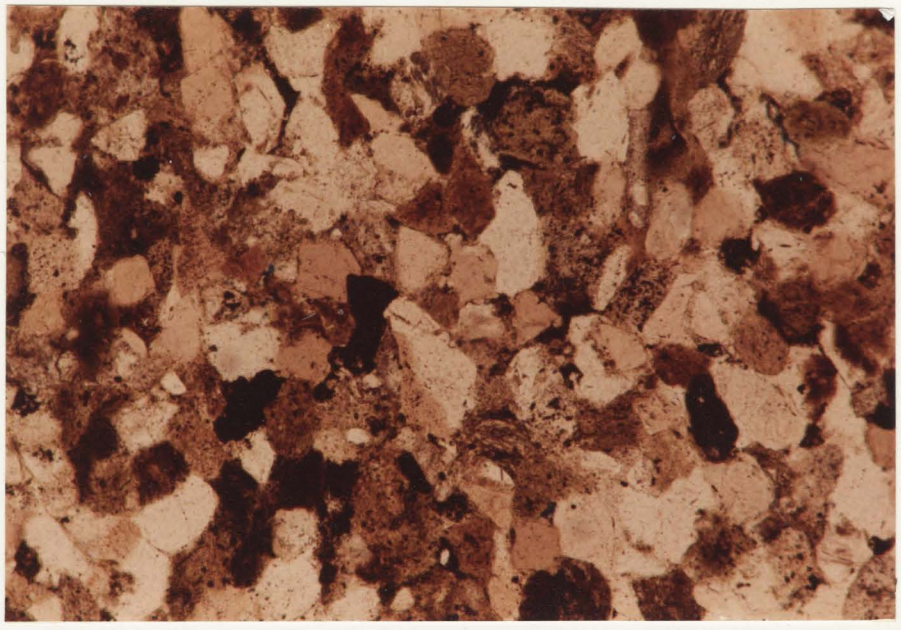

Plate 4-1 Classification of the Notikewin sands as sublitharenites-litharenites is based on the abundance of chert and rock fragments. Sample 1, magnification 63X, PPL.

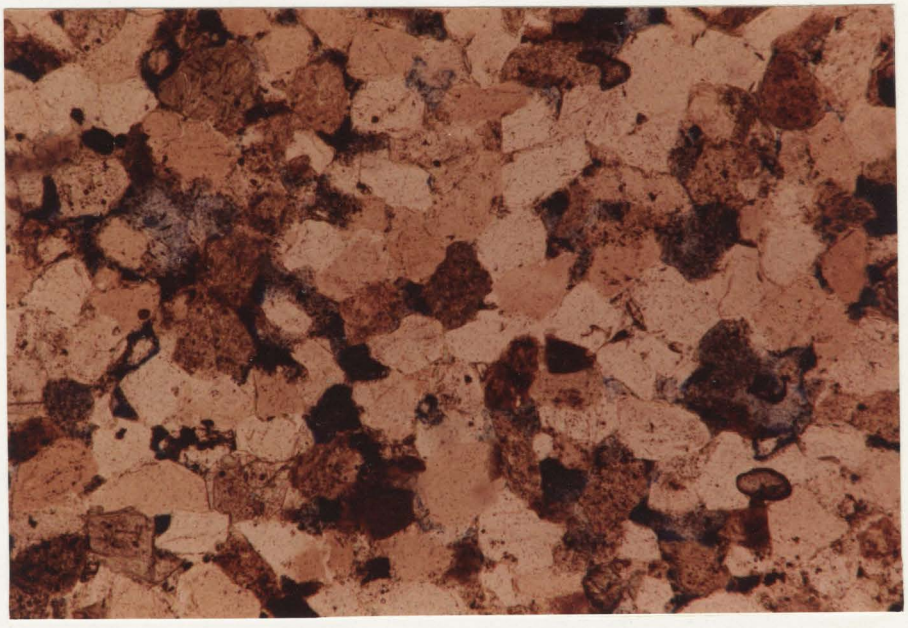

Plate 4-2 Similar composition as above but with highest observed porosity in Facies B (9.7%) (porosity infilled with blue epoxy). Sample 6, magnification 63X, PPL.

lent quartz overgrowths developed in coarser sands and conglomerates (plates 4-3 and 6-4). Overgrowths are observed to occlude pore space totally in some cases. Polycrystalline quartz comprises an average of 10% of total quartz grains.

The degree of roundness of grains varies in each of the facies. In Facies A and B, grains are rounded to well rounded. Sub-angular to sub-rounded grains comprise Facies D. Uncertainty in determining degree of roundness is encountered due to the quartz overgrowths which cause pseudo-angularity.

Overall grain size is variable, from 2ϕ (0.25 mm.) to larger than -2ϕ (4.0 mm.). Within Facies B grain size is consistently 0ϕ (1.0 mm.) to 1ϕ (0.5 mm.). Facies D has relatively greater variation in grain size and is difficult to measure due to the angularity of grains. Grain sizes vary from 1ϕ (0.5 mm.) to 3ϕ (0,125 mm.).

Few inclusions are observed in quartz grains. Most commonly bubble trains and "dust" are found. "Dust" on the perimeter of the detrital quartz grains before the formation of overgrowths facilitates recognition of the latter (plate 4-3). The dust is due to void space between the overgrowth and the nucleus (Pittman, 1972). Unidentifiable needle-like inclusions are rare. One grain contained a plagioclase feldspar inclusion (plate 4-4).

Most grain contacts are tangential or long. Sutured contacts are rare except internally in polycrystalline quartz

Plate 4-3 Syntaxial quartz overgrowths. Note the roundness of the detrital grain emphasized by "dust" around the perimeter (arrow). Sample 17, magnification 63X, XN.

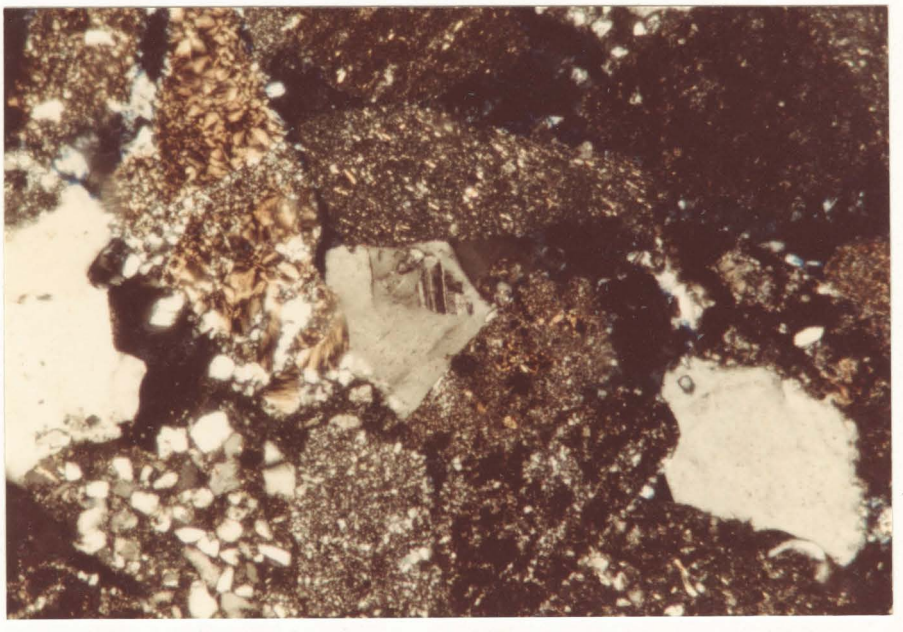

Plate 4-4 Plagioclase feldpsar inclusion in quartz grain in centre of photomicrograph. Sample 23, magnification 63X, XN.

grains.

Quartz also occurs as drusy, fracture filling cement in chert grains (plate 4-5).

The four types of monocrystalline and polycrystalline quartz described previously are distinctive indicators of original provenance (Basu et al., 1975). Table 4.6 summarizes point count results. A plot of these quartz varieties (figure 4.2) indicates that the majority of quartz has been derived from a middle to high grade metamorphic source area.

Chert

Although chert is a rock fragment it will be considered separately. Chert is present in all samples and is most abundant (30% to 70%) in Facies A (conglomerate). Chert content increases with increasing grain size. It ranges from coarse crystalline to cryptocrystalline (plate 4-6). Microcrystalline chalcedony exhibiting a radiating pattern is observed (plate 4-7). Rare fossiliferous sponge spicules were observed. In addition one fossil (identity unknown) was found infilled with crystalline quartz (plate 4-8). Radiolarian chert was also recognized.

The chert is well rounded. Contacts with other chert grains in Facies A are commonly sutured. Light to dark brown coloured varieties are phosphatic.

Rock Fragments

Apart from chert, which has been considered separately, there are four types of rock fragments: carbonate, shale/

Table 4.6 Point count results – Quartz types

FACIES	SAMPLE NO.	NON-UNDULOSE	UNDULOSE	2-3 CRYSTALS GRAIN POLYCRYSTALLINE	>3 CRYSTALS GRAIN POLYCRYSTALLINE
A	23	25	67	03	05
	29	33	58	04	05
B	4	59	35	-	06
	6	69	26	02	03
	9	72	12	02	14
	15	60	28	05	07
	24	64	27	05	07
D	12	70	09	04	18
	16	82	14	03	01
	33	85	10	-	05

n = 100 point counts per slide

Figure 4.2 Quartz varieties of the Notikewin Member plotted on diagram proposed by Basu et al. (1975) suggests a provenance of medium to high grade metamorphic terrain.

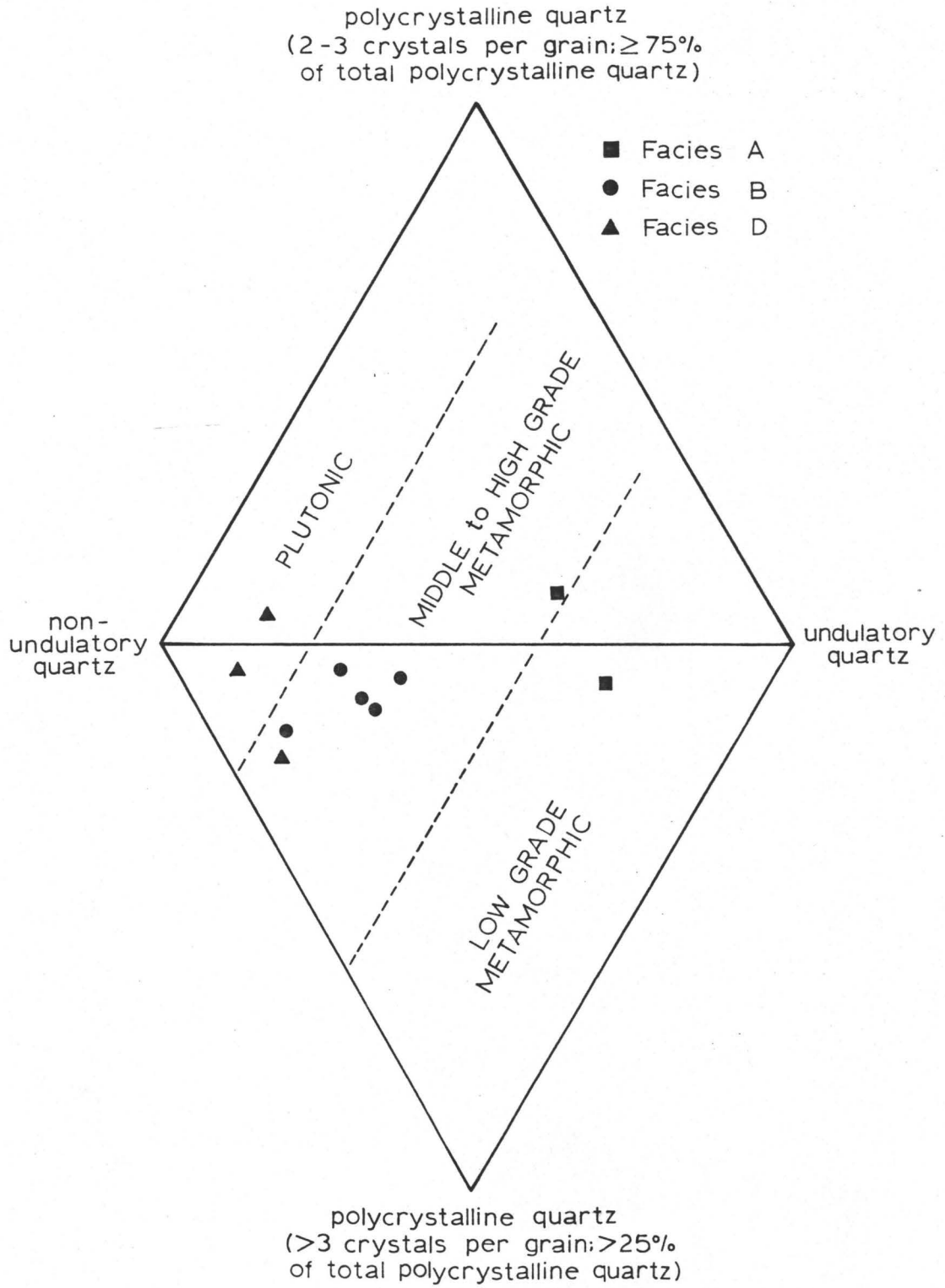
polycrystalline quartz
(2-3 crystals per grain; ≥ 75%
of total polycrystalline quartz)
Facies A
Facies B
Facies D
PLUTONIC
MIDDLE to HIGH GRADE
METAMORPHIC
non-
undulatory
quartz
undulatory
quartz
LOW GRADE
METAMORPHIC
polycrystalline quartz
(>3 crystals per grain; >25%
of total polycrystalline quartz)

Plate 4-5 Drusy, fracture filling quartz cement in chert grain. Sample 17, magnification 25X, XN.

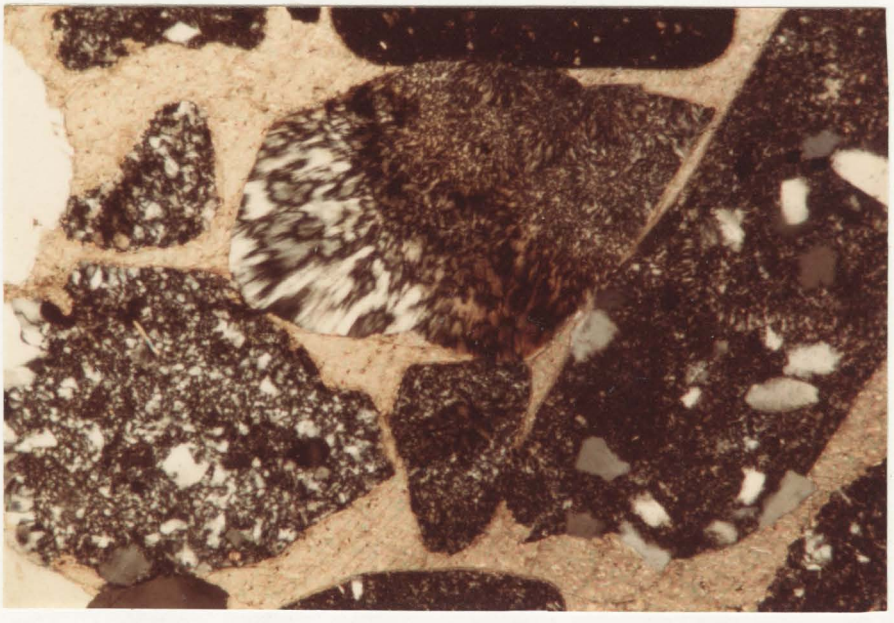

Plate 4-6 Various types of chert ranging from coarse crystalline to cryptocrystalline. Radiating chalcedony is common. Sample 28, magnification 63X, XN.

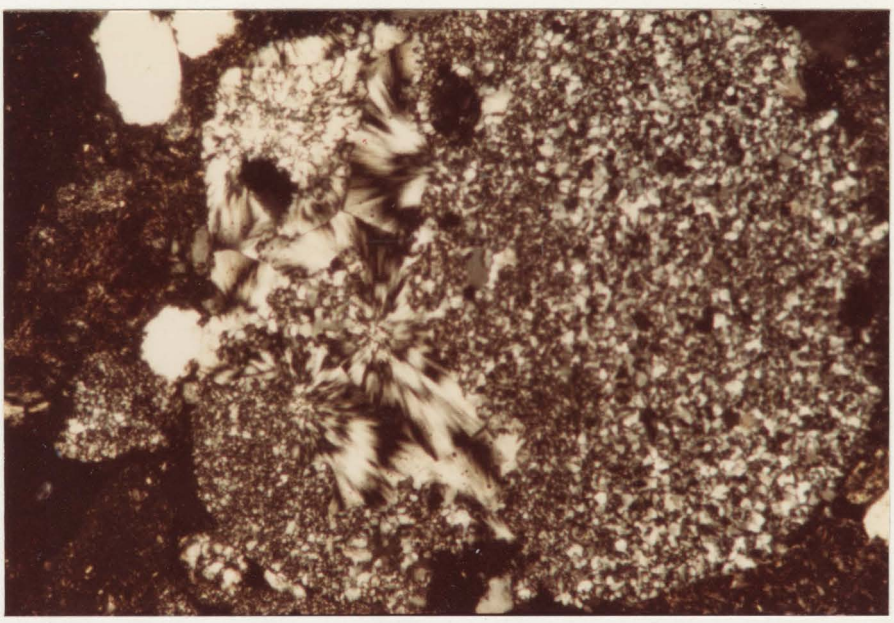

Plate 4-7 Radiating chalcedony in chert. Sample 23, magnification 63X, XN.

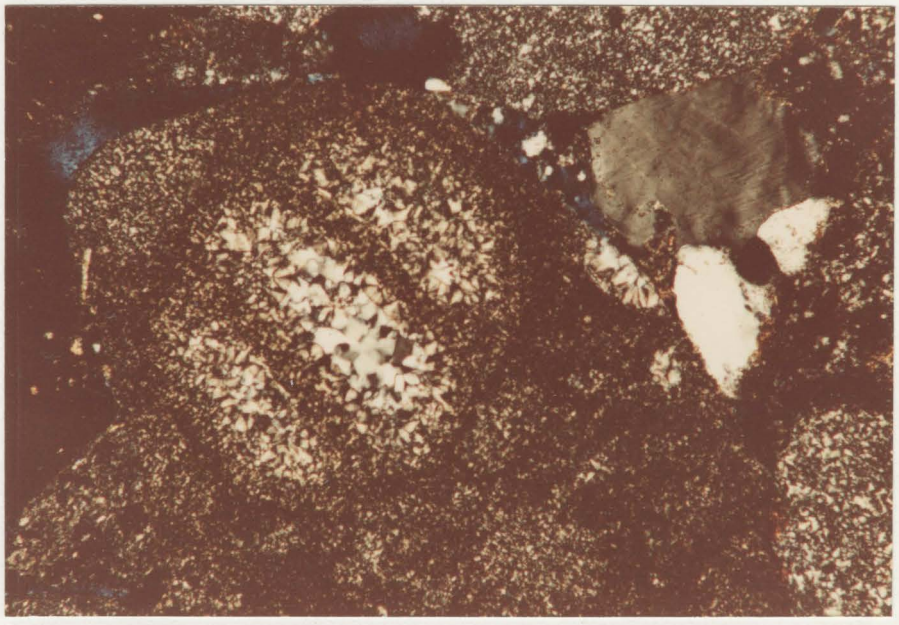

Plate 4-8 Fossil infilled with crystalline quartz within chert fragment. Sample 17, magnification 63X, XN.

mudstone, sandstone and metamorphic rock fragments. The most common types are sandstone sedimentary rock fragments and metamorphic rock fragments (plates 4-9 and 4-10). Sandstone rock fragments are well rounded, translucent grains composed of clean quartz sand grains with concavo-convex contacts within the grain. They can be distinguished from metamorphic (polycrystalline quartz) fragments by the presence of irregular, sutured internal grain contacts in the metamorphic fragments. Sutured polycrystalline quartz was the only type of metamorphic rock fragment recognized. The division between these two types of rock fragments and polycrystalline quartz is subject to the writer's discretion.

Carbonate and shale/mudstone rock fragments were less common. Facies D contained the largest proportion of carbonate rock fragments (plate 4-11). Their high birefringence is masked by the tan brown colour of the grain. The shale/mudstone rock fragments exhibit deformation due to compaction around more competent grains.

Feldspar

Plagioclase feldspar exhibiting albite type twinning was the only detrital feldspar recognized. Samples from Facies D contained the largest amount of feldspar. Carbonate replacing plagioclase was common in the carbonate cemented sands of Facies D (plate 4-12).

Carbonate

Most carbonate present is authigenic calcite cement

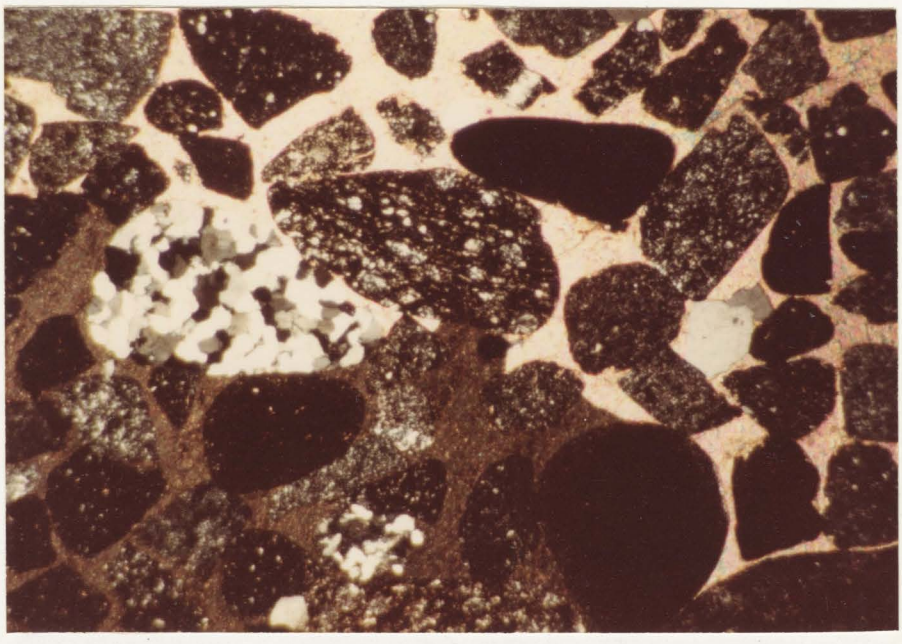

Plate 4-9 Sedimentary sandstone rock fragment in left centre. Grains cemented with poikilotopic carbonate cement. Sample 28, magnification 25X, XN.

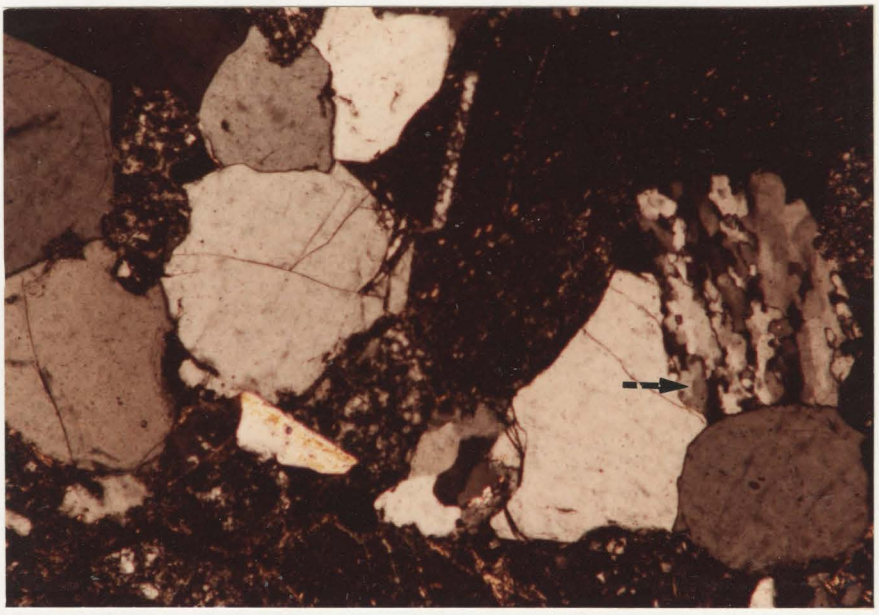

Plate 4-10 Metamorphic, polycrystalline grain with sutured internal grain contacts (arrow). Sample 25, magnification 63X, XN.

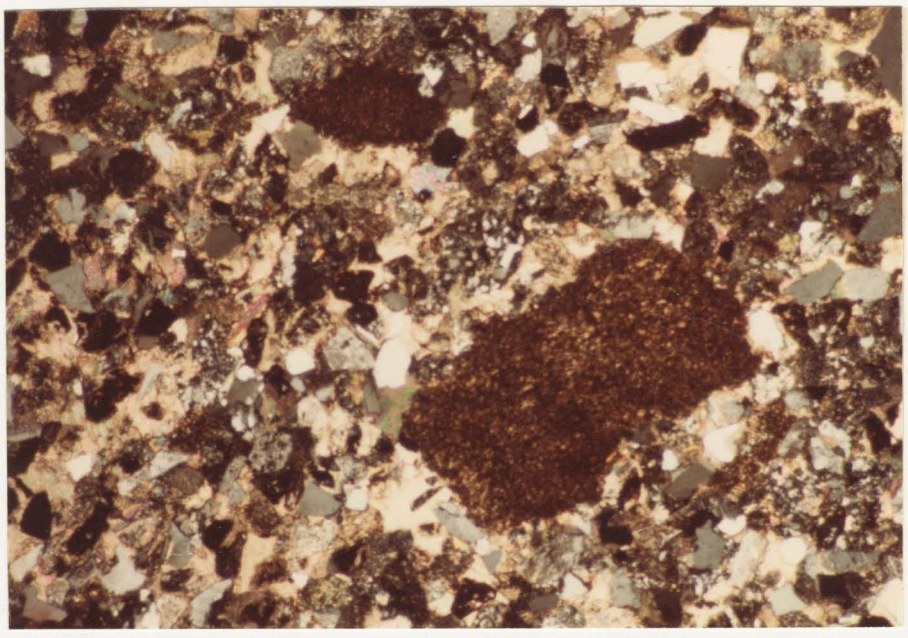

Plate 4-11 Carbonate rock fragment in angular, carbonate cemented sand of Facies D. Sample 33, magnification 25X, XN.

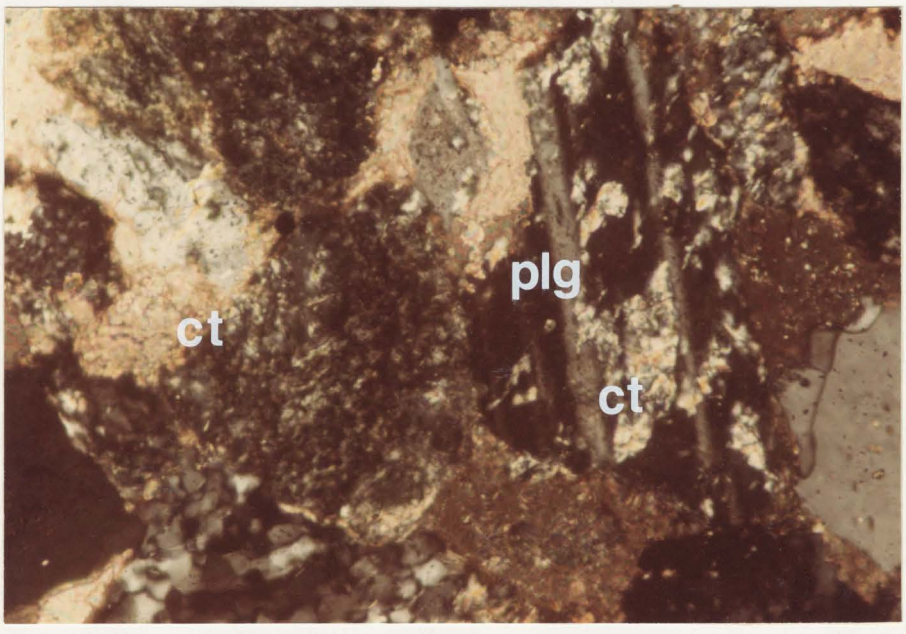

Plate 4-12 Calcite (ct) replacing albite twinned plagioclase (plg) feldspar grain in carbonate cemented sand of Facies D. Sample 33, magnification 125X, XN.

which occurs in Facies A and more abundantly in Facies D. The cement of Facies D is poikilotopic (plate 4-9). Siderite cement was identified previously by May (1967) as an important carbonate constituent. It is recognized by greenish brown limonite staining, high relief and high birefringence. Dolomite rhombs are present in Facies D also.

Glauconite

The presence of glauconite is exclusive to Facies B. It is recognized by its green colour, high birefringence and round pelletal morphology. It is uniformly disbributed with some rare concentrated laminae observed.

Minor Minerals and Constituents

Heavy minerals such as sphene, and zircon, mica flakes, opaques and bitumen constitute minor accessories. Bitumen and other hydrocarbon residue is most common in the pores of Facies A and B. The remainder of these accessories are most abundant in finer fractions of the other facies. Sphene, zircon and opaques occur in horizontal laminae on a millimetre scale. The opaques vary in size and degree of roundness. Most occur as irregular masses and aggregates. No attempt to identify opaques was made.

Porosity

Point counts were made to determine per cent porosity, with no differentiation between primary and secondary types.

The bulk of porosity is primary intergranular poros-

ity. In addition there is strong evidence for secondary porosity, particularly in Facies B. Secondary porosity is recognized by several textural features. Local patchy porous areas are indicative of secondary porosity (Schmidt and McDonald, 1979a)b)). Shrinkage cracks around glauconite produce minor secondary porosity (plate 4-13). Microfractures also produce minor secondary porosity (plate 4-14). Abnormally large, oblong pores suggest dissolution (plate 4-15). Also, rounded or well formed pore geometry suggests the presence of a precursor mineral which has been subsequently removed to produce secondary porosity (plate 4-16).

The high porosity of non-carbonate cemented Facies A conglomerate appears equal to the minus-cement porosity of carbonate cemented Facies A conglomerates with the same grain size and composition (plates 4-17 and 4-18). This suggests that regional dissolution of carbonate cement has resulted in widespread secondary porosity in Notikewin conglomerates. Schmidt and McDonald (1979a)b)) claim that the dissolution of carbonates is the most important cause of secondary porosity in reservoirs.

The porosity of Facies A (conglomerate) was largest on average (12%-20%) as anticipated (plate 4-19). Porosity of clast-supported conglomerates is larger than those with fine-grained sand matrix. The porosities determined from point counts for Facies A agree with core plug analyses and with porosities determined from sonic/acoustic velocity logs.

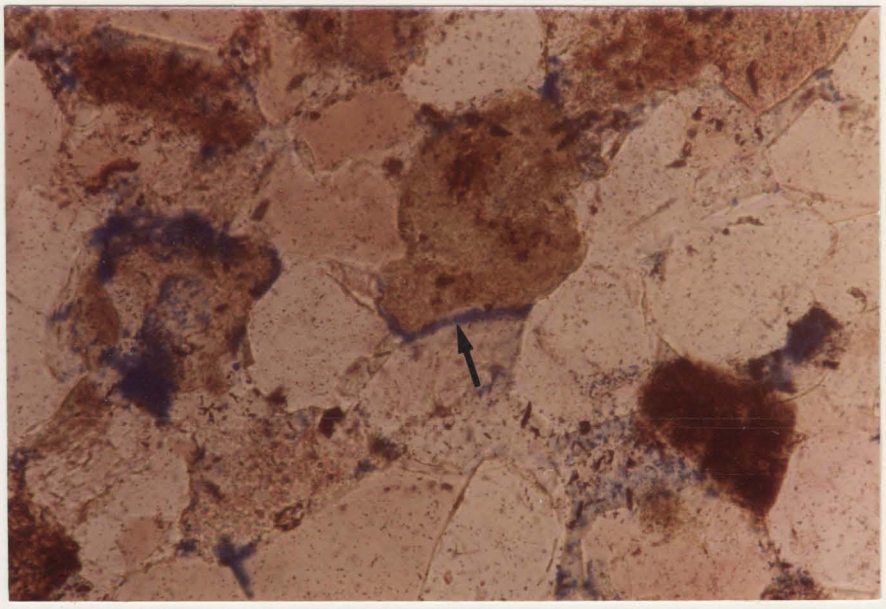

Plate 4-13 Shrinkage of glauconite producing minor secondary porosity (arrow). Sample 6, magnification 125X, PPL.

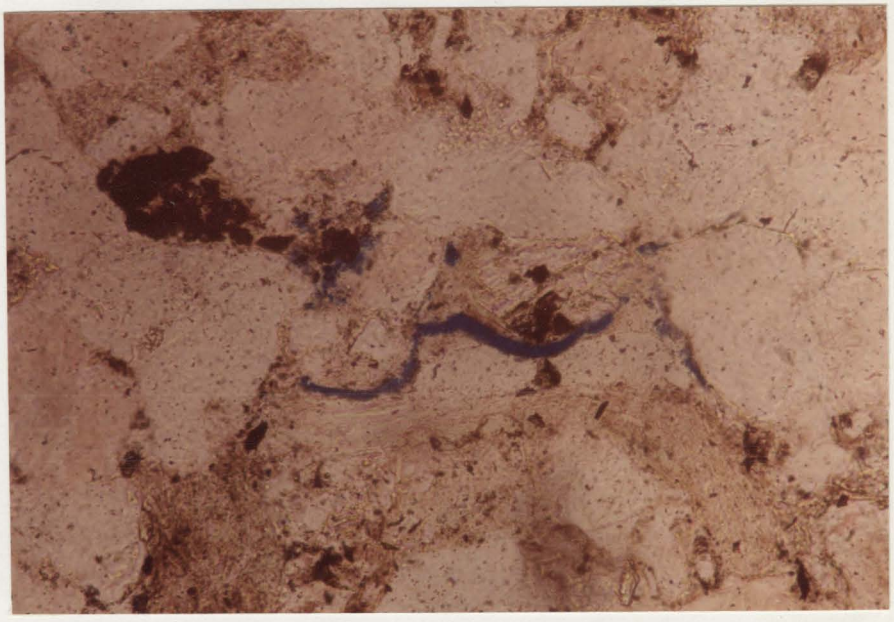

Plate 4-14 Secondary porosity due to microfracturing. Sample 5, magnification 125X, PPL.

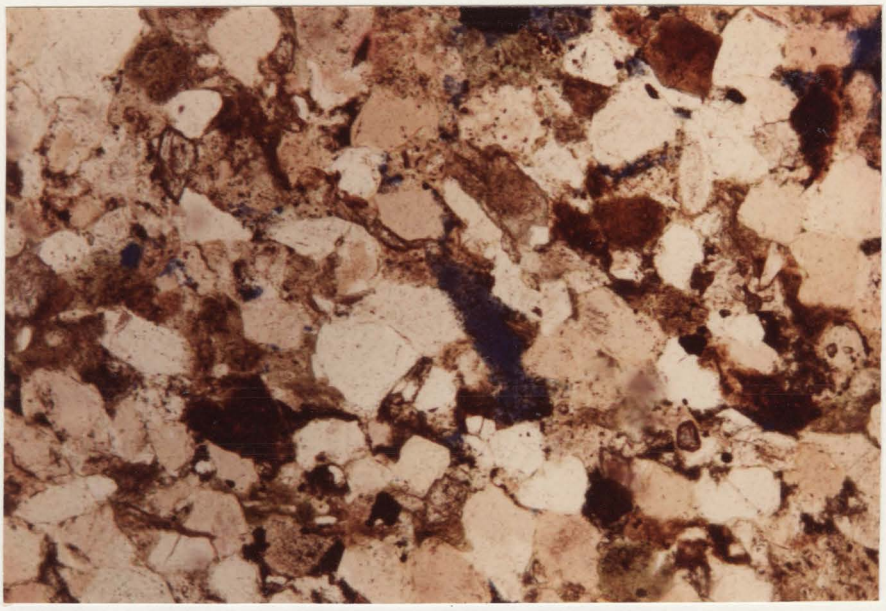

Plate 4-15 Large oblong pores suggest dissolution to produce secondary porosity has occurred. Sample 15, magnification 63X, PPL.

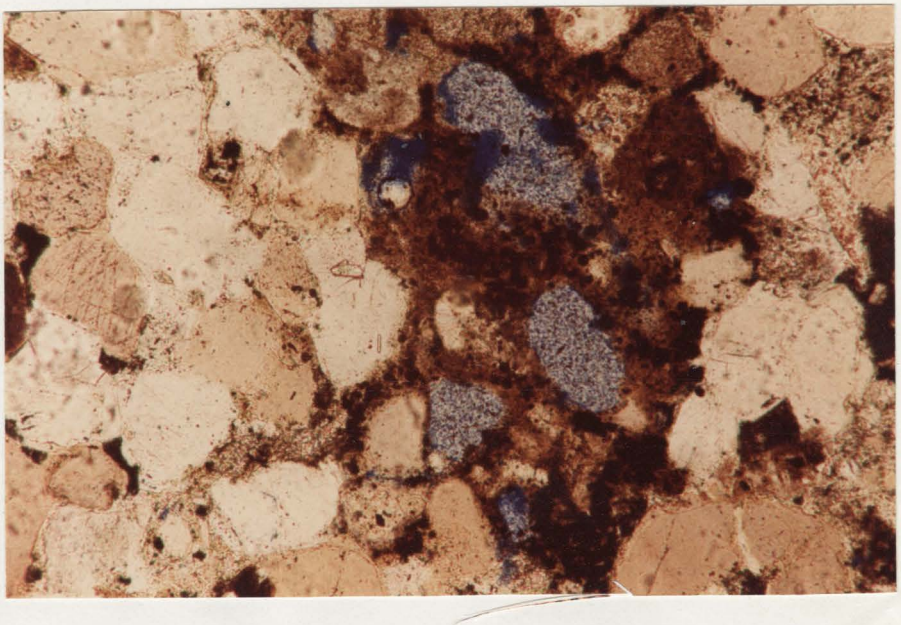

Plate 4-16 Rounded or well shaped pores indicate presence of a previous grain. Sample 24, magnification 63X, PPL.

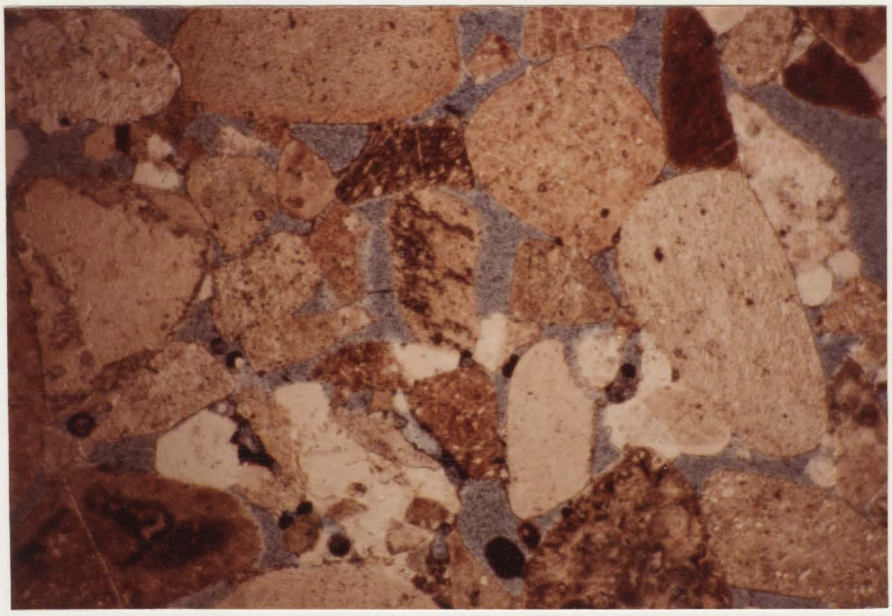

Plate 4-17

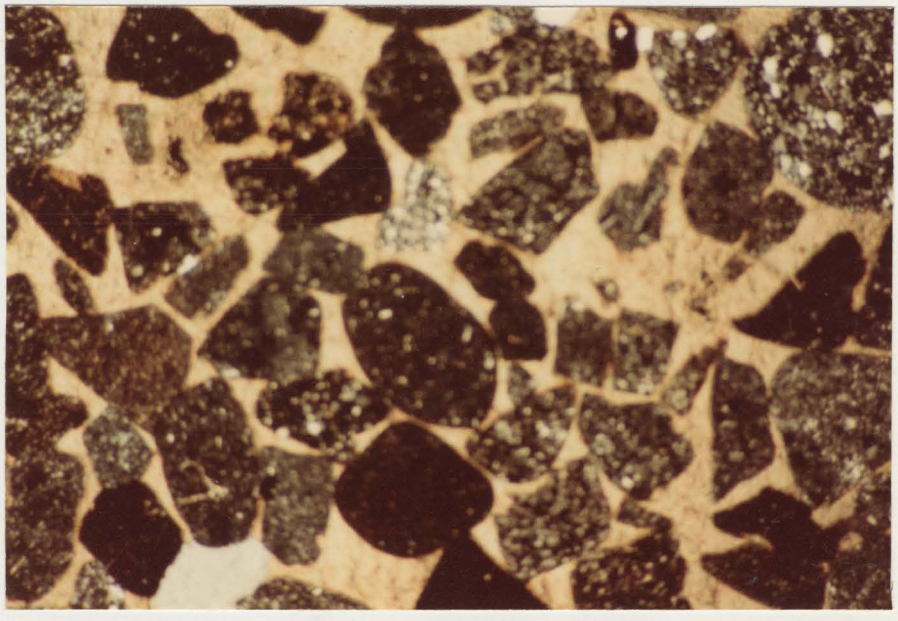

Plate 4-18 The high porosity of Sample 25 (top) PPL is similar to the minus-cement porosity of Sample 28 (bottom) XN suggesting regional dissolution of carbonate cement to produce secondary porosity. Both magnifications 25X.

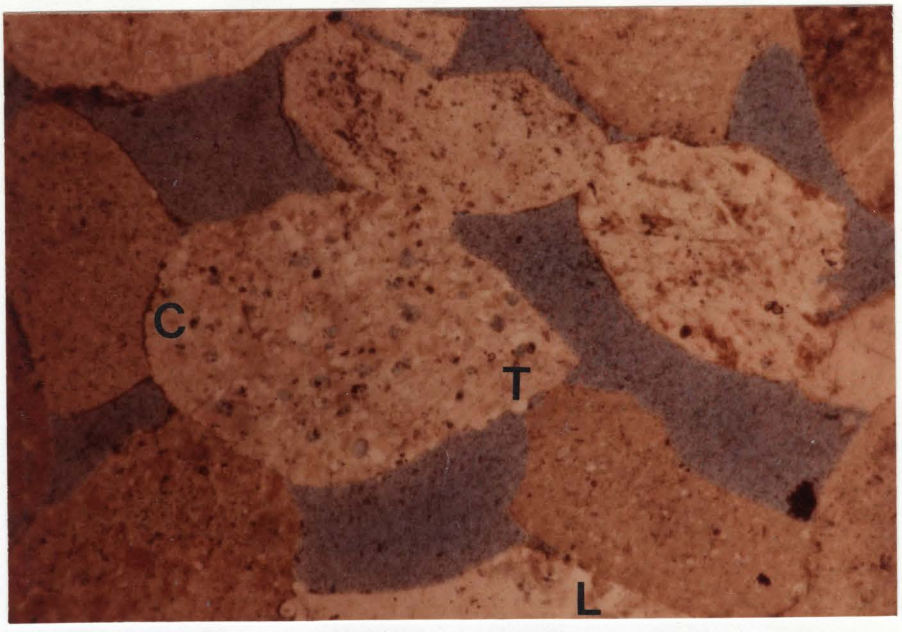

Plate 4-19 High porosity (20.3%) in chert conglomerates of Facies A. Note concavo-convex (C), long (L), and tangential (T) types of grain contacts. Sample 18, magnification 25X, PPL.

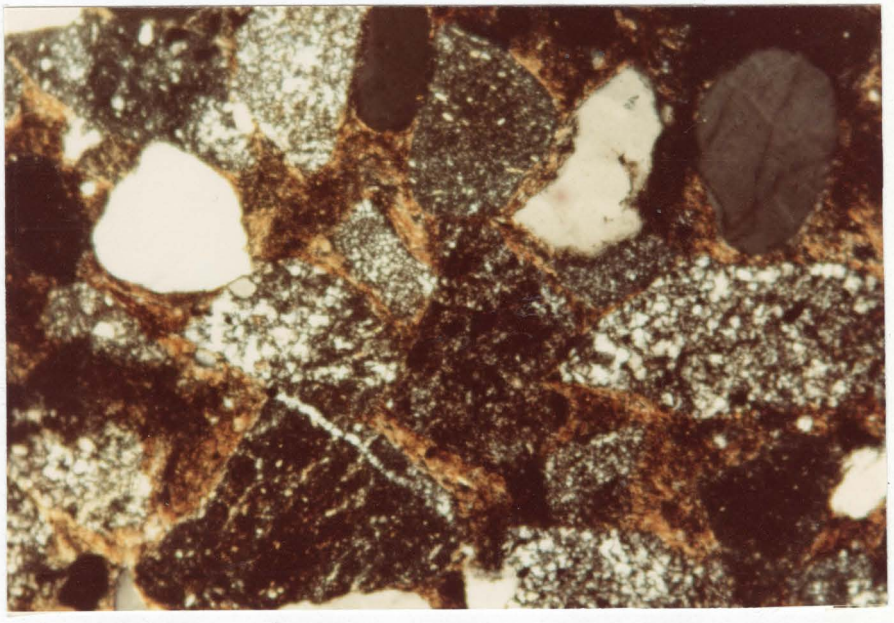

Plate 4-20 Allogenic (detrital) clay existing as dispersed matrix. Sample 29, magnification 63X, XN.

Porosities determined for Facies B (4.7%-9.7%) are significantly lower than those determined from core plug analyses and sonic/acoustic velocity logs which suggest porosities of 10%-18%. This may be the result of the presence of secondary porosity, resulting in more intergranular contacts than primary porosity, thus causing shorter interval transit times (Schmidt and McDonald, 1979a). The porosity of Facies D is very small (<4.0%).

The pore geometry of Facies A varies from Facies B in that pores in Facies A (conglomerate) are bounded by smooth, round chert grain surfaces with minor pore-lining clay and quartz overgrowths. In contrast, pores in Facies B are much more irregularly shaped, smaller, and have patchy distribution (compare plate 4-1 (Facies B) and plate 4-19 (Facies A)).

Clay Minerals

Clay mineral identification will be dealt with in detail in chapter five. Petrographic description here serves only as a preliminary examination. The detail of clay mineralogy is best determined by the use of X-ray diffraction (XRD) and scanning electron microscopy (SEM) since individual clay particles are on the order of a few microns, beyond the resolution limit of the light microscope.

The bulk of the clay is allogenic (detrital) and forms matrix. However, because recognition of authigenic clay is difficult the abundance of authigenic clay may be

underestimated. Allogenic clay exists as dispersed matrix (plate 4-20), infiltration residues, thin intercalated laminae and floccules. Authigenic clay exists as pore linings (plate 4-21), pore bridging and pore fillings (plates 4-22 and 4-23). From visual estimates Facies B contains the most clay (authigenic and allogenic). Facies A contains abundant authigenic clay existing as pore lining and pore bridging types with pore filling clay absent. Pore filling clay is more abundant in Facies B. Pore lining clay is usually absent at the contacts between detrital grains. Rarely it is observed along the contact between detrital grains and surrounding detrital quartz grains within quartz overgrowths. This has genetic implications.

Due to the low porosity (<4.0%) and carbonate cemented nature of Facies D a discussion of clay types in this facies is omitted.

Interpretation and Provenance

Results from petrographic data indicate sedimentary and metamorphic source areas for Notikewin sands.

Evidence for a sedimentary source lies in the presence of chert. The chert in clastic rocks is derived from either nodules in carbonate rocks or from beds of "deep water" chert in geoclinal settings (Blatt et al., 1980). The chert was probably derived from Paleozoic (Devonian and Mississippian) carbonates in the Cordilleran highlands. If chert is derived from carbonates then the presence of carbonate rock

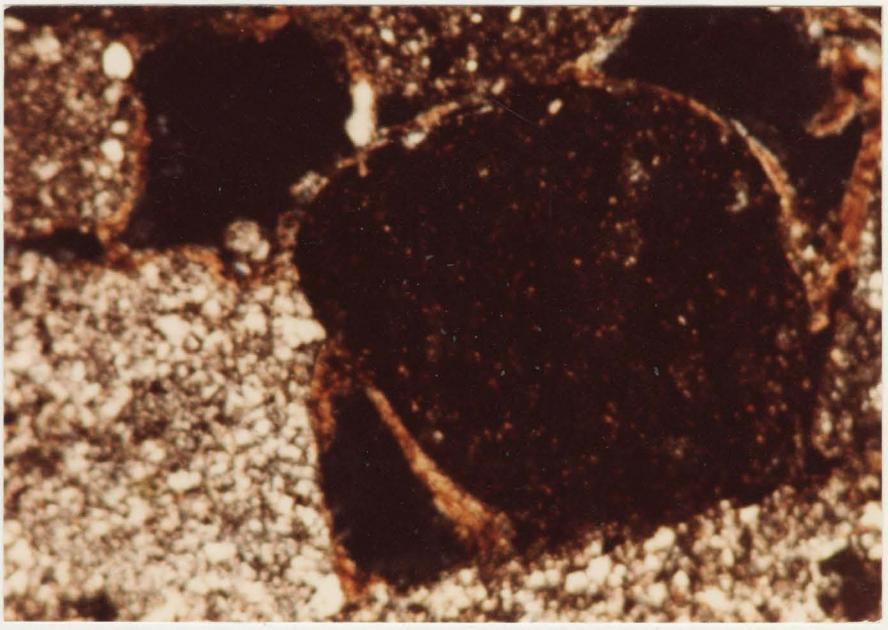

Plate 4-21 Pore lining authigenic clay surrounding chert grain. Note absence of clay along grain contacts. Sample 17, magnification 63X, XN.

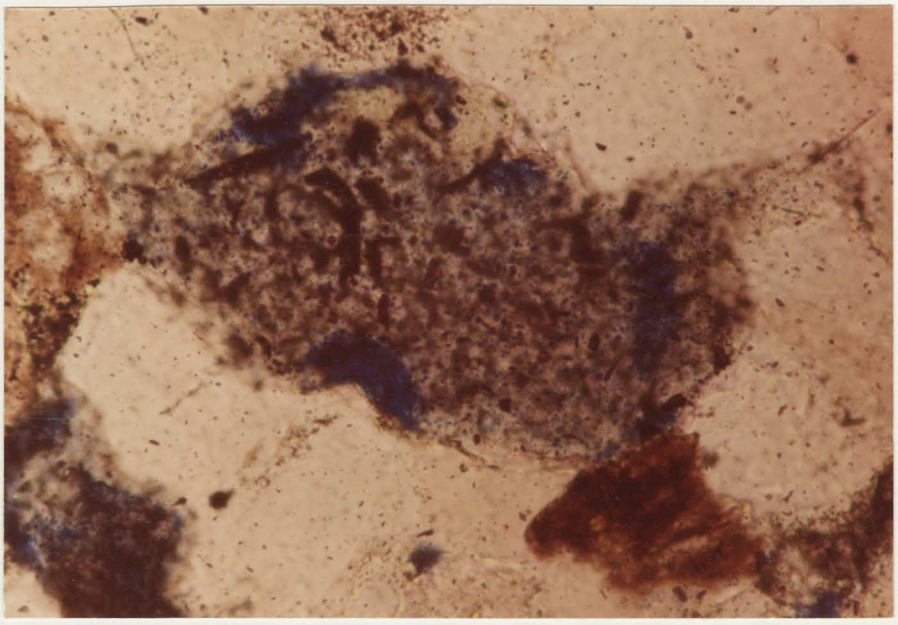

Plate 4-22

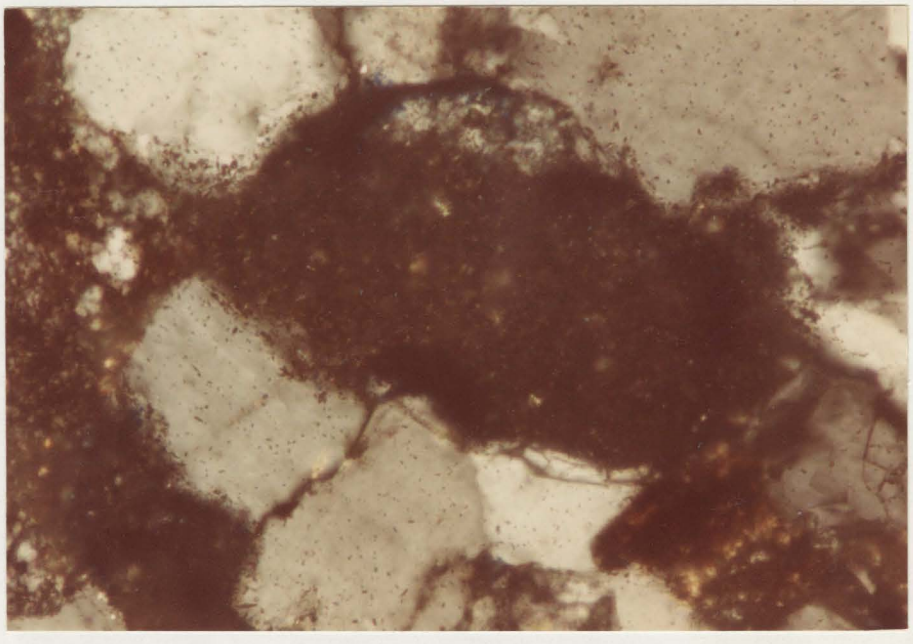

Plate 4-23 Pore filling clay in PPL (top) and same view in XN (bottom). Sample 6, magnification 63X.

fragments is anticipated. This explains the presence of carbonate rock fragments in the fluvial Facies D. Carbonate is preferentially dissolved and is therefore not preserved in other sand facies. This is also true for feldspar which is observed only in Facies D.

The well rounded nature of the quartz grains along with the presence of sandstone sedimentary rock fragments confirms that quartz has survived at least one previous erosion cycle before deposition at Notikewin time. The sandstone source of these grains is also of Paleozoic or Late Proterozoic age.

Data plotted according to Basu et al. (1975) suggests a dominant medium to high grade metamorphic source terrain which existed in the Cordillera. It is observed that Facies A, B and C do not plot decisively in the same regions (figure 4.2). This may be the result of an insufficient number of samples point counted. Alternatively, it may indicate a change in source areas for Notikewin sediments. A change in sediment source could be substantiated by paleoflow determinations but this is not possible in subsurface core studies of this type. Furthermore, a change in paleoflow direction in Notikewin time is not anticipated according to the regional geology.

Young (1976) states that if the detrital monocrystalline quartz population of a sandstone is comprised of significant amounts of non-undulatory polycrystalline quartz

derived from mature sedimentary rocks then the method of Basu et al. (1975) is less effective. Furthermore, Basu's method indicates a primary ultimate source for quartz grains whereas it is realized that many quartz grains are from a secondary, sedimentary source. Therefore, the interpretation of the plotted quartz types is subjective.

Feldspar present may have been derived from a metamorphic source also in the Cordilleran highlands. The alternative is the Precambrian shield which lies a great distance to the northeast. Jardine (1974) indicates that this is a potential source of sediment in Notikewin time. Paleoflow determinations would aid in this interpretation but as mentioned are not possible in subsurface core studies.

5. CLAY MINERALOGY

Introduction

An investigation of the clay mineralogy of Facies A and B was undertaken to identify allogenic and authigenic clay constituents and interpret their effects on porosity and permeability of these potential reservoir rocks. Clay mineral identification was determined by X-ray diffraction techniques. However, X-ray analysis alone cannot be used effectively to distinguish between allogenic and authigenic clays although analysis of detrital clay rich (argillaceous) samples may indicate possible detrital clay types. Differentiation between allogenic and authigenic clays is determined by observing morphology and textural relationships under the scanning electron microscope (SEM). Clay mineral identification based on morphologies observed under the SEM is useful for many authigenic clay minerals. Petrographic study can also supplement these textural observations.

X-ray Diffraction

Method

A total of 5 samples were prepared for X-ray analysis: Sample 17 from Facies A, Samples 6 and 9 from Facies B and two argillaceous samples (see Appendix I for sample

locations).

Samples weighing 15 to 20 grams were reduced to a fine powder using a mortar and pestle. To the disaggregated sediment 150 to 200 ml of distilled water and a deflocculating agent was added. This mixture was placed in an ultrasonic bath for twelve hours. Ultrasonic vibration treatment achieves dispersal of the fine fraction. The suspension is then transferred to one litre cylinders and diluted with distilled water. After 225 minutes the top 200 ml is removed using a pipette. According to Stoke's Law this volume should contain <2 micron-sized particles. A suitable volume of clay rich suspension was then vacuum filtered through a 0.45 micron circular millipore filter pad. The resulting thin clay residue was mounted on glass slides by pressing the filtered material firmly onto a glass slide while still damp. This achieves a thin, roughly basally-oriented sample. Two slides were made for each sample.

One slide from each sample was scanned from 7° 2θ to 42° 2θ at a scanning speed of 1° 2θ per minute using CuK α radiation at 16 Ma, 45 Kv. The second slide was kept in an atmosphere of ethylene glycol for 2 hours at 60°C. Following glycoclation the sample was scanned again from 7° 2θ to 42° 2θ. The first sample was subsequently heated at 550°C for 2 hours and then scanned from 7° 2θ to 42° 2θ. These processes were not completed for each slide, only those which initially had suitable sharp peaks.

Results

Kaolinite

Kaolinite was identified in the untreated samples by intense peaks at approximately 12.55° 2θ (7.12Å) and 25.15° 2θ (3.56Å) representing the 001 and 002 plane reflections. Upon heating to 550°C for 1.5 hours these peaks collapsed (see figure 5.1) as the result of the formation of an amorphous meta-kaolin structure (Carroll, 1970). Glycolation had no effect on the kaolinite peaks, as expected. Other anticipated kaolinite peaks could not be resolved from the background noise of the diffractogram.

Chlorite

Chlorite could not be accurately identified on the diffractogram. The most intense diagnostic chlorite peak represents the 001 basal reflection (14.0Å) which occurs at less than 7° 2θ. Because the X-ray equipment used is limited to scanning 2θ ranges commencing at approximately 7° 2θ this chlorite peak could not be determined. The 002 plane reflection of chlorite at 12.50° 2θ (7.0Å) coincides with the 001 reflection of kaolinite. The only evidence of chlorite occurs at approximately 19.0° 2θ (4.70Å) which is the 003 plane reflection (figure 5.1). This peak collapsed upon heating to 550° C, similar to what is characteristic of kaolinite peaks after heat treatment. However, kaolinite does not exist at this d-spacing. Therefore, the identity of this peak is uncertain.

Q – Quartz
K – Kaolinite
I – Illite

X-ray diffractogram: Sample 23

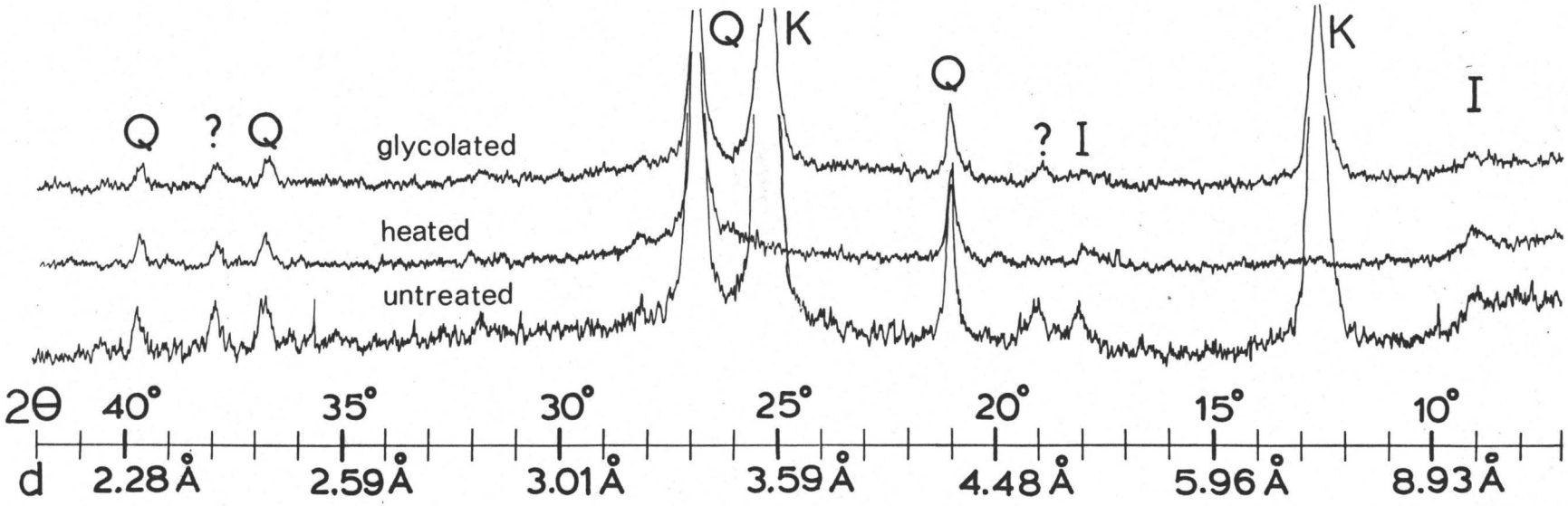

Figure 5.1

Illite

Illite did not produce sharp intense peaks on the diffractogram. However in the untreated samples it is identified based on broad diffuse peaks at 8.9° 2θ (10.04Å) and 18.0° 2θ (4.96Å) representing the 001 and 002 plane reflections (Thorez, 1975). Because the peaks are broad and diffuse, the illite is poorly crystallized (detrital 1Md polytype). The low intensity of peaks indicates the likelihood of relatively low concentrations of illite in the samples by semi-quantitative estimates (Vemuri, 1967).

No change of the nature or location of illite peaks occurred in the heated or glycolated samples. This indicates the absence of illite-mixed layer clay combinations.

Others

In addition to the clay mineral peaks there are also four quartz peaks at approximately 2.10° 2θ (4.25Å), 26.75° 2θ (3.34Å), 36.75° 2θ (2.47Å) and 39.63° 2θ (2.28Å). These represent the 100, 011, 110 and 102 planes respectively (Borg and Smith, 1969). These intense peaks result from sand grains reduced to less than 2 microns in the crushing process of sample preparation. The remaining peak at 37.87° 2θ (2.30Å) is unidentified. It undergoes no change upon glycolation or heating to 550°C. The d-spacing is not characteristic of any of the common clay minerals.

Scanning Electron Microscopy

Method

Ten samples were examined; three from Facies A (i.e. samples 17, 18 and 25) and seven from Facies B (i.e. samples 5, 6, 9, 15, 24 and 35). According to petrographic observations these samples have the highest porosity excepting samples 21 and 35. Core samples were broken to form specimens of approximately 1 cm^3 suitable for mounting on aluminum stubs with silver conductive paint. A gold coating 360 Å thick was applied to each sample using a Polaron E 5100 sputter coater. Finally, samples were examined with a Phillips 501B scanning electron microscope (with no energy dispersive analyzer (edax)).

Results

Kaolinite

Kaolinite occurs as vermicular stacks of pseudohexagonal plates, many of which are curved and intertwining, forming vermicular aggregates (plate 5-1). These vermicular aggregates are common in both Facies A and B. Kaolinite is the most common recognizable clay observed. However, it can be difficult to recognize because the morphology is not the "textbook example" of stacked booklets. Commonly, the Kaolinite booklets appear disaggregated and broken (plate 5-2a) b)). One must question this appearance. It is possible that this is detrital Kaolinite but a detailed origin is found in chapter 6. Kaolinite occurs as pore filling authigenic cement (plate 5-3). Pore filling aggregates reduce potential

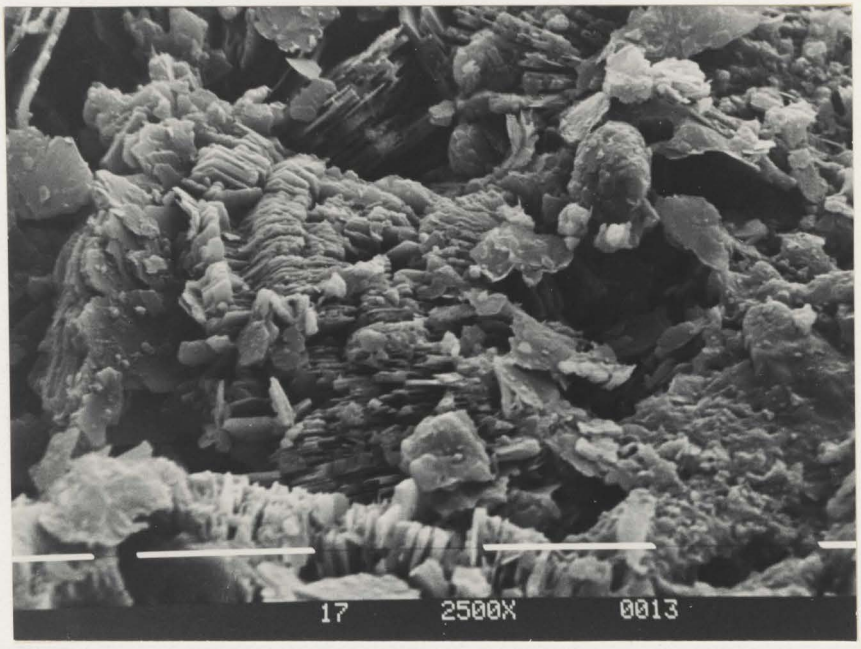

Plate 5-1 Kaolinite booklets curved and intertwining, forming worm-like appearance. Sample 17. Scale bar divisions equal 10 microns.

a)

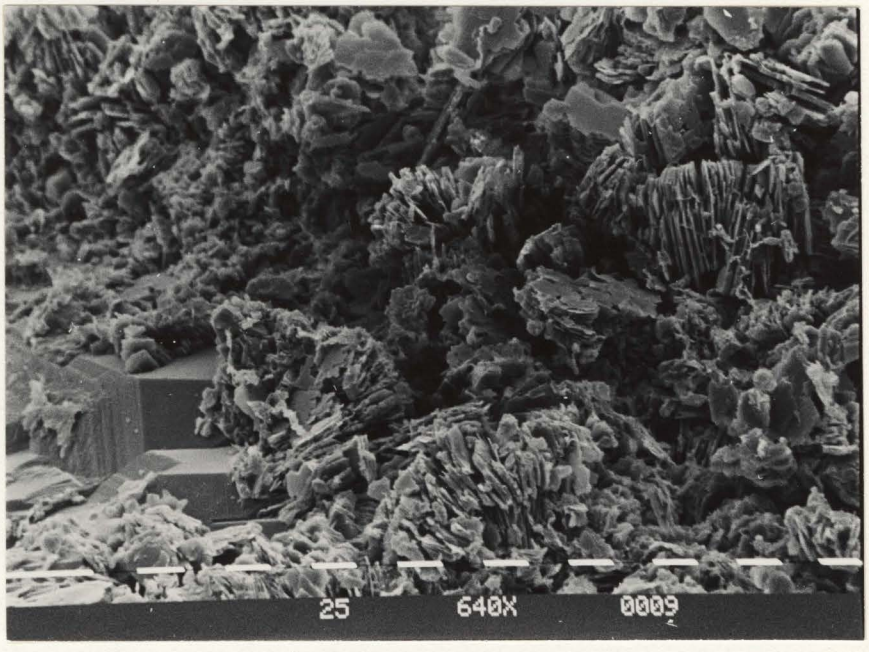

b)

Plate 5-2 Disaggregated and fragmented Kaolinite. It postdates quartz overgrowth in lower left of b). Samples 17 and 25 respectively. Scale bar equals divisions equal 10 microns.

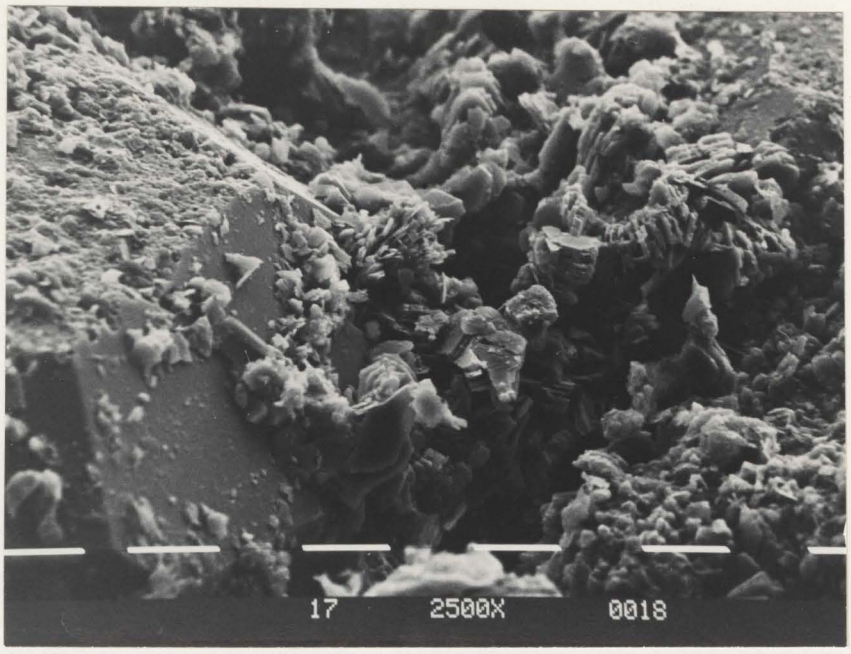

Plate 5-3 Kaolinite occurs as pore filling cement; here post-dating quartz overgrowth. Sample 17. Scale bar divisions equal 10 microns.

Plate 5-4 Idiomorphic plate-like chlorite flakes were the only observed chlorite morphology. Sample 6. Scale bar divisions equal one micron.

porosity to microporosity. This cement is commonly found on the surface of euhedral quartz overgrowths therefore post-dating overgrowth formation.

Chlorite

Individual idiomorphic plate-like crystals is the only chlorite morphology observed in Notikewin sands (plate 5-4). Of the four chlorite polytypes this morphology resembles the Ib polytype (Hayes, 1970). Facies B contained relatively more chlorite than Facies A. The chlorite plates are euhedral and intact signifying their authigenic origin. It occurs as a rim on detrital grains (plate 5-5). Although ubiquitous, chlorite is more concentrated in areas where there are no other authigenic growths. Where small quartz overgrowths or detrital material is present chlorite is recognized only as scattered individual flakes (plate 5-6) or in small clusters (plate 5-7). In several samples a mixture of predominantly authigenic chlorite and other unrecognized material completely occluded porosity (plates 5-8a)b)) by forming pore linings and pore bridgings. These chlorite textures can greatly affect permeability and interactions with pore fluids due to their great surface area.

Illite

Although illite was identified by X-ray diffraction methods it was difficult to recognize by scanning electron microscopy because no classic "textbook" morphologies were observed. Illite is tentatively identified in the conglomerate

Plate 5-5 Chlorite rims on detrital grains. Sample 9. Magnification on left side is 640X.

Plate 5-6 Chlorite flakes occur scattered and sparse, post-dating quartz overgrowths. Sample 18. Scale bar divisions equal 10 microns.

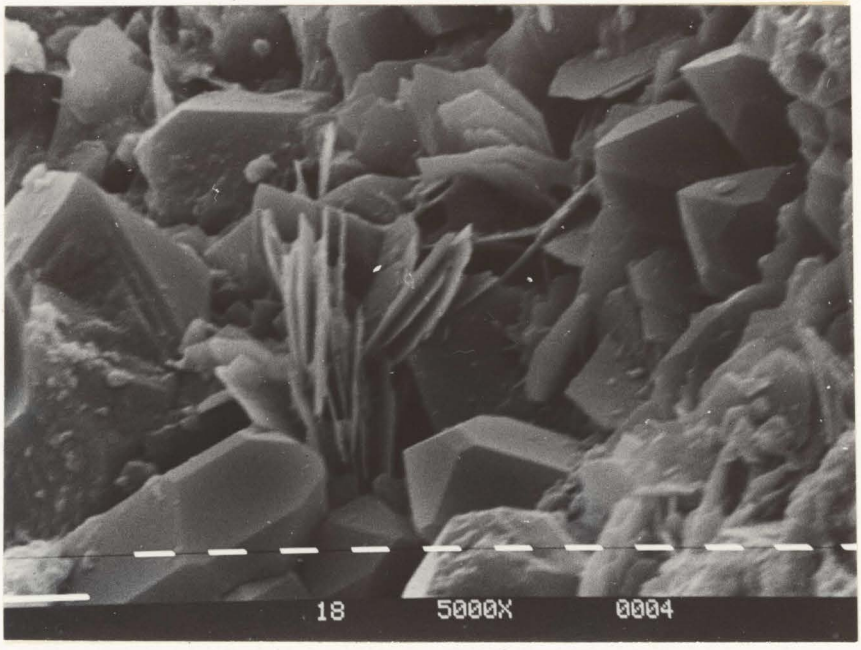

Plate 5-7 Small isolated cluster of chlorite flakes. Sample 18. Scale bar divisions equal one micron.

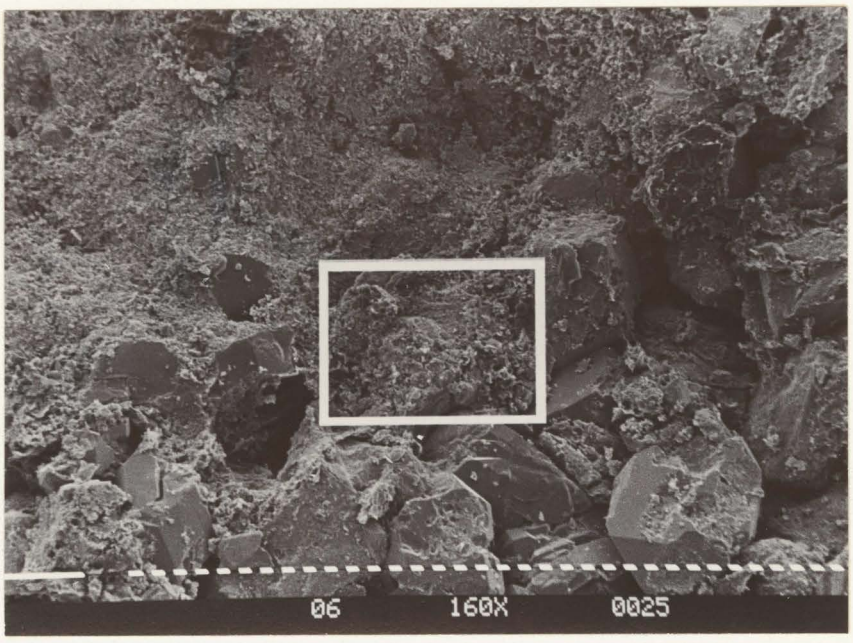

a)

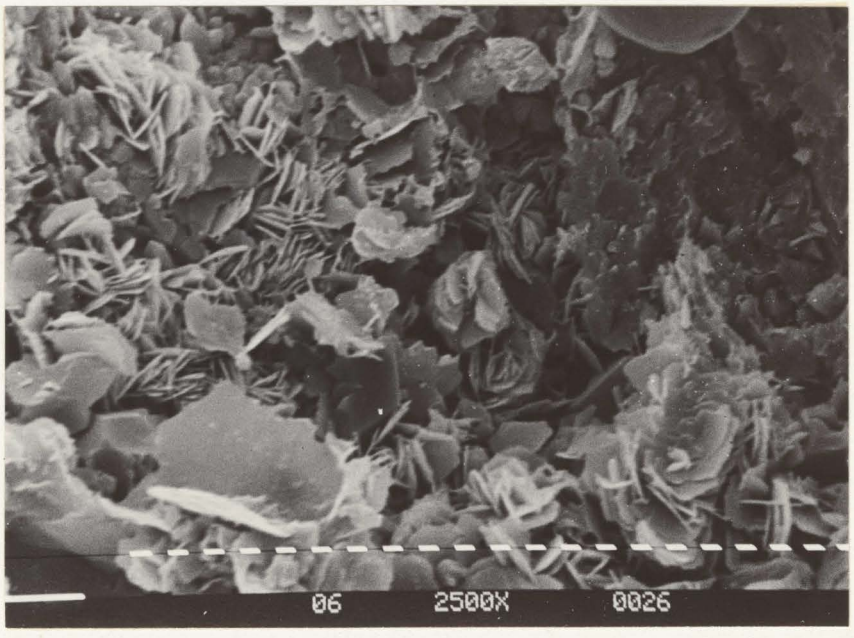

b)

Plate 5-8 Chlorite rims on detrital grains completely occlude porosity. The outlined area in a) is shown magnified in b). Sample 6. Scale bar divisions equal 10 microns and one micron respectively.

of Facies A (plate 5-9). It occurs in pore bridging and pore lining forms (plate 5-10). Also it forms a mudcrack-type morphology on the surface of pebbles (plate 5-11). One problem is that these morphologies and clay morphologies in general are not usually observed at magnifications lower than approximately 1250X to 2500X. However, these textures were observed at 160X or less. One exception is a possible illite morphology observed in plate 5-12. This shows the initiation of growth of delicate laths which indicates authigenic formation.

In addition to authigenic illite, detrital muscovite which has a similar structure (Grim, 1968), was observed (plate 5-13). Detrital clays and micas are difficult to recognize and identify on the SEM used in this study for two reasons: 1) with no energy dispersive analyzer attachment, compositions of unknown morphologies are inaccessible; 2) little documentation of detrital clay morphologies is present in the literature. For example plate 5-14 shows a very common microscopic landscape observed in many samples which contains no recognizable material, detrital or authigenic. Observations such as this are eluded in most texts in favour of well formed, decisively authigenic examples.

Discussion

In general the observed clay mineral assemblage is in accord with Carrigy and Mellon (1964). Table 5.1 relates the numbered samples to the clay types identified by X-ray

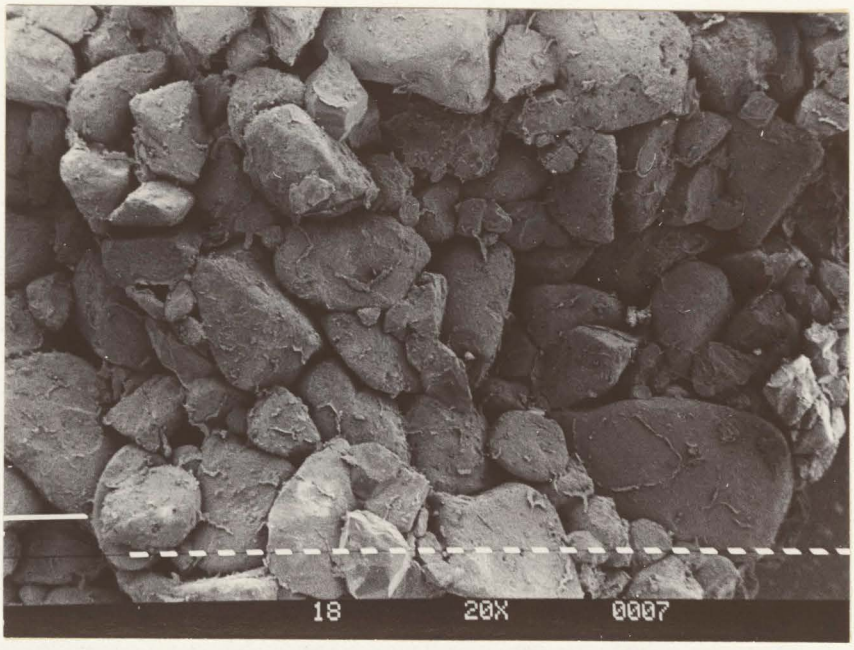

Plate 5-9 High porosity and minor illite clay of Facies A conglomerate. Sample 18. Scale bar divisions equal 100 microns.

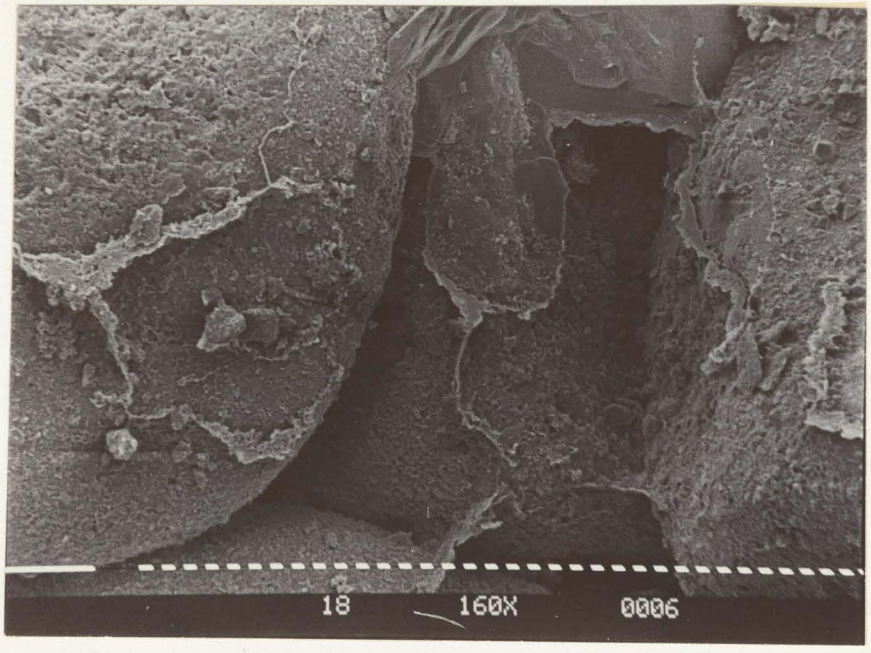

Plate 5-10 Pore bridging and pore lining illite in conglomerate. Sample 18. Scale bar divisions equal 10 microns.

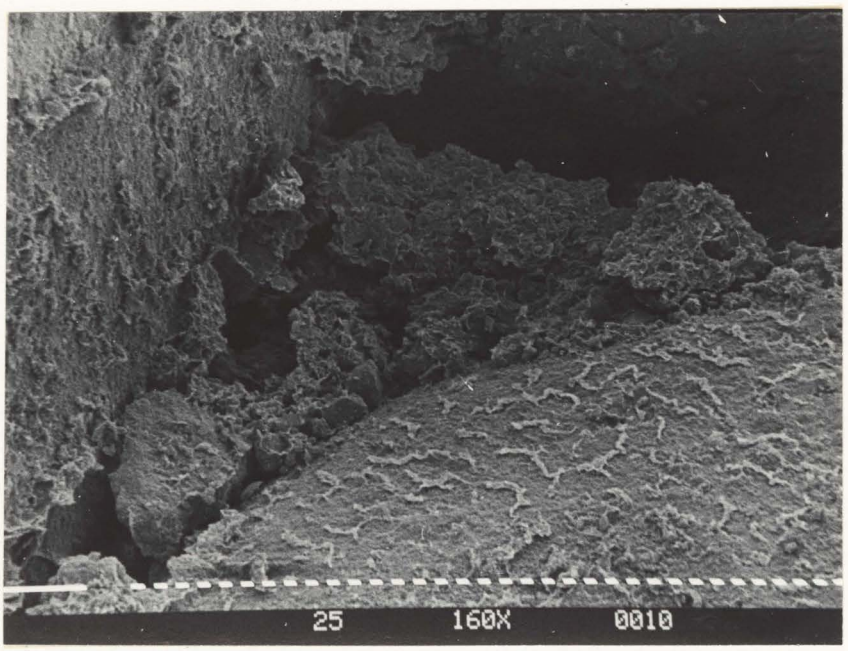

Plate 5-11 Mudcrack type illite morphology on detrital chert grain. Sample 25. Scale bar divisions equal 10 microns.

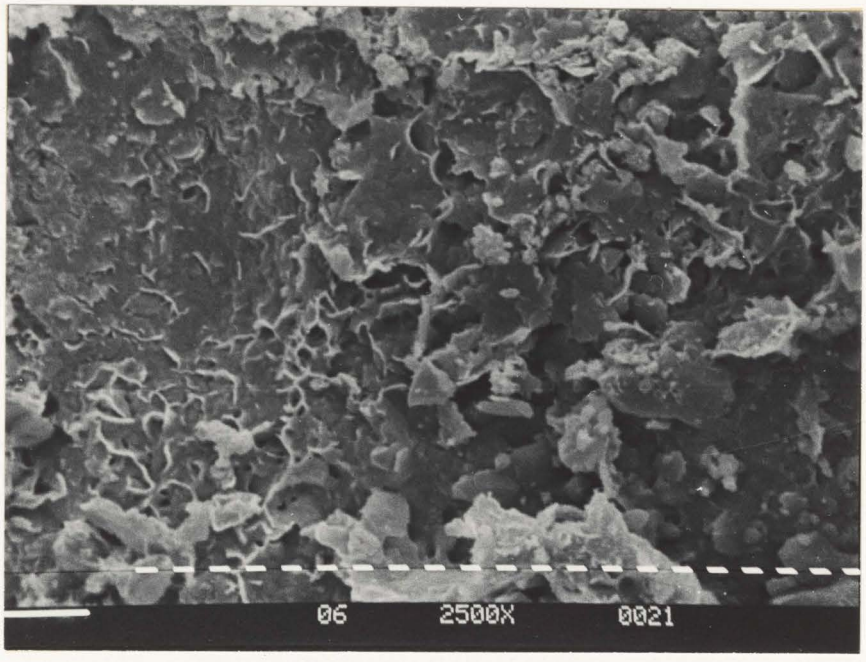

Plate 5-12 Possible illite morphology (lower left). Sample 6. Scale bar divisions equal one micron.

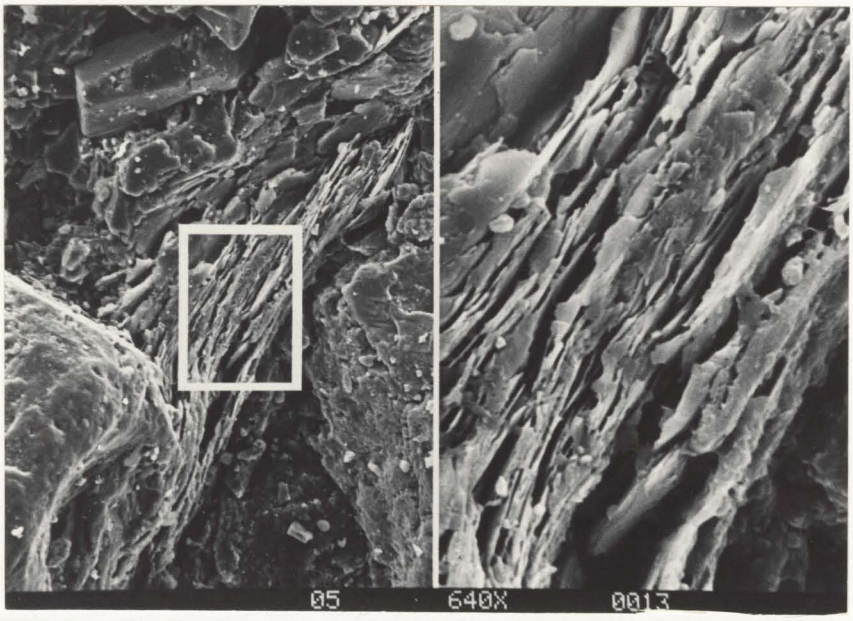

Plate 5-13 Detrital muscovite bent between grains due to compaction. Sample 5. Magnification on left side is 640X.

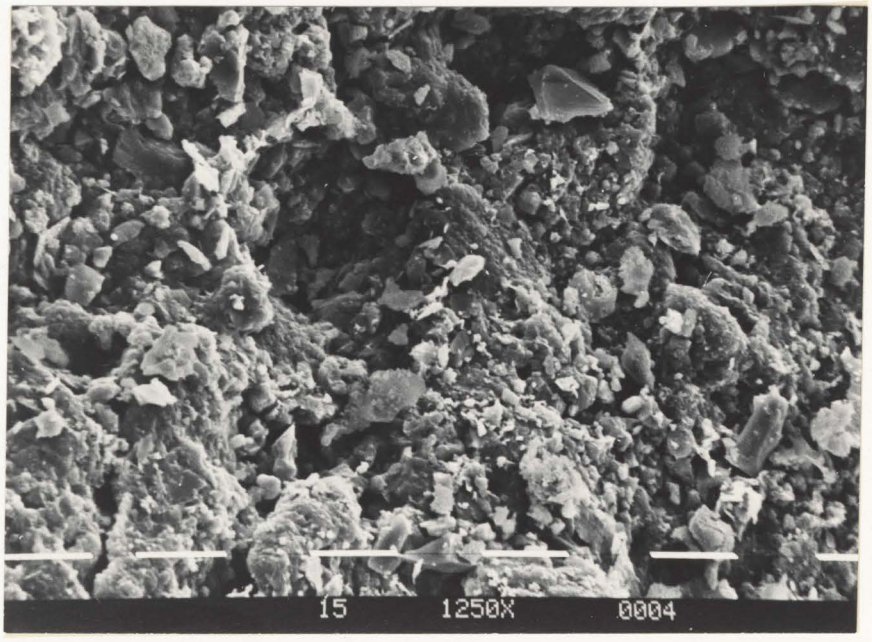

Plate 5-14 Very commonly observed microscopic landscape containing no identified material (based on morphology) Sample 15. Scale bar divisions equal 10 microns.

Table 5.1 Summary of clay types identified by scanning electron microscopy and X-ray diffraction

	X-RAY DIFFRACTION*		SCANNING ELECTRON MICROSCOPY		
SAMPLE	KAOLINITE	ILLITE	KAOLINITE	ILLITE	CHLORITE
06	X	X	-	-	X
09	X	X	-	X	X
15	not examined		X	-	-
17	X	X	X	-	-
18	X	X	-	X	X
25	not examined		X	-	-
34 (argill)	X	X	not examined		

*chlorite could not be accurately identified by X-ray methods

diffraction and scanning electron microscopy found therein. Some discrepancies become apparent upon examination of this table. For example, in sample 06, Kaolinite and illite are recognized peaks on the X-ray diffractogram but were not recognized in the scanning electron microscopy of the same sample. Therefore, this suggests that although Kaolinite and illite are present perhaps their morphology as viewed under the SEM was not recognizable. However, it is possible that the recognizable morphologies were present but not encountered upon examination.

To aid in determining the detrital components of clay mineralogy, a very argillaceous sample (no. 34) was examined by X-ray diffraction. Although Kaolinite and illite were found suggesting their existence as detrital clay components one could argue that the peaks resulted from authigenic clay mineral growth. However, this seems unlikely since the argillaceous samples have little or no pore space which would accommodate authigenic mineral growth. Therefore allogenic (detrital) Kaolinite and illite are common constituents of Notikewin Member sandstones in addition to observed authigenic cementing components. A discussion of the authigenesis of clay minerals during paragenesis is contained in chapter six.

6. DIAGENESIS

Introduction

As soon as a sediment is buried, diagenesis begins. The sediment will undergo various diagenetic processes as conditions change in the subsurface. There are five factors which influence the diagenetic history of a clastic rock (McDonald, 1979). These are:

i) original composition and texture of sands;
ii) pore fluid compositions;
iii) burial history in terms of pressure;
iv) burial history in terms of temperature;
v) time.

The sand, originally a non-equilibrium assemblage, seeks to adjust to changing physical and chemical conditions. The sequence of temperatures and pressures that the sediment has experienced can be estimated from known burial depths and geothermal gradients. Using these one can interpret the observed paragenetic sequence of mineral formation, and the progressive effects on porosity and permeability. One can then assess potential reservoir problems for production treatment and anticipate future plays in light of diagenetic

trends in the subsurface.

Burial Conditions

The Notikewin Member sandstones and conglomerates presently lie approximately 5000 ± 200 feet (1525 ± 60 metres) below the present erosional surface in the study area (assume regional dip is negligible). However, they once existed at greater burial depths and have undergone uplift and erosion in post-Cretaceous time. Magara (1978) suggests that the original burial depths can be determined by examining increased shale compaction (decreased shale porosity) with increased depth in order to determine an estimate of the thickness of erosion using acoustic velocity/sonic logs. The sum of the erosion thickness and the present burial depth approximates the maximum depth of burial of the sediment. Using this burial depth and an estimate of the geothermal gradient, an approximate maximum diagenetic temperature can be determined. These values are very subjective however, since higher (or lower) temperatures may have been attained only for geologically short periods.

Interval transit times are directly proportional to shale porosity values. If no erosion occurred, a plot of shale transit time versus depth extrapolated to the present surface would indicate a transit time of 200 microseconds per foot (Magara, 1978).

Figure 6.1 indicates approximately 2800 feet (853 metres) of erosion has occurred. This is in accord with

Figure 6.1 Approximate erosion thickness of 2800 feet (853 metres) using shale porosity from sonic/acoustic velocity logs (method after Magara, 1978).

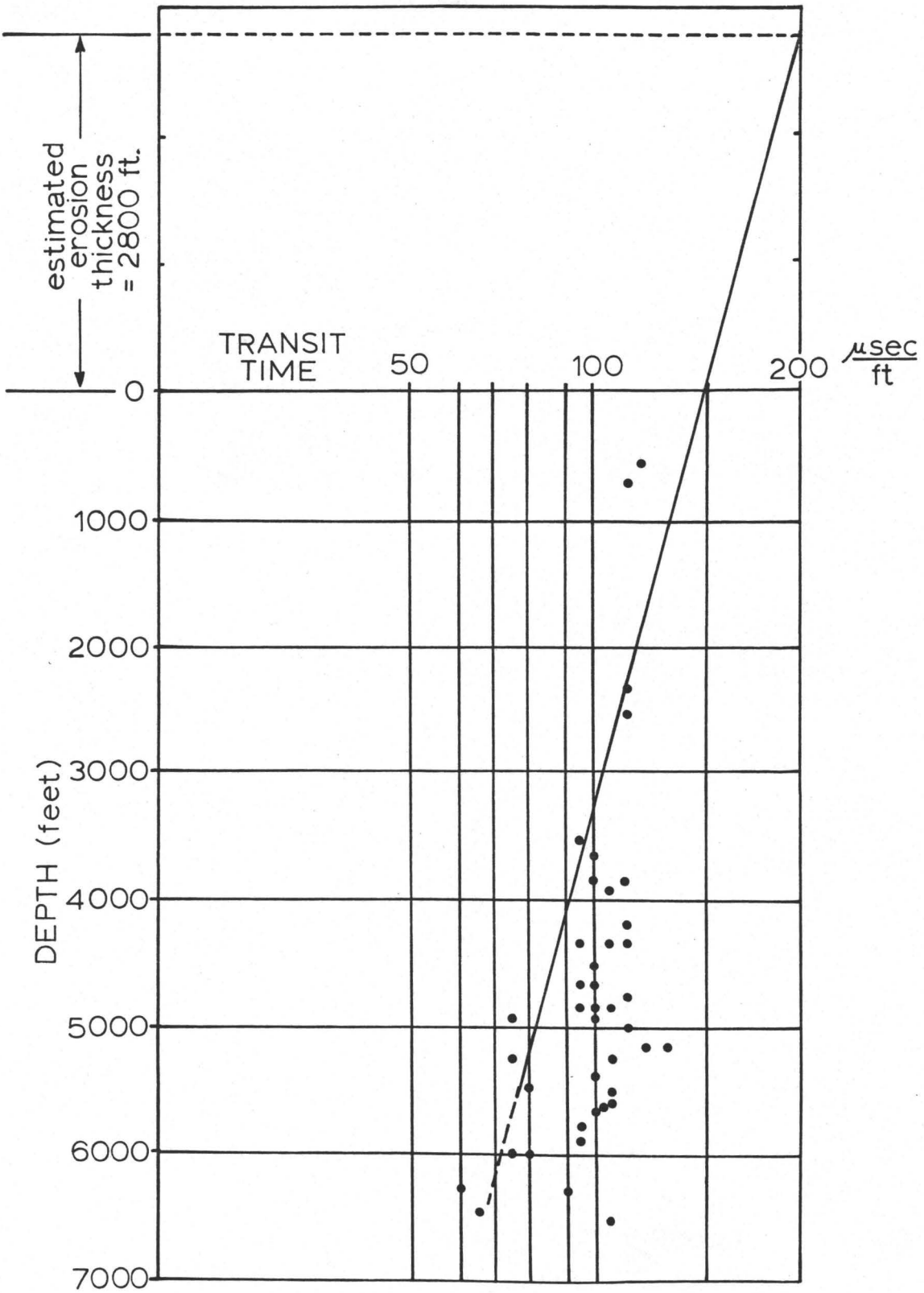
estimated erosion thickness = 2800 ft.
TRANSIT TIME
50
100
200
μsec/ft
0
1000
2000
3000
4000
5000
6000
7000
DEPTH (feet)

Magara's (1978) results which indicate an erosion thickness ranging from 1000 to 3000 feet (305 to 914 metres). Therefore the maximum burial depth is estimated to be 7800 feet (2377 metres) (i.e. 2800 feet (853 metres) + 5000 feet (1524 metres)).

The approximate burial temperature can be determined using an average geothermal gradient of 3°C ± 0.4/100 m. (1.7°F ± 0.1/100 ft.) (Magara, 1978) and the calculated maximum burial depth. The resulting inferred maximum burial temperature is 71°C ± 10 (160°F ± 50).

Alternatively, Fuchtbauer (1967) documents a plot of porosity versus depth of burial for sandstones which can be used to determine burial depths for the generalized cases of calcareous and quartz-rich sandstones. This method could not be applied to the Notikewin Member for two reasons:

1) the observed porosity of Notikewin sands is too low ($\lesssim$ 10%);
2) detrital composition is not favourable (i.e. not quartz-rich).

Other methods commonly in use to determine diagenetic temperatures include conodont colouration and vitrinite reflectence. Unfortunately these methods are outside the scope of this study. However, chlorite polytypes have been used to determine pre-metamorphic subsurface temperatures (Hayes, 1970). The chlorite polytype Ib_d, recognized by the scanning electron microscope study, does not persist above temperatures of 70°C to 80°C (158°F to 176°F) (Hoffman and Hower, 1979;

Hayes, 1970). Therefore, the existence of this chlorite polytype indicates a diagenetic temperature which is in agreement with the value determined by Magara's method.

Hoffman and Hower (1979) have determined relationships between clay mineral assemblages and diagenetic temperature in both sandstones and shales. However, the technique does not permit a precise determination of temperature when applied to the authigenic chlorite and Kaolinite assemblages of Notikewin Member sands.

Eodiagenesis

Mechanical Porosity Reduction

The term eodiagenesis, applied to clastic rocks, refers to the regime at or near the surface of sedimentation where the interstitial water chemistry is controlled by the surface environment (Schmidt and McDonald, 1979a). The mechanical reduction of porosity is the main process operating during eodiagenesis. Mechanical porosity reduction predominates over cementation to burial depths of approximately 3000 to 5000 feet (1000 to 1524 metres) after which chemical porosity reduction by cementation is paramount (ibid.).

Initially, mechanical porosity reduction occurs by grain slippage, rotation and ductile grain deformation (i.e. micas, see Plate 5-13). Visual evidence of mechanical porosity reduction by slippage and rotation is not found. However, these processes are associated with pressure solution which results in the generation of silica, formation of

sutured and concavo-convex grain boundaries (plate 4-19) and the resultant syntaxial quartz overgrowths during meso-diagenesis (plate 4-3).

Early Pore Fluid Chemistry

Ideally, in order to study the chemical reactions characterizing the diagenetic history of a sandstone, the geologist must determine the types and ranges of compositions of pore waters (Pettijohn, pg. 411, 1973). Pore waters originally in the sediment range from brackish to marine. As compaction increases, original pore fluids are replaced by fluids expelled from the adjacent shales.

Aerobic bacteria present near the sediment-water interface utilize available free oxygen and release CO_2 when consuming organic constituents in the sediment. As a result, the pH of pore fluids decreases from 8.0 to approximately 6.5 (Collins, 1975). Detrital carbonate, if accessible to pore waters, will buffer the pH thus maintaining it above neutrality. At depths greater than 0.5 metres below the sediment-water interface oxygen is no longer available. Anaerobic bacteria cause pore fluid pH values to become alkaline with pH approximately equal to 9.0 (Collins, 1975). If detrital carbonate survives to this burial depth it is now protected from further dissolution until later diagenesis. Organic matter which survives down to the anoxic conditions below 0.5 metres is destined to generate hydrocarbons at greater depth.

Early Clay Diagenesis

Although there are initial reactions between dissolved species in seawater and clay minerals in river water entering the sea (halmyrolsis), post-halmyrolitic reactions affect detrital clays before later stage diagenesis involving neo-formation and transformation. Early clay diagenesis takes place in the top few metres of accumulated sediment (Berner, pg. 185, 1971). At this time, excess bicarbonate not reacting to form carbonate, reacts with cation free clay containing K^+, Na^+ or Mg^+ by a reverse weathering process such as:

$$2K^+_{aq} + 2HCO_3^-{}_{aq} + 3Al_2Si_2O_5(OH)_4 \rightarrow 2KAl_3Si_3O_{10}(OH)_2 + SH_2O + 2CO_2$$

(Berner, pg. 181, 1971). Therefore some authigenic clay formation occurs to help remove excess HCO_3^- from rivers in the deltaic depositional environment. This has been hypothesized after experimental work by Mackenzie and Garrels (1966). However, the bulk of authigenic clay minerals form at greater depth in subsequent diagenesis. Experimental work by Whitehouse and Carter (1958) indicated that conversion of montmorillonite to illite and chlorite may take place in early diagenesis. This process may be inhibited by dissolved organics which block interlayer sites which would alternatively be available for cation exchange (Berner, pg. 184, 1971).

The boundary between halmyrolsis and early diagenesis is uncertain. Relative to later diagenesis this period is much less important to clay mineral authigenesis (Blatt et al.,

pg. 385, 1980).

Carbonate (siderite) Formation

In Facies D carbonate bands, tan brown in colour, are sideritic (recall plate 3-7 and 3-8). May (1967) also observed this in samples from the source wells coincident with this study (i.e. 10-1 and 10-24). Authigenic siderite has no stability field in marine sediments since Eh must be low and pS^{2-} must be high (Berner, pg. 199, 1971). Also, the iron concentration must be greater than five per cent of the calcium concentration. However, in non-marine settings anaerobic bacterial decay of organic matter forms low Eh and high PCO_2 with minimal H_2S formation. Therefore, siderite typically forms in poorly drained bogs or swamp environments which may be adjacent to the channel sandstones of Facies D.

Ironstone/sideritic concretions found in Facies C do not necessarily indicate a similar environment. The concretions may be post-depositional forming as a result uplift and exposure of marine beds to non-marine anaerobic ground waters (Berner, pg. 200, 1971).

Mesodiagenesis

Mesodiagenesis, as defined by Schmidt and McDonald (1979a), refers to the burial regime under strata that seal the interstitial fluids of the sandstone from chemical reagents at or near the surface. It is during mesodiagenesis that the bulk of porosity and permeability reduction occurs by overgrowth formation. Secondary porosity also forms in

this regime (ibid.).

Four textural stages of mesodiagenesis have been recognized (figure 6.2) (ibid.). This terminology will be used in this discussion.

Carbonatization

The formation of calcite cement and pore fillings is pervasive in the fluvial Facies D and sporadic in the chert conglomerates of Facies A. Some of the carbonate in the fluvial sands may be eogenetic but the carbonate cement in the conglomerate probably formed mesogenetically in the late immature to semi-mature stages. Evidence for this cementation occurring early in the paragenetic sequence is the high minus-cement porosity (35% to 40%). This early cementation lithifies the rock inhibiting mechanical compaction leaving individual grains scarcely in contact (recall plate 4-18). The presence of rare authigenic quartz overgrowths surrounded by carbonate cement suggests that the introduction of carbonate post-dates the immature mesodiagenetic stage although the two processes may be simultaneous (Dapples, 1979). The source of carbonate is principally from the dissolution of shell material (McDonald, 1979). The reprecipitation as cement is in response to a drop in CO_2 pressure due to the diffusion of CO_2 from organic decay upward through the sediment column.

Partial calcite replacement of plagioclase feldspar in Facies D is probably a mesodiagenetic feature (recall plate 4-12), the timing of which is uncertain.

Figure 6.2 Textural changes of porosity during mesodiagenesis indicating progressive burial (after Schmidt and McDonald, 1979a)).

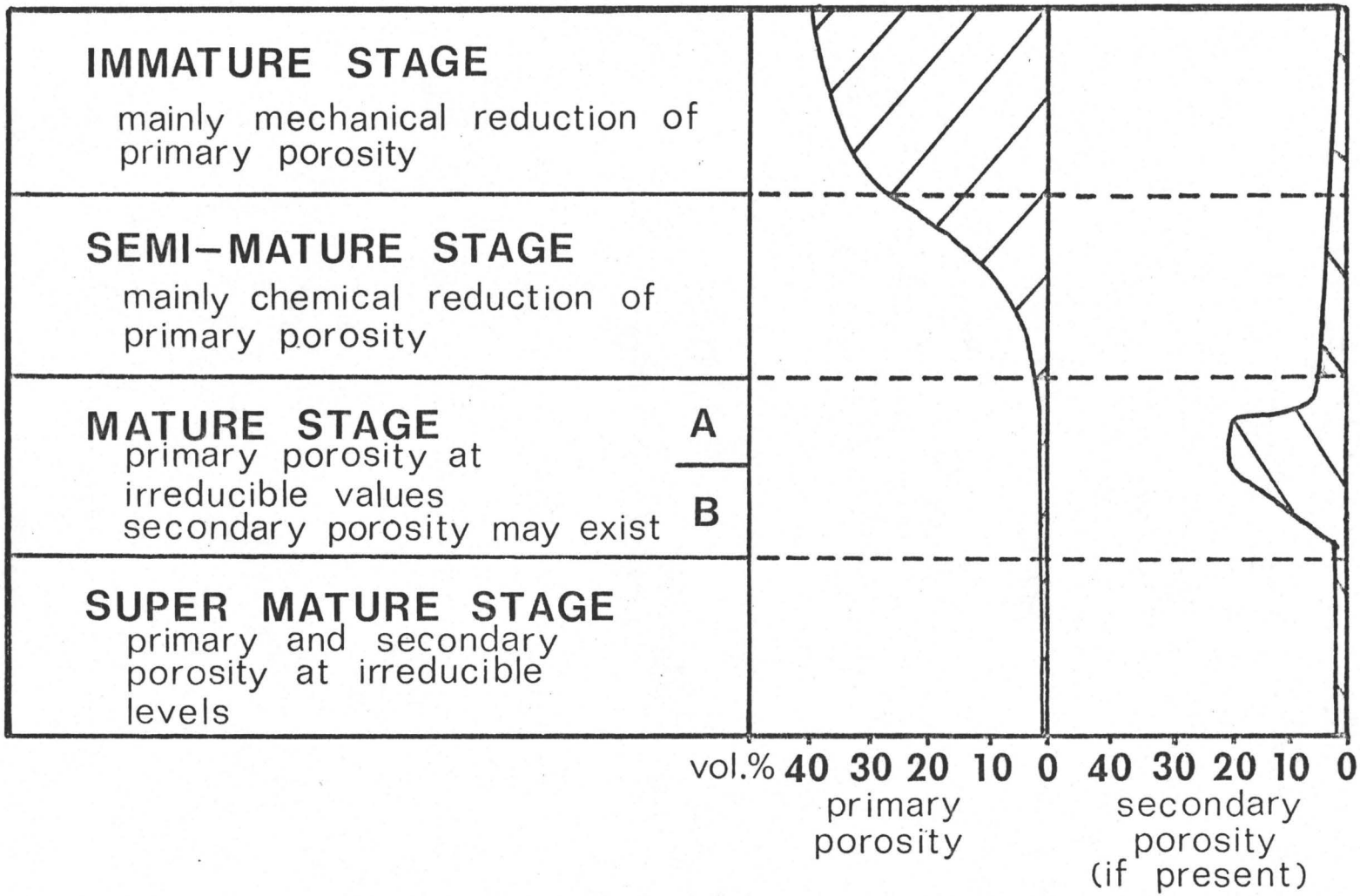
IMMATURE STAGE
mainly mechanical reduction of primary porosity
SEMI–MATURE STAGE
mainly chemical reduction of primary porosity
MATURE STAGE
primary porosity at irreducible values
secondary porosity may exist
A
B
SUPER MATURE STAGE
primary and secondary porosity at irreducible levels
vol.% 40 30 20 10 0 40 30 20 10 0
primary porosity
secondary porosity (if present)

An intriguing point is that the carbonate cement of Facies A conglomerate is regionally localized. It is confined to the 10-27 well in this study. In addition to lateral localization it is vertically localized within the conglomerate of a given well. Furthermore, in non-carbonate cemented conglomerates with excellent porosity there is no relict carbonate. Indeed this indicates that there has been local protection of the deposits either from the cement precipitating fluid or from the decarbonatizing acid porewater causing dissolution. The latter possibility will be discussed later (see decarbonatization).

Quartz Overgrowths

Deposition of this cement occurs in the semi-mature mesodiagenetic stage. At this time pore fluids are oversaturated with respect to silica causing precipitation out of solution, nucleating on detrital quartz grains (Collins, 1975). This would occur at or near the maximum depth of burial (G.V. Middleton, personal communication).

There are several postulated sources of silica. In the Notikewin Member it is probable that silica was derived from pressure solution due to compaction, especially in the chert conglomerate. This is suspected on the basis of the many concavo-convex and sutured contacts between chert grains and the excellent development of interstitial quartz overgrowths. Clay minerals surrounding grains may have a catalytic effect on pressure solution at points of contact (Pettijohn

et al., pg. 425, 1973).

In part, silica may be derived from the dissolution and hydrolysis of feldspar grains (plate 6-1) by water containing carbon dioxide according to the following equation:

$$2KAlSi_3O_8 + 2H^+ + 2HCO_3^- + 9H_2O \rightarrow$$
$$Al_2Si_2O_5(OH)_4 + 4H_4SiO_4 + 2K^+ + 2HCO_3^-$$

Alternatively, Hoffman and Hower (1979) indicate that feldspar decomposition may contribute to clay formation in addition to forming quartz according to the reaction:

smectite + K-feldspar → quartz + illite + chlorite.

The balance of the silica required to produce overgrowths was probably derived from the diagenetic change of mixed-layer smectite-illite to pure illite in shales proximal to the Notikewin sands (Blatt et al., pg. 344, 1980).

Where sufficient space is available, quartz overgrowths are observed to totally occlude porosity, particularly in Facies B (plate 6-2). In addition, overgrowth development appears to post-date development of some unidentified authigenic clay constituents (plate 6-3).

Decarbonatization

The relative timing of carbonate cement dissolution in the Notikewin Member is uncertain. It is probably localized and may occur simultaneously with carbonatization in adjacent areas. Mesogenetic decarbonatization to produce secondary porosity probably occurred during the entire mesodiagenetic history of the Notikewin Member but is pre-eminent in the semi-

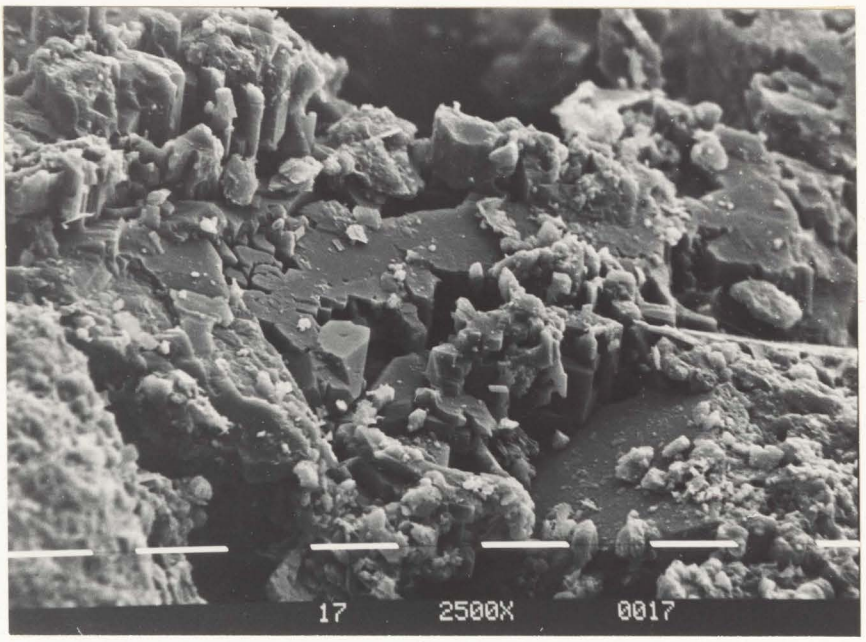

Plate 6-1 Feldspar exhibiting evidence of dissolution. Sample 17. Scale bar divisions equal 10 microns.

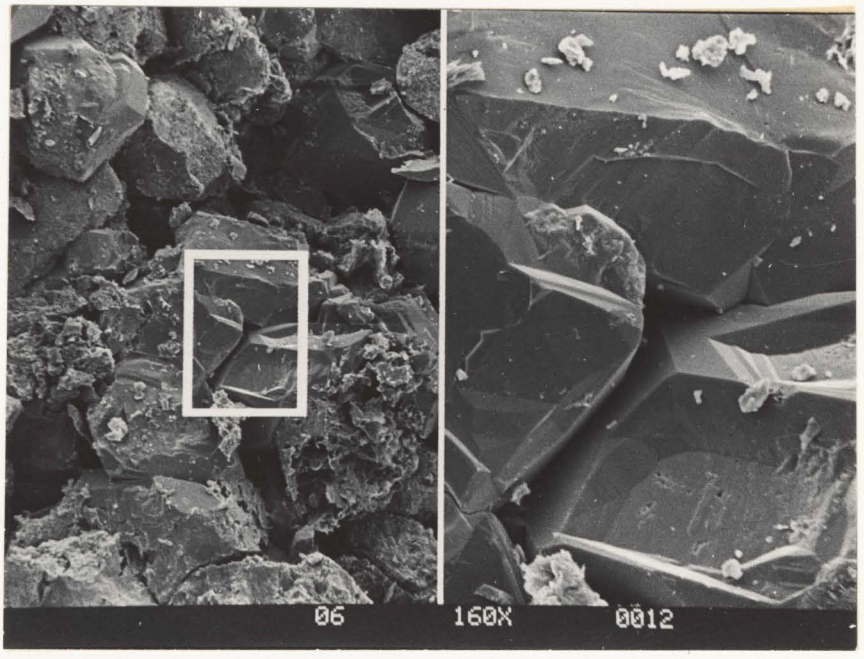

Plate 6-2 Quartz overgrowths completely occluding porosity. Sample 6. Magnification on left side is 160X.

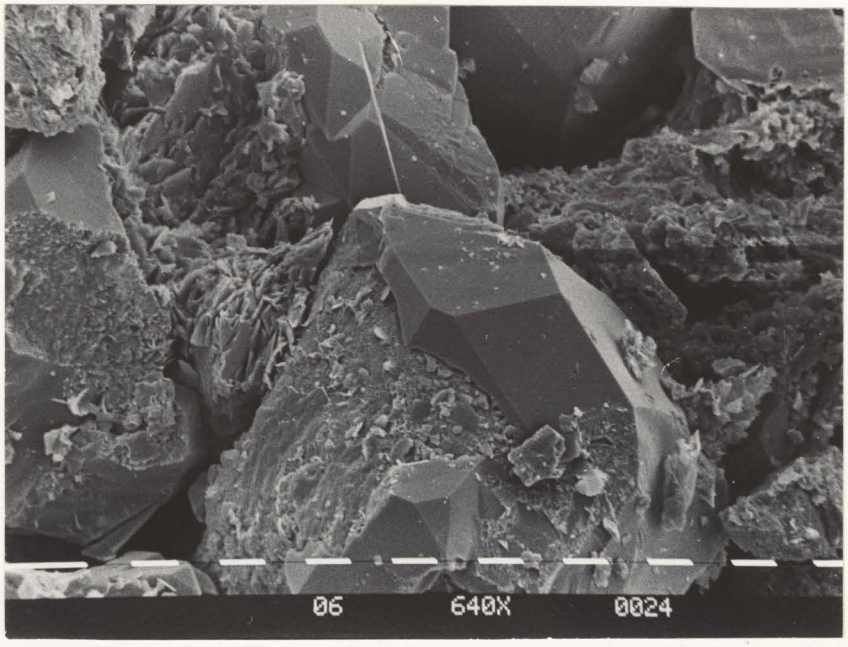

Plate 6-3 Development of quartz overgrowth on detrital grain. Minor evidence of authigenic growth observed on grain pre-dating quartz overgrowth. Sample 6. Scale bar divisions equal 10 microns.

mature to mature stages. Dissolution of carbonate material is a result of catagenesis (50°C to 200°C, 122°F to 392°F) of organic material in source rocks (Hunt, 1979). At this time the oxygen-containing groups in organic matter undergo thermocatalytic decomposition to yield CO_2 and H_2O (ibid.) producing acidic conditions conducive to carbonate dissolution. Another source of CO_2 is the decarboxylation of COOH but the products are utilized by microbes or dissolve as HCO_3^- (ibid.). H_2S formed by the thermal alteration of organic sulphur compounds also enhances the mesogenetic dissolution of carbonate. The decomposition of limestone and/or dolomite is not anticipated to be a source of CO_2 since carbonates are not stratigraphically close by. Tissot et al. (1974) found that the release of mesogenetic CO_2 occurs over a wide range of diagenetic temperature/time exposures. Therefore, carbonate dissolution may occur continually throughout the diagenetic history of the sediment.

Illite

Illite found in the Notikewin Member has two possible origins. Firstly, the majority of the illite present in the Notikewin Member resulted from the recrystallization of pre-existing detrital (2M polytype) illite. The incomplete recrystallization causes the X-ray diffractogram peaks to be low amplitude, broad and diffuse (as observed, Chapter 5). This recrystallization or transformation process involves agradation of the allogenic illite which regularizes the crys-

tal lattice by addition of K^+ ions from alkaline, cation rich pore solutions (Millot, 1970). The source of K^+ ions may be from feldspar dissolution (plate 6-1) in Facies D or other adjacent sands.

Secondly, a minor amount of the illite is the product of neoformation (i.e. direct precipitation from pore fluids) based on the rare delicate morphologies observed under the SEM.

Alternatively, the tentative identification of this clay as illite may be in error. One possibility is that the clay may be drilling mud (montmorillonite) residue. The high porosities and permeabilities (100 md to 1 darcy) in Facies A might permit considerable infiltration of drilling fluids. However, the high birefringence and textural relationships of the clay rule out this possibility (plate 6-4a)). Plates 6-4a) and b) illustrate the textural relationships of illite (recall also plates 5-10 to 5-12). Because illite exists both between grain contacts and around quartz overgrowths (plate 6-4, see arrows) the original illite may have pre-dated compaction and later recrystallized with some authigenesis post-dating authigenic quartz overgrowth formation.

Chlorite

Apart from minor neoformation of illite, the timing of which is uncertain, authigeneic chlorite is the only stable clay mineral present in the Notikewin Member. This indicates that it was probably the last authigenic mineral to form and

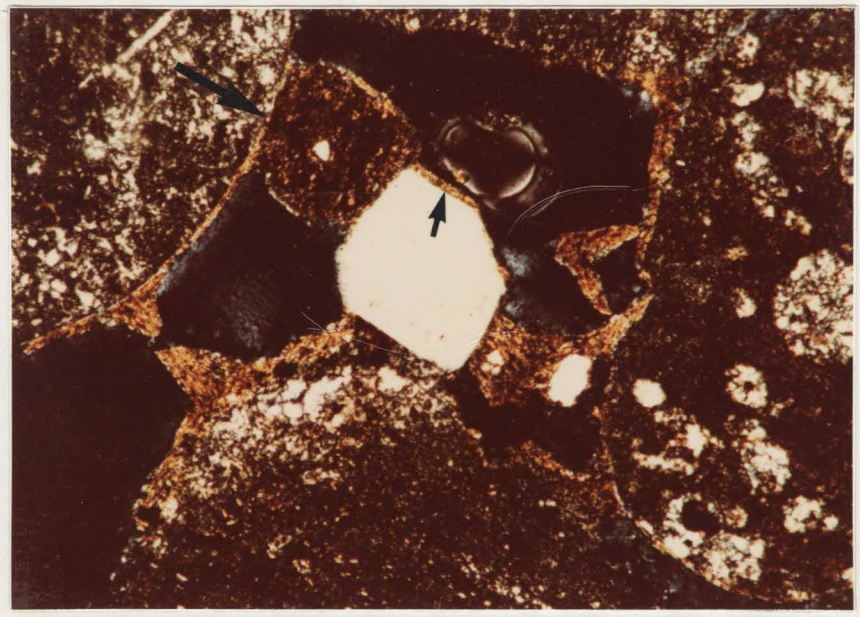

Plate 6-4a) Authigenic illite on perimeter of quartz overgrowth (arrow). Pore lining and pore bridging illite also present. Note clay rim between detrital grains (arrow). Sample 17. Magnification 63X. XN.

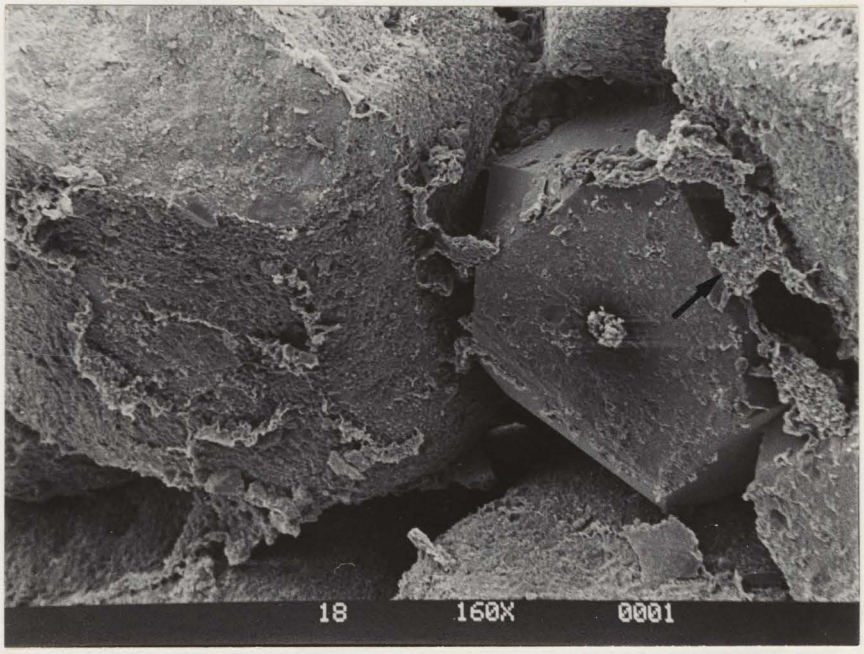

Plate 6-4b) Similar relationships to a) as viewed under the scanning electron microscope. Note authigenic illite around quartz overgrowth (arrow). Magnification 160X.

was in equilibrium with the final pore fluid composition. Plate 5-7 indicates that chlorite post-dates quartz overgrowth formation. Chlorite is a common authigenic constituent in clastic rocks containing rock fragments. In the Cretaceous sandstones of Alberta Carrigy and Mellon (1964) commonly found chlorite to be an early diagenetic cement which is contrary to observations in the Notikewin Member made by this writer.

The diagenesis of chlorite polytypes has been studied in detail by Hayes (1970). The initial diagenetic chlorite polytype, Ib_d forms at relatively low temperature. With increasing burial and associated temperature increased crystallization and ordered stacking produces the Ib polytype. Recall that the Ib_d polytype cannot persist above 80° (Hayes, 1970). Unfortunately, the detailed chemistry of the authigenic chlorite produced (Fe versus Mg composition) was not determined. As a result, stability diagrams involving chlorite are used for generalization only. The only certainty is that the final composition of pore fluid chemistry remained in equilibrium with chlorite since it shows no signs of instability.

Kaolinite

From X-ray analysis of argillaceous samples it was determined that kaolinite was in part, allogenic. However vermicular booklets indicate authigenic (neoformative) origin also.

Corroded detrital feldspar is commonly associated with

kaolinite authigenesis (Shelton, 1964). However, corroded feldspar observed under the SEM was "clean", with no associated authigenic kaolinite. Furthermore, it seems unlikely that the minor amounts of feldspar in Facies B and absence in Facies A could account for the amount of kaolinite observed. Abundant feldpsar is present in the fluvial Facies D but is inaccessible to pore waters due to carbonate cementation. Therefore, the kaolinite developed from reactants outside the immediate area of the Notikewin sandstone and conglomerate.

Cation poor, alumina enriched, acidic pore waters are favourable for kaolinite neoformation (Keller, 1970). If cation concentration increases due to poor circulation of pore water kaolinite neoformation will terminate.

The abraded, imperfect nature of the kaolinite booklets (recall plates 5-1 and 5-2) is questioned. This abraded appearance might be anticipated if the kaolinite was transported, signifying an allogenic origin. However, because the booklets are pore-filling around quartz overgrowths (plate 5-3), they post-date quartz authigenesis confirming a neoformative origin. Therefore, kaolinite was <u>not</u> in equilibrium with the most recent pore fluid in the sediments of the Notikewin Member.

<u>Changes in Pore Fluid Chemistry</u>

Ideally, in order to infer the pathway of changing chemical composition of pore fluids one needs two critical

compositions; the initial composition (seawater) and the present composition observed in the reservoir rock.

The composition of seawater is known. Unfortunately fluid analysis of formation waters was not available at the time of writing. Hitchon et al., 1971 have summarized the major and minor chemical components in pore waters of numerous oil and gas fields in the Western Canada Sedimentary Basin. Their data do not include the Kaybob field where this study is located, but they do indicate the general range of probable water composition. As a result, one can make some inferences about the path of porewater compositional changes based on the presence of certain clay minerals, their morphologies and inter-relationships starting from an original pore water composition of seawater.

The seawater pore fluid composition is indicated on figures 6.3, 6.4, 6.5 and 6.6 (data obtained from Blatt et al., pg. 224, 1980). The stability boundaries on these diagrams were calculated for 25°C but are still useful as a guide for mesodiagenetic temperature conditions of 70°C to 80°C. From this starting point the following pathway has been inferred.

An increase of orthosilicic acid (H_4SiO_4) moves the pore fluid composition toward quartz saturation at 10^{-4} moles/litre. At this time, which is approximately at the maximum burial depth, quartz overgrowths form. The pore fluid never falls to H_4SiO_4 concentrations below this value since overgrowths are observed to be in equilibrium with the fluid.

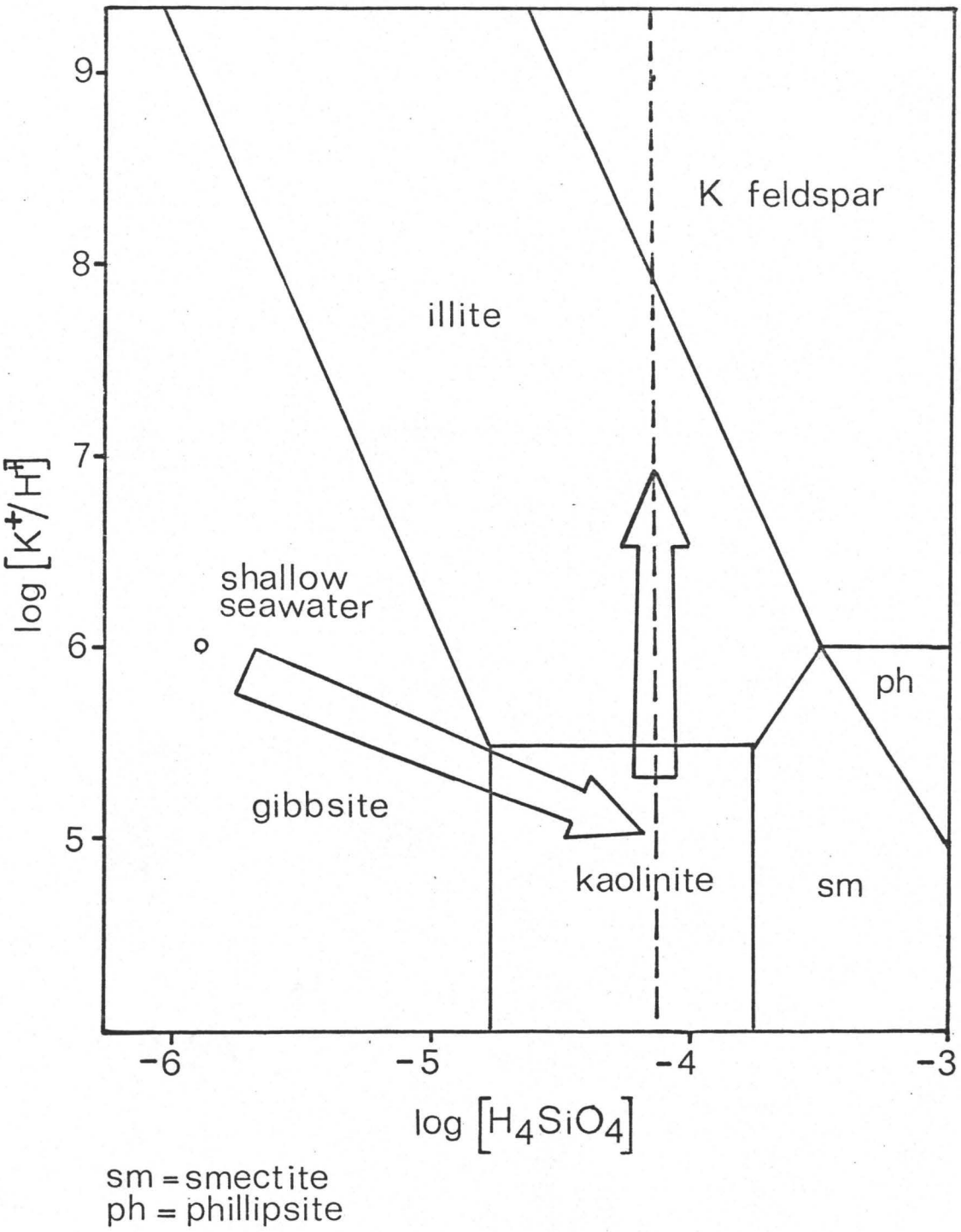

Figure 6.3 The arrow indicates the changing chemical composition of pore fluids first reaching quartz saturation forming quartz overgrowths. Kaolinite neoformation occurred with waters later becoming aggressive toward Kaolinite forming illite transformation and neoformation (after Drever, pg. 102; Blatt et al., pg. 262, 1980).

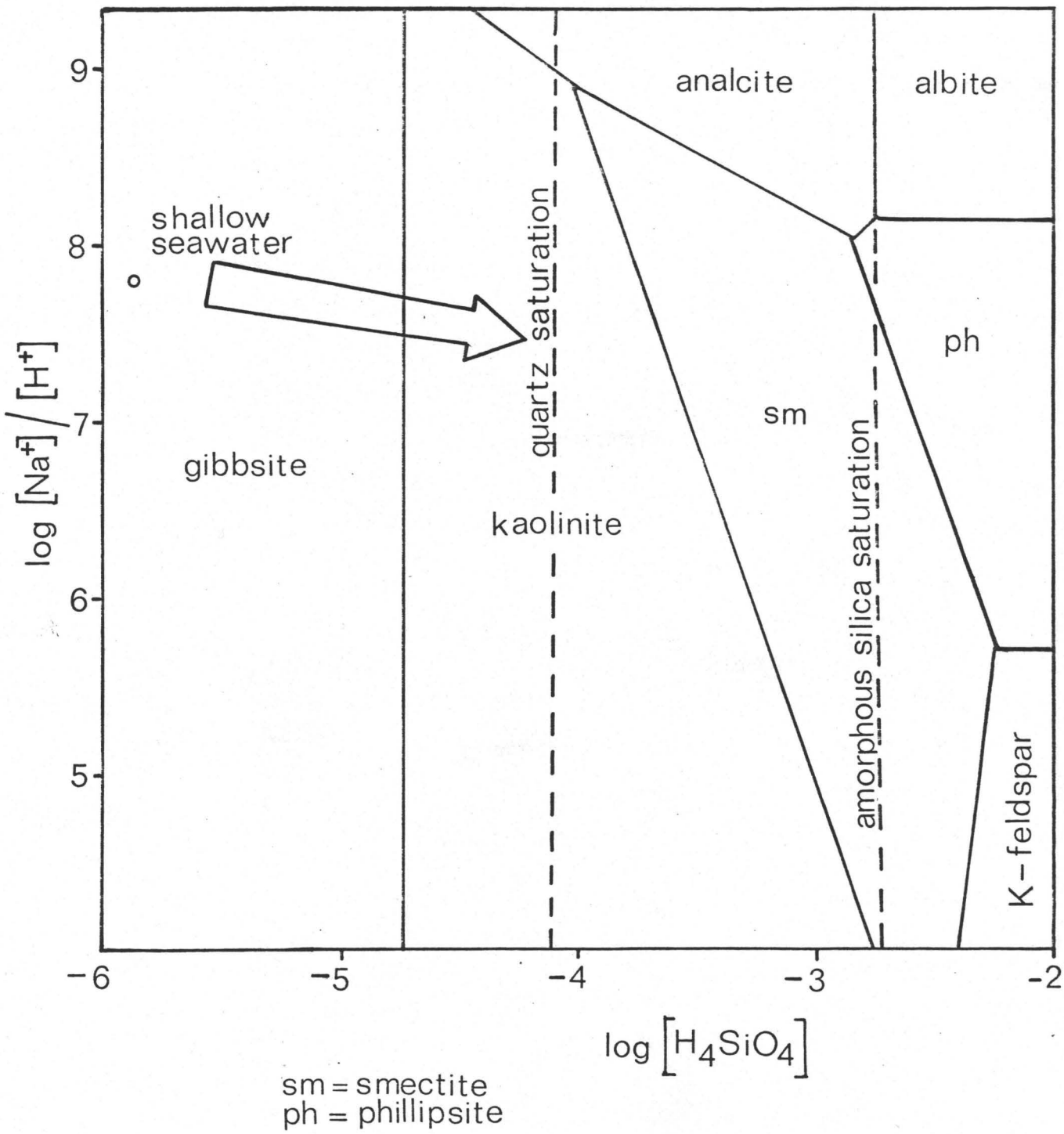

Figure 6.4 With increasing burial pore waters become rich in Na^+ up to 1 to 3 times its concentration in sea-water (after Drever, pg. 102, 1982).

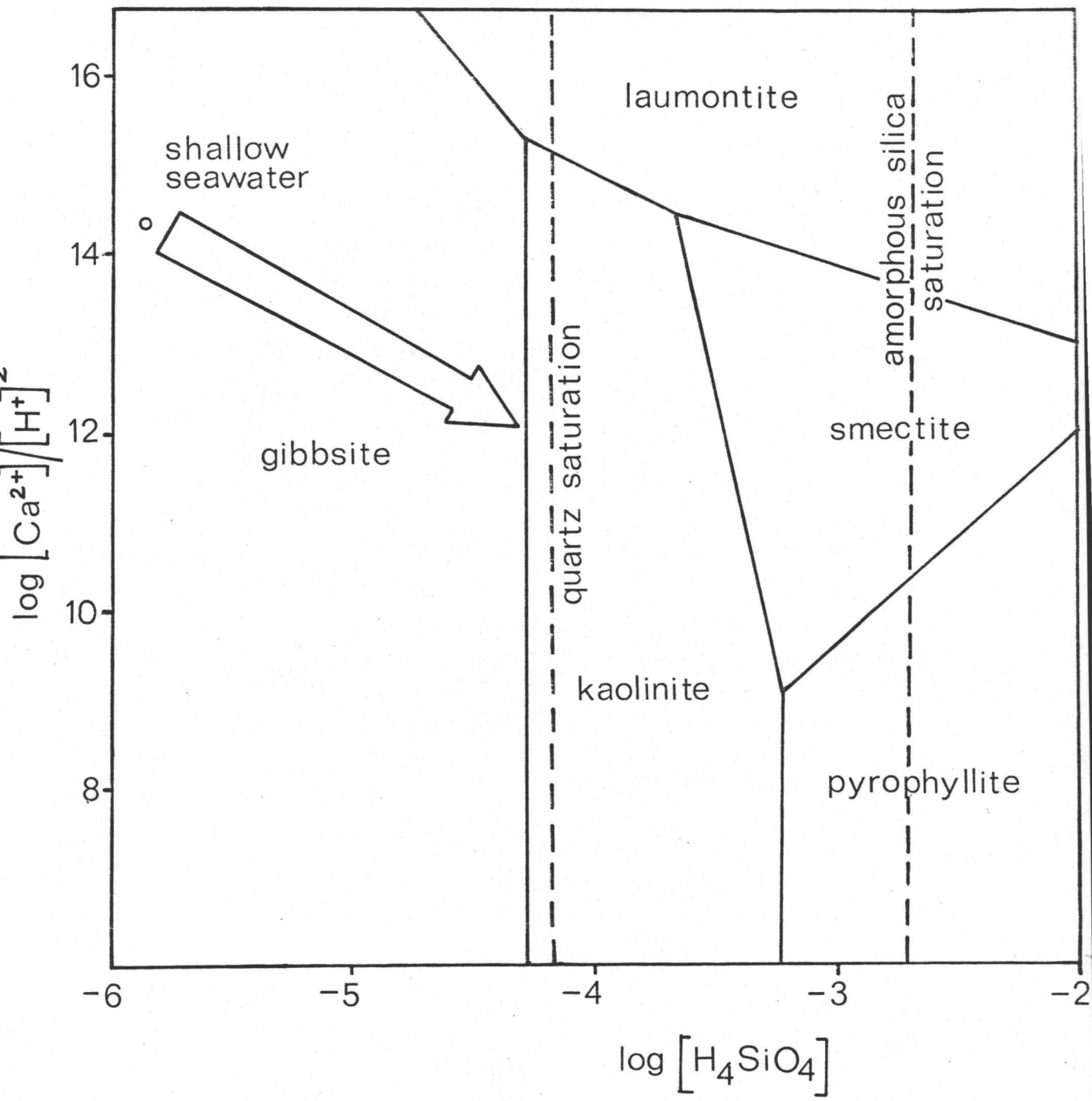

Figure 6.5 Calcium ions may be used early in the diagenetic history resulting in carbonate cementation and depletion of Ca^{2+}. The trend of the path is unknown once quartz saturation is reached (after Drever, pg. 104, 1982).

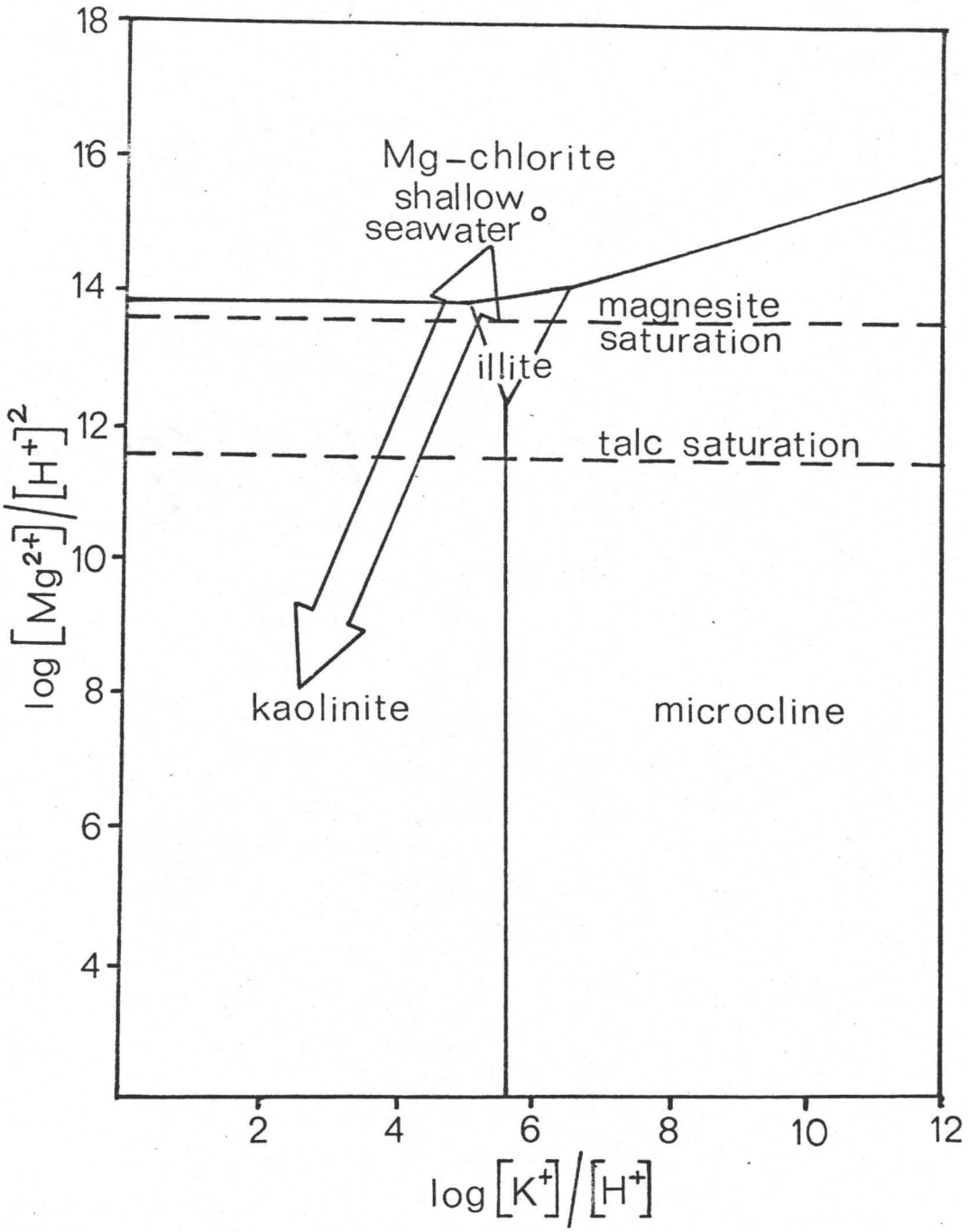

Figure 6.6 Chlorite is initially stable in seawater. It subsequently forms Kaolinite after the formation of quartz overgrowths. Later, Kaolinite becomes unstable as the Mg^{2+} activity increases and chlorite forms authigenically (after Helgeson, pg. 41, 1969b)).

Although montmorillonite is not observed in the Notikewin Member it is possible that it formed during progressive burial and subsequently became unstable. Montmorillonite disappears at approximately 80°C to 130°C corresponding to burial depths of 2666 metres (8747 feet) to 4333 metres (14200 feet) (Ghent and Miller, 1974). The burial temperature of 70°C to 80°C calculated for the Notikewin Member may be sufficient to break down montmorillonite, if present. The products of this breakdown may combine to form chlorite which will be discussed later.

Following the formation of quartz overgrowths kaolinite neoformation occurs. Kaolinite is known to post-date the quartz overgrowths based on textural evidence observed under the scanning electron microscope (recall plate 5-3). According to Hitchon et al. (1971) the pore fluids should be enriched in cations, particularly Na^+ and Cl^-, in the order of three times their concentrations in seawater. Therefore a problem comes to light. How does one explain the formation of kaolinite at a time when pore fluids should be cation enriched? Kaolinite usually forms in freshwater or at least in water relatively depleted of cations. There are two possible explanations for the observed formation of kaolinite at this time:

1) the sediment was exposed to freshwater;

2) waters were locally depleted in cations.

Possibility 1) is highly unlikely. The depth of burial of approximately 2377 metres (7800 feet) would rule out the pos-

sibility of the introduction of freshwater at such depth.

The second possibility is more feasible. The difficulty lies in explaining why cations are depleted locally and where the cations have gone. Answers to these questions are not known. Facies A, due to its high porosity and permeability (1 darcy) may have acted as a conduit for pore fluids in the subsurface which may have introduced fluids of varying compositions to the sediment at high rates. This may be related to the anomalous appearance of kaolinite since cations may be given up to form cation-rich clay minerals in another laterally adjacent formation with the depleted waters moving rapidly through the Notikewin Member porous sediments.

Chlorite is the last clay mineral to form authigenically (figure 6.6). Chlorite in the Notikewin Member forms at the expense of kaolinite which is observed to be dissolving and therefore unstable (plates 5-1, 5-2 and 5-3). The reaction is:

$$3Al_2Si_2O_5(OH)_4 + 10Mg^{2+} + 9H_2O \rightarrow 2Mg_5Al_2Si_3O_{10}(OH)_8 + 14H^+ + 2Al^{3+}$$

(Helgeson, 1969a)). The observation that kaolinite and chlorite do not usually occur together was also made by Ghent and Miller (1974). For this reaction to occur there must be considerable addition of Mg^{2+}. Adjacent marine shales may supply the required Mg^{2+}. From figure 6.6 it is evident that less Mg^{2+} is required to form chlorite as pH increases. Furthermore, some Fe^{2+} may combine with the Mg^{2+} thereby

reducing the Mg^{2+} requirements.

Chlorite may also be generated from montmorillonite, if it was present, according to the following reaction (Hitchon et al., 1971):

$$1.7Al_2O_3.0.9MgO.8SiO_2.2H_2O + 9.2MgO \rightarrow$$
$$10.1MgO.1.7Al_2O_3.6.4SiO_2.8H_2O + 1.6SiO_2$$

However, as mentioned previously there is no evidence for or against the presence of montmorillonite.

Although the illite observed in Facies A formed by transformation not authigenesis it still must have been stable with the final pore fluid composition (figure 6.3). As mentioned previously the timing of the transformation is uncertain.

From these interpretations the overall pathway for the pore fluid composition is:

$$\text{seawater} \rightarrow \text{quartz saturation} \rightarrow \text{kaolinite} \rightarrow \text{chlorite}$$
$$\nearrow \text{(illite)}$$

Discussion

Figure 6.7 indicates the paragenetic sequence of minerals formed and processes occurring during diagenesis. This sequence is the result of textural observations in thin section and using scanning electron microscopy. Although the individual timing of mineral formation with respect to the diagenetic stages is uncertain, the overall sequence of minerals relative to one another is known from textural evidence.

Figure 6.7 Paragenetic sequence of events during progressive burial and diagenesis (dashed lines indicate uncertainties).

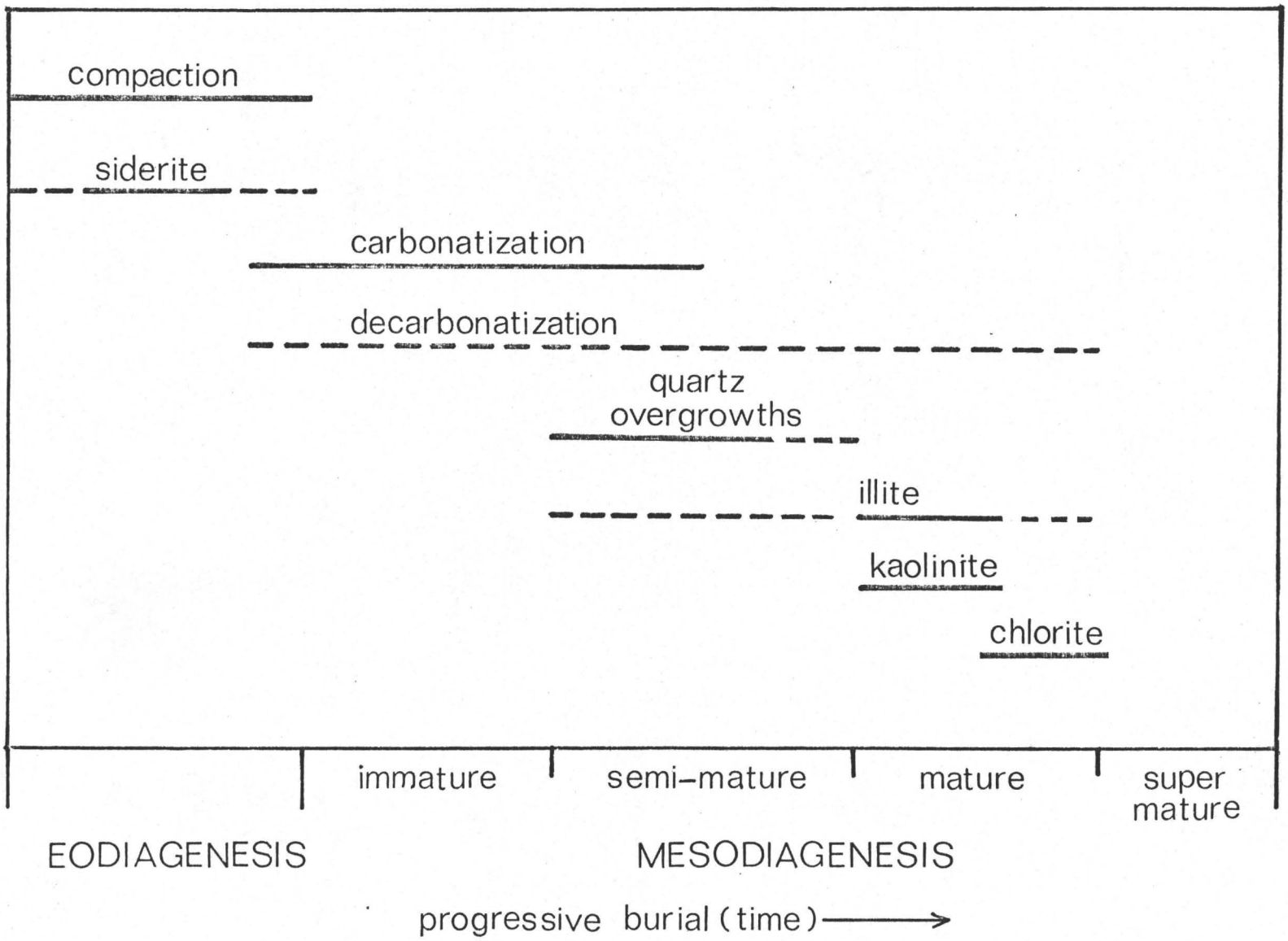
compaction
siderite
carbonatization
decarbonatization
quartz overgrowths
illite
kaolinite
chlorite
immature
semi-mature
mature
super mature
EODIAGENESIS
MESODIAGENESIS
progressive burial (time) ⟶

7. CONCLUSIONS

1. Sands and conglomerates of the Notikewin Member were influenced by both fluvial and beach processes. Sediment transported via fluvial channels from the south to southwest forms distributary month bar depocentres. These are subsequently modified by wave energy and littoral currents to form beaches (trending east-west) within or adjacent to the wave dominated deltaic environment.

2. Clast supported Notikewin Member conglomerates are excellent potential reservoirs. They may represent fluvial deposits or high energy beaches. Distinguishing between these two possibilities is difficult. Beach sands (Facies B) are also good reservoirs but there is extensive diagenetic control on their potential as gas producers. Porosities indicated by sonic/acoustic velocity logs may be overestimated due to many intergranular contacts resulting from secondary porosity.

3. Notikewin Member sands and conglomerates are classified as sublitharenites to litharenites (chert-rich). The provenance is variable from a high grade metamorphic terrain to

sedimentary rocks, both located in the Cordilleran highlands. The Precambrian Shield is also a potential sediment source.

4. Burial diagenetic temperatures were approximately 70°C ±10 (160°F ±50). This has allowed for the progressive assemblage of carbonate, quartz overgrowths, kaolinite and chlorite. Allogenic illite has been recrystallized by transformation. Secondary porosity occurs mainly be decarbonatization. It may occur throughout the mesodiagenetic history.

5. Pore fluid compositions have changed with time. Originally, oversaturation with respect to carbonate allowed for local precipitation of carbonate cement. Where carbonate cement is absent, pore waters permitted silica overgrowths to nucleate on detrital quartz grains. Kaolinite neoformation post-dates quartz overgrowth formation. Pore fluids at this time were locally depleted in ions. This was not due to the influx of freshwater. Chlorite formed from the breakdown of kaolinite with considerable influx of Mg^{2+} ions from adjacent shales. Montmorillonite, although not observed, may have contributed to chlorite authigenesis. Allogenic illite underwent transformation due to K^{+} ions supplied to the pore waters, the timing of which is uncertain. Throughout the progressive burial pore fluids became acidic due to dissolved CO_2 supplied by catagenesis of organic matter. This allowed for the removal of carbonate cement producing secondary porosity.

6. Apparently identical chert-rich sandstones and conglomerates may be welded or unaffected, carbonate cemented or porous. The explanation for porous (non-carbonate cemented) conglomerates is a lack of exposure to carbonate precipitating fluids, or once cemented, protection from acidic pore fluids which promote dissolution. Protection may be from hydrocarbon saturation or overpressuring restricting fluid movement.

7. Low porosities and permeabilities in thick deposits of the Notikewin Member are a result of: (listed in order of importance)

1) fine grained sand matrix in the conglomerate and to a lesser extent clay matrix in the sandstone;

2) porosity occlusion by quartz overgrowths, kaolinite and chlorite. Illite transformation has had little effect on the reservoir potential of the Notikewin Member;

3) carbonate cementation.

BIBLIOGRAPHY

Alberta Study Group, 1954, Lower Cretaceous of the Peace River Region; Western Canada Sedimentary Basin, Rutherford Memorial volume, Am. Assoc. Petrol. Geol., Tulsa, Oklahoma.

Badgley, P.C., 1952, Notes on the subsurface stratigraphy and oil and gas geology of the Lower Cretaceous series in Central Alberta, Geol. Surv. Can. paper 52-11, 12 p.

Basu, A., Young, S.W., Suttner, L.J., James, W.C. and Mack, G.H., 1975, Re-evaluation of the use of undulatory extinction and polycrystallinity in detrital quartz for provenance interpretation, Jour. Sed. Petrol. v. 45, pp. 873-882.

Berner, R.A. (ed.), 1971, Principles of Chemical Sedimentology, McGraw-Hill Book Co., New York, 239 p.

Blatt, H., Middleton, G.V. and Murray, R. (eds.), 1980, The Origin of Sedimentary Rocks, 2nd ed., Prentice-Hall Inc., 782 p.

Bluck, B.J., 1967, Sedimentation of beach gravels: Examples from South Wales, Jour. Sed. Petrol. v. 37, pp. 128-157.

Borg, I.Y. and Smith, D.K., 1969, Calculated X-ray Powder Patterns for Silicate Minerals, Geol. Soc. Amer. Memoir 122.

Brindley, G.W., 1980, Quantitative X-ray mineral analysis of

clays, in "Crystal Structures of Clay Minerals and their X-ray Identification", (G.W. Brindley and G. Brown eds.), Ch. 7, Mineral Soc. London.

Brindley, G.W., 1981, X-ray identification (with ancillary techniques) of clay minerals, in "Clays and the Resource Geologist", F.J. Longstaffe (ed.), Mineral Assoc. Can. Short course handbook.

Carrigy, M.A. and Mellon, G.B., 1964, Authigenic clay mineral cements in Cretaceous and Tertiary sandstones of Alberta, Jour. Sed. Petrol. v. 34, pp. 461-472.

Carroll, D., 1970, Clay Minerals: A guide to their X-ray Identification, Geol. Soc. Amer. Spec. Paper 126, 80 p.

Clark, L.M., 1954, (ed.), Lower Cretaceous of the Peace River Region in the Western Canada Sedimentary Basin, Amer. Assoc. Petrol. Geol. Rutherford memorial volume, Tulsa, Oklahoma.

Clifton, H.E., 1981, Progradational sequences in Miocene shoreline deposits, Southeastern Caliente Range, California, U.S.A., Jour. Sed. Petrol. v. 51, pp. 165-184.

Clifton, H.E., Hunter, R.E. and Philipps, R.L., 1971, Depositional structures and processes in the non-barred high energy nearshore, Jour. Sed. Petrol. v. 41, pp. 651-670.

Coleman, J.M. and Wright, L.D., 1975, Modern river deltas: variability of processes and sand bodies, in Deltas, models for exploration, M.L. Broussard (ed.), Houston

Geol. Soc., pp. 99-149.

Collins, A.G. (ed.), 1975, Geochemistry of Oilfield waters, Developments in Petroleum Science 1, Elsevier Scientific Publ. Co., New York, 496 p.

Dapples, E.C., 1979, Physical classification of carbonate cement in quartzose sandstones, Soc. Econ. Paleont. and Mineral. Reprint Series No. 9.

Dawson, G.M., 1881, Report on an exploration from Port Simpson on the Pacific coast to Edmonton on the Sasdatchewan, embracing a portion of the northern part of B.C. and Peace River country, 1879 Geol. Surv. Can. Prog. Rep't., 1879-1880, pt. 6, pp. 1-142.

Drever, J.I., 1982, The Geochemistry of Natural Waters, Prentice-Hall Inc., New Jersey, 388 p.

Dupré, W.R. and Clifton, H.E., 1979, Modern and ancient coastal sedimentary facies, Monterey Bay, California. Field trip guidebook for the Geol. Soc. Amer. Cordilleran Section meeting at San Jose, California, 50 p.

Folk, R.L. (ed.), 1974, Petrology of Sedimentary Rocks, Hemphill Publishing Co., Austin, Texas, 182 p.

Füchtbauer, H., 1967, Influence of different types of diagenesis on sandstone porosity, 7th World Petrol. Congr., Mexico, Panel Disc., 3, v. 2, pp. 353-369.

Füchtbauer, H. (ed.), 1974, Sediments and Sedimentary Rocks I, John Wiley and Sons Inc., 464 p.

Garrels, R.M. and Christ, C.L., 1965, Solutions, Minerals and

Equilibria, Harpers and Row Inc., New York, 450 p.

Ghent, E.D. and Miller, B.E., 1974, Zeolite and clay-carbonate assemblages in the Blairmore Group (Cretaceous), Southern Alberta Foothills, Canada, Contr. Miner. Petr. v. 44, pp. 313-329.

Glaister, R.P., 1959, Lower Cretaceous of Southern Alberta and adjoining areas, Bull. Am. Assoc. Petrol. v. 43, no. 3, pp. 590-640.

Grim, R.E. (ed.), 1968, Clay mineralogy, New York, McGraw-Hill Book Co., 2nd edition.

Güven, N., Hower, W.F. and Davies, D.K., 1980, Nature of authigenic illites in sandstone reservoirs, Jour. Sed. Petrol. v. 50, pp. 761-766.

Hayes, J.B., 1970, Polytypism of chlorite in sedimentary rocks, Clays and Clay Minerals v. 18, pp. 285-306.

Helgeson, H.G., 1969, Thermodynamics of hydrothermal systems at elevated temperatures and pressures, Am. Jour. Sci. v. 267, pp. 729-804.

Helgeson, H.C., Brown, T.H. and Leeper, R.H. (eds.), 1969, Handbook of Theoretical Activity Diagrams Depicting Chemical Equilibria in Geologic systems Involving an Aqueous Phase at One Atm. and 0° to 300° C, Freeman, Cooper and Co., San Francisco, 253 p.

Heward, A.P., 1981, A review of wave dominated clastic shore-line deposits, Earth Sci. Review, vol. 17, pp. 223-276.

Hitchon, B., Billings, G.K. and Klovan, J.E., 1971, Geochemistry and origin of formation waters in the Western Canada Sedimentary Basin - III. Factors controlling chemical composition, Geochim. Cosmochim. Acta v. 35, pp. 567-598.

Hoffman, J. and Hower, J., 1971, Clay mineral assemblages as low grade metamorphic geothermometers: Application to the thrust faulted disturbed belt of Montana, U.S.A., Soc. Econ. Paleont. and Mineral. Spec. Publ. No. 26, pp. 55-79.

Hunt, J.M. (ed.), 1979, Petroleum Geochemistry and Geology, W.H. Freeman and Co. Publ., 617 p.

Jardine, D., 1974, Cretaceous oil sands of Western Canada in Hills, L.V. (ed.), Oil Sands: Fuel of the Future, Can. Soc. Petrol. Geol., pp. 50-67.

Keller, W.D., 1970, Environmental aspects of clay minerals, in Symposium on Environmental Aspects of Clay Minerals, Jour. Sed. Petr. v. 40, No. 3, pp. 788-854.

Leckie, D.A., 1981, Shallow-marine transitional to non-marine sedimentation in the Upper Moosebar Formation - Lower Gates Member (Wilrich-Falher equivalents), Fort St. John Group, N.E. British Columbia; Storm and tidally influenced shorelines, McMaster University Dept. of Geology Tech. - Memo 81-1, Hamilton, Ontario.

Leckie, D.A. and Walker, R.G., 1982, Storm and tide-dominated shorelines in Cretaceous Moosebar - Lower Gates Interval—

Outcrop equivalents of Deep Basin gas traps in Western Canada, Am. Assoc. Petrol. Geol. Bull. v. 66, pp. 138-157.

Mackenzie, F.T. and Garrels, R.M., 1966, Chemical balance between rivers and oceans, Am. Jour. Sci. v. 264, pp. 507-525.

Maxwell, J.C., 1977, Influence of depth, temperature, and geologic age on porosity of quartzose sandstone, Amer. Assoc. Petrol. Geol. Reprint Series No. 20, pp. 83-95.

May, R.W., 1967, Geology of the Peace River, Viking, Joli Fou and "Notikewin" Formations, Kaybob Area, northern Alberta, M.Sc. thesis, Dept. of Geology, University of Calgary.

McCrossan, R.G. and Glaister, R.P. (eds.), 1964, Geological History of Western Canada, Alta. Soc. Petrol. Geol., 232 p.

McDonald, D.A., 1979, Concepts in Sandstone diagenesis, Can. Soc. Petrol. Geol. Clastic Diagenesis Workshop Publication.

Mellon, G.B., 1967, Stratigraphy and Petrology of the Lower Cretaceous Blairmore and Mannville Groups, Alberta Foothills and Plains, Alberta Research Council Bull. 21.

Miall, A.D., 1979, Deltas, in Facies Models Walker, R.G. (ed.), Geoscience Canada Reprint Series I, pp. 43-56.

Millot, G. (ed.), 1970, Géologie des Argilles (Geology of Clays), Springer-Verlag, New York, 499 p.

Nauss, A.W., 1945, Cretaceous stratigraphy of Vermillion Area, Alberta, Canada, Bull. Am. Assoc. Petrol. Geol. v. 29, pp. 1605-1629.

Nelson, S.J. (ed.), 1970, The Face of Time, Can. Soc. Petrol. Geol., 133 p.

Pettijohn, F.J., Potter, P.E. and Siever, R. (eds.), 1973, Sand and Sandstone, Springer-Verlang, New York, 618 p.

Pittman, E.D., 1972, Diagenesis of quartz in sandstones as revealed by scanning electron microscopy, Jour. Sed. Petrol. v. 42, pp. 507-519.

Reading, H.G. (ed.), 1980, Sedimentary Environments and Facies, Elsevier-North Holland Publ., 556 p.

Reineck, H.B. and Singh, I.B. (eds.), 1980, Depositional Sedimentary Environments, Springer-Verlag Publ., 542 p.

Rudkin, R.A., 1964, Lower Cretaceous in Geological History of Western Canada, S.J. Nelson, R.P. Glaister and R.G. McCrossan (eds.), Alta. Soc. Petrol. Geol. Publ., pp. 156-168.

Sarkisyan, S.G., 1971, Application of the scanning electron microscope in the investigation of oil and gas reservoir rocks, Jour. Sed. Petrol. v. 41, pp. 289-292.

Schmidt, V., McDonald, D.A. and Platt, R.L., 1977, Pore geometry and reservoir aspects of secondary porosity in sandstones, Can. Petrol. Geol. Bull. v. 25, pp. 271-290.

Schmidt, V. and McDonald, D.A., 1979a), The role of secondary porosity in the course of sandstone diagenesis, Soc.

Econ. Paleont. and Mineral. Spec. Publ. No. 26, pp. 175-207.

Schmidt, V. and McDonald, D.A., 1979b), Texture and recognition of secondary porosity in sandstones, Soc. Econ. Paleont. and Mineral. Spec. Publ. No. 26, pp. 209-225.

Scholle, P.A. (ed.), 1979, A Colour Illustrated Guide to Constituents, Textures, Cements and Porosities of Sandstones and Associated Rocks, Amer. Assoc. Petrol. Geol. memoir 28.

Shelton, J.W., 1964, Authigenic kaolinite in sandstone, Jour. Sed. Petrol. v. 34, pp. 102-111.

Singh, C., 1971, Lower Cretaceous microfloras of the Peace River Area, Northwestern Alberta, Alberta Research Council Bull. 28, 542 p.

Stott, D.F., 1961, Summary account of the Cretaceous Alberta group and equivalent rocks, Rocky Mountain Foothills, Alberta, Geol. Surv. Can. paper 61-2.

Stott, D.F., 1963, Stratigraphy of the Lower Cretaceous Fort St. John Group and Gething, Cadomin Formations, foothills of N. Alberta and B.C., Can. Geol. Surv. paper 62-39, 48p.

Stott, D.F., 1968, Lower Cretaceous Bullhead and Fort St. John Groups, between Smoky and Peace Rivers, Rocky Mountain Foothills, Alberta and British Columbia, G.S.C. Bulletin 152, Ottawa.

Stumm, W. and Morgan, J.J. (eds.), 1981, Aquatic Chemistry, 2nd edition, John Wiley and Sons Inc., New York, 583 p.

Thorez, J., 1975, Phyllosilicates and Clay Minerals - A laboratory handbook for their X-ray diffraction analysis. G. Lelotte (ed.), 604 p.

Thorez, J., 1976, Practical Identification of Clay Minerals, G. Lelotte (ed.), 90 p.

Tissot, B., Durand, B., Espitalie, J. and Combay, A., 1974, Influence of nature and diagenesis of organic matter in formation of petroleum, Am. Assoc. Petrol. Geol. Bull. v. 58, pp. 499-506.

Vemuri, R., 1967, Practical notes on the semi-quantitative analysis of clay minerals in sediments by X-ray diffraction, McMaster University Dept. of Geology Tech.-Memo 67-9, Hamilton, Ontario.

Williams, G.D., 1963, The Mannville Group (Lower Cretaceous) of Central Alberta, Bull. Can. Petrol. Geol. v. 11, pp. 350-368.

Wilson, M.D. and Pittman, E.D., 1977, Authigenic clays in sandstones: Recognition and influence on reservoir properties and paleoenvironmental analysis, Jour. Sed. Petrol. v. 47, pp. 3-31.

Young, S.W., 1976, Petrographic textures of detrital polycrystalline quartz as an aid to interpreting crystalline source rocks, Jour. Sed. Petrol. v. 46, no. 3, pp. 595-603.

APPENDIX I

Core lithologies and associated log response

LEGEND

LITHOLOGY

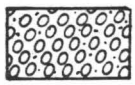
pebble conglomerate

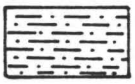
siltstone


fine grained congl./ coarse grained sandstone

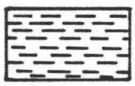
shale

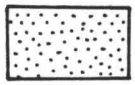
sandstone


coal

STRUCTURES and CONSTITUENTS

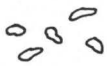
pebble lag

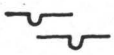
bioturbation

cross stratification (angle to horizontal)


churned


vague horizontal laminae

G glauconite

H homogeneous


carbonaceous fragments


non-parallel convolute laminae


carbonaceous laminae


microfaulted convolute laminae


rootlet


scour and fill


fossil shell mould


lenticular bedding


chert

S siderite


ironstone

6-36-64-20 W5

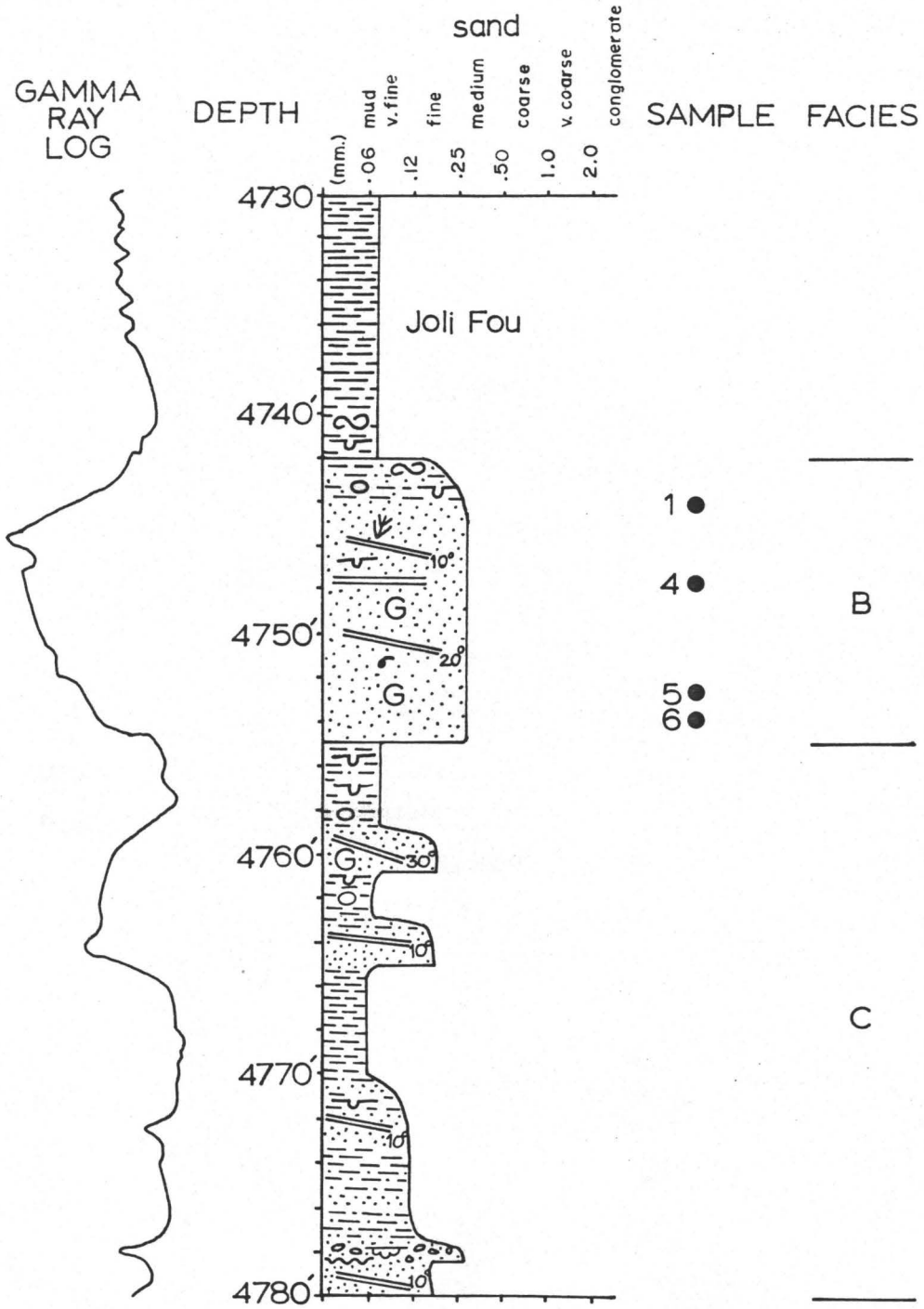
sand
GAMMA RAY LOG
DEPTH
(mm.)
.06 mud
.12 v. fine
.25 fine
.50 medium
1.0 coarse
2.0 v. coarse
conglomerate
SAMPLE
FACIES
4730
Joli Fou
4740
4750
4760
4770
4780
1
4
5
6
B
C
G
10°
20°
30°

7-13-63-19 W5

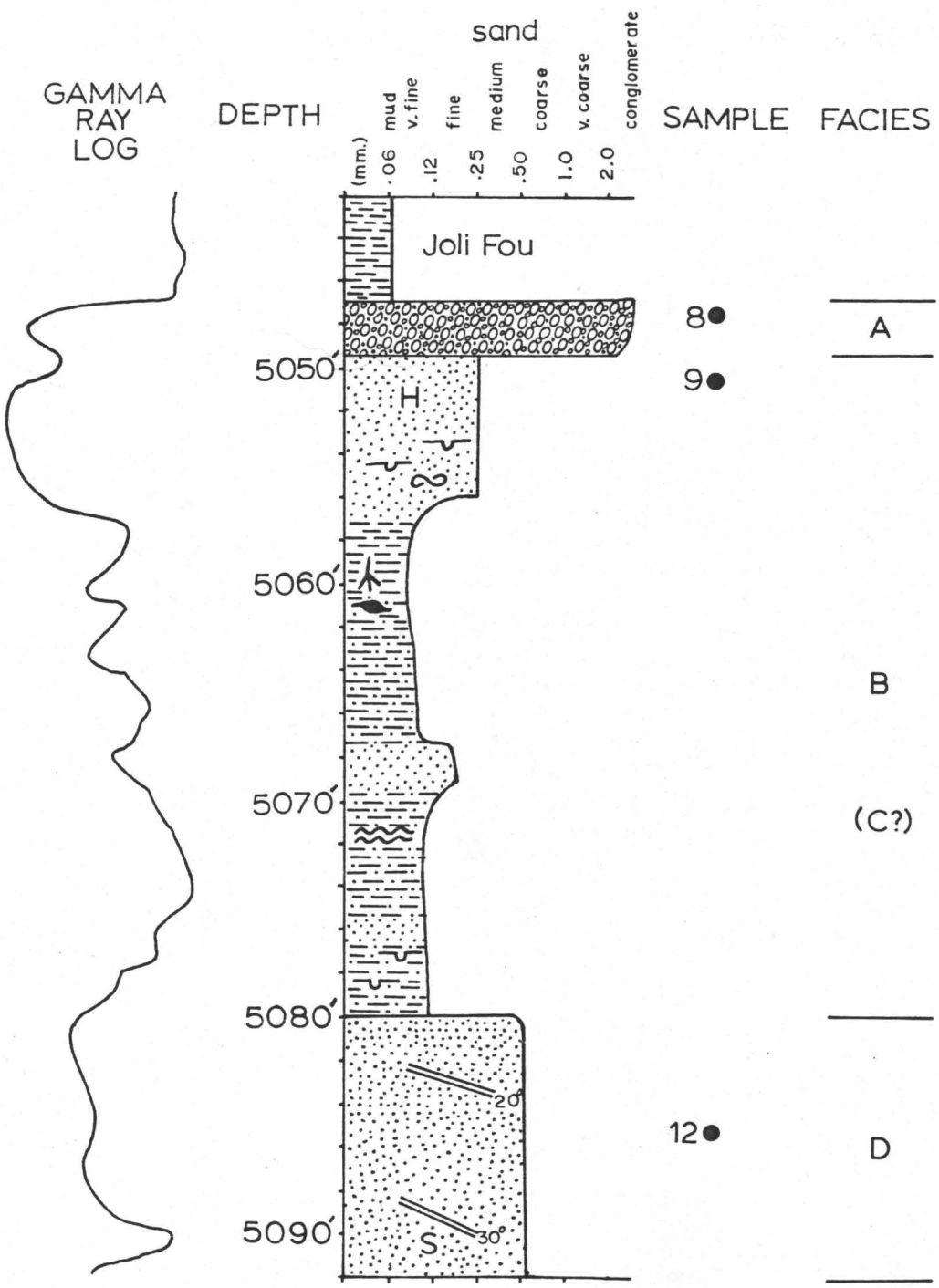
GAMMA RAY LOG
DEPTH
sand
(mm.)
.06
mud
v.fine
.12
fine
.25
medium
.50
coarse
1.0
v. coarse
2.0
conglomerate
SAMPLE
FACIES
Joli Fou
8
9
12
A
B
(C?)
D
5050'
5060'
5070'
5080'
5090'
H
S
20°
30°

10-24-64-20 W5

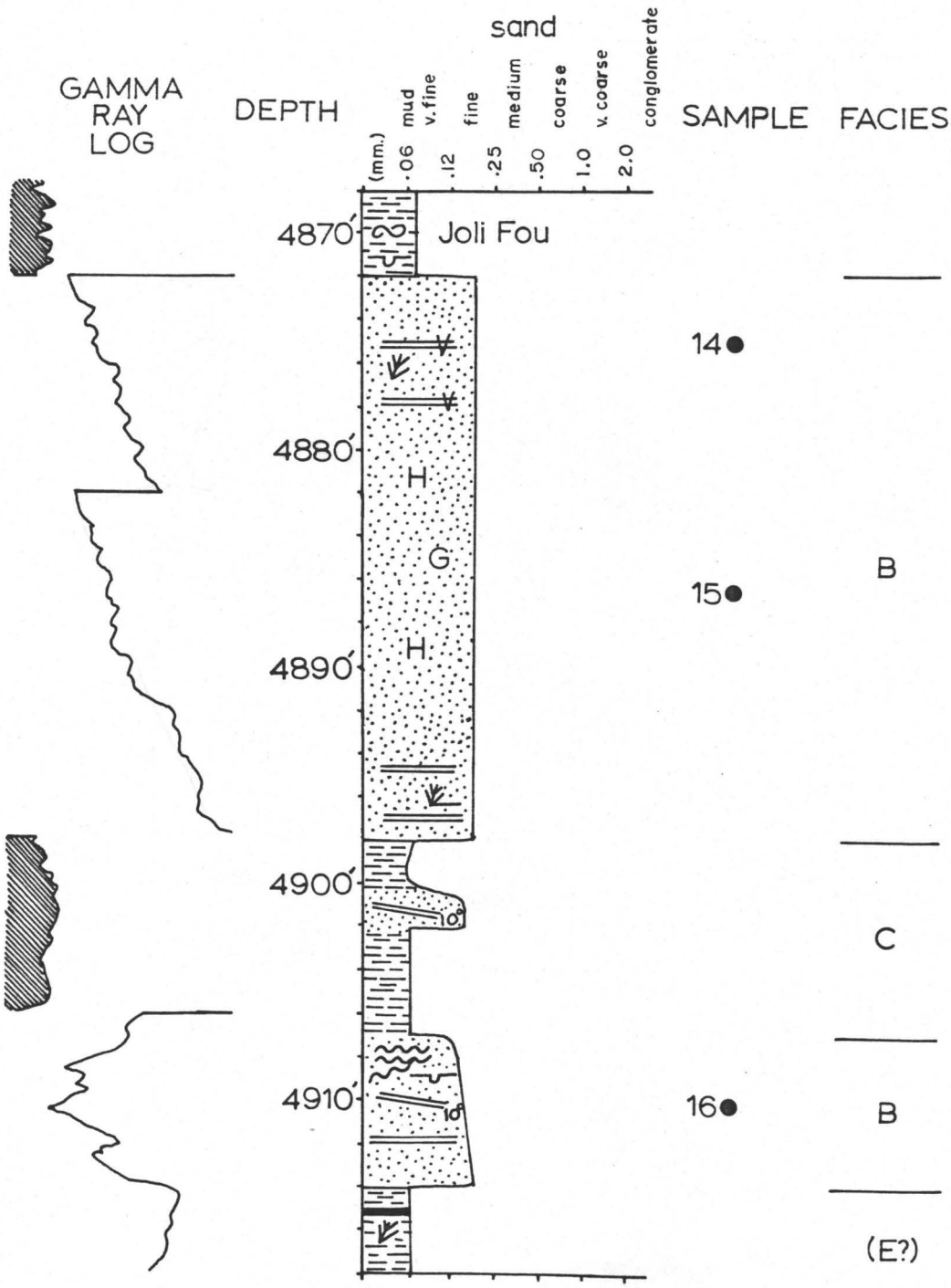
GAMMA RAY LOG
DEPTH
sand
(mm.)
.06 mud
v.fine
.12
fine
.25
medium
.50
coarse
1.0
v. coarse
2.0
conglomerate
SAMPLE
FACIES
4870'
Joli Fou
14
4880'
H
G
15
B
4890'
H
4900'
C
4910'
16
B
(E?)

10-1-65-18 W5

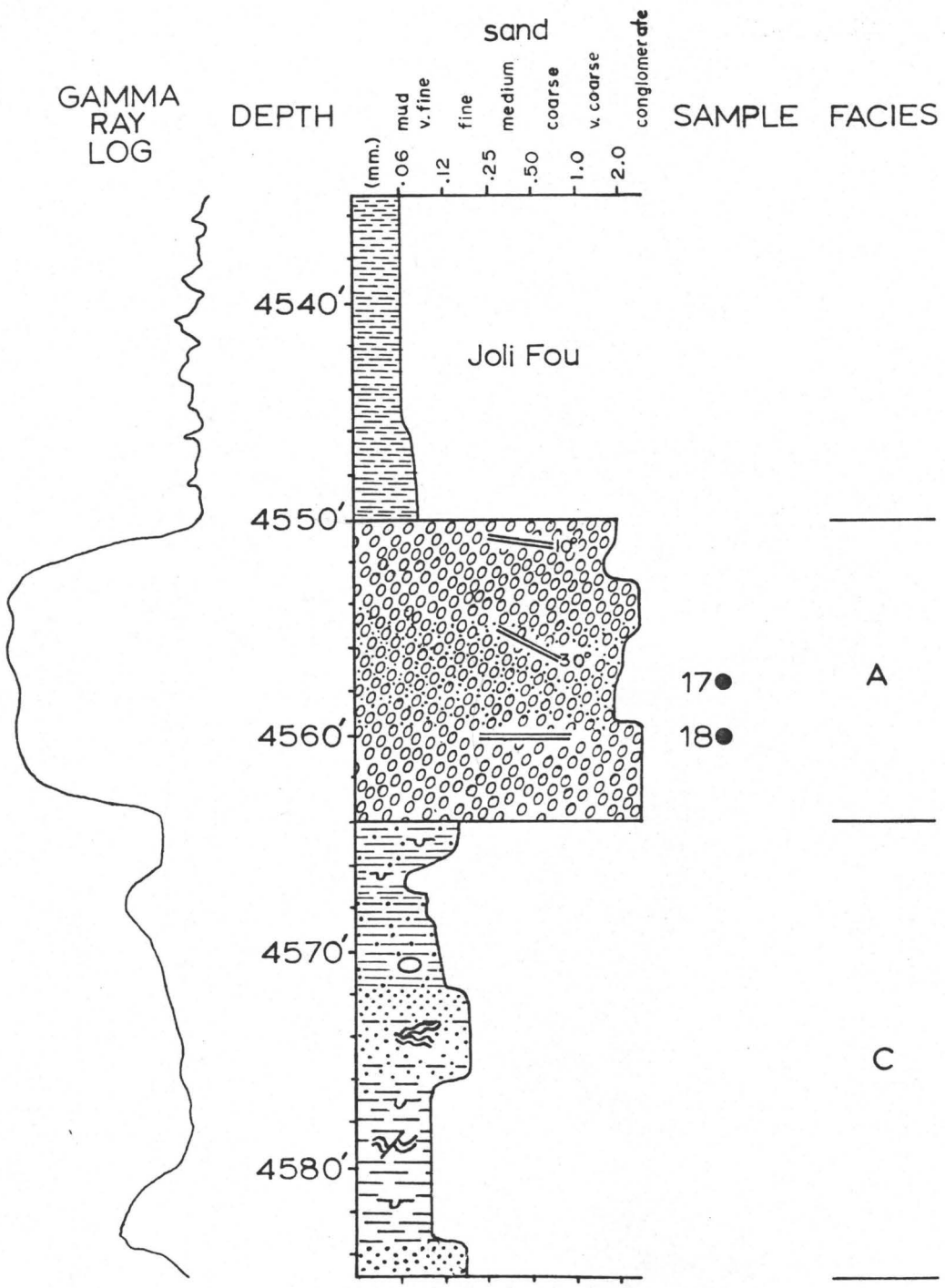
sand
GAMMA RAY LOG
DEPTH
mud
v. fine
fine
medium
coarse
v. coarse
conglomerate
(mm.)
.06
.12
.25
.50
1.0
2.0
SAMPLE
FACIES
4540'
Joli Fou
4550'
10°
30°
17
18
A
4560'
4570'
C
4580'

12-10-64-19 W5

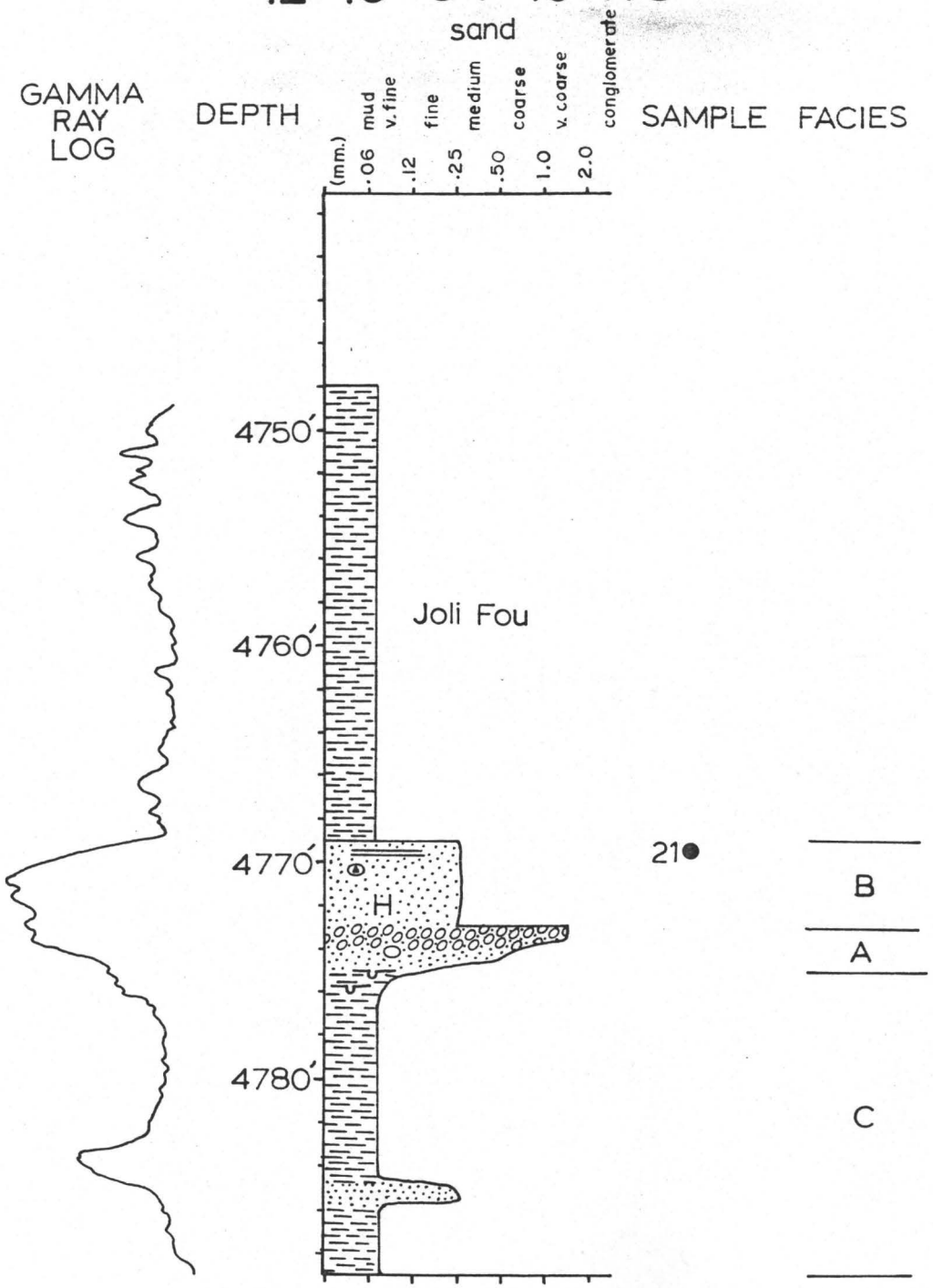
sand
GAMMA RAY LOG
DEPTH
(mm.)
.06
mud
v. fine
.12
fine
.25
medium
.50
coarse
1.0
v. coarse
2.0
conglomerate
SAMPLE
FACIES
4750'
4760'
4770'
4780'
Joli Fou
21
H
B
A
C

12-15-63-19 W5

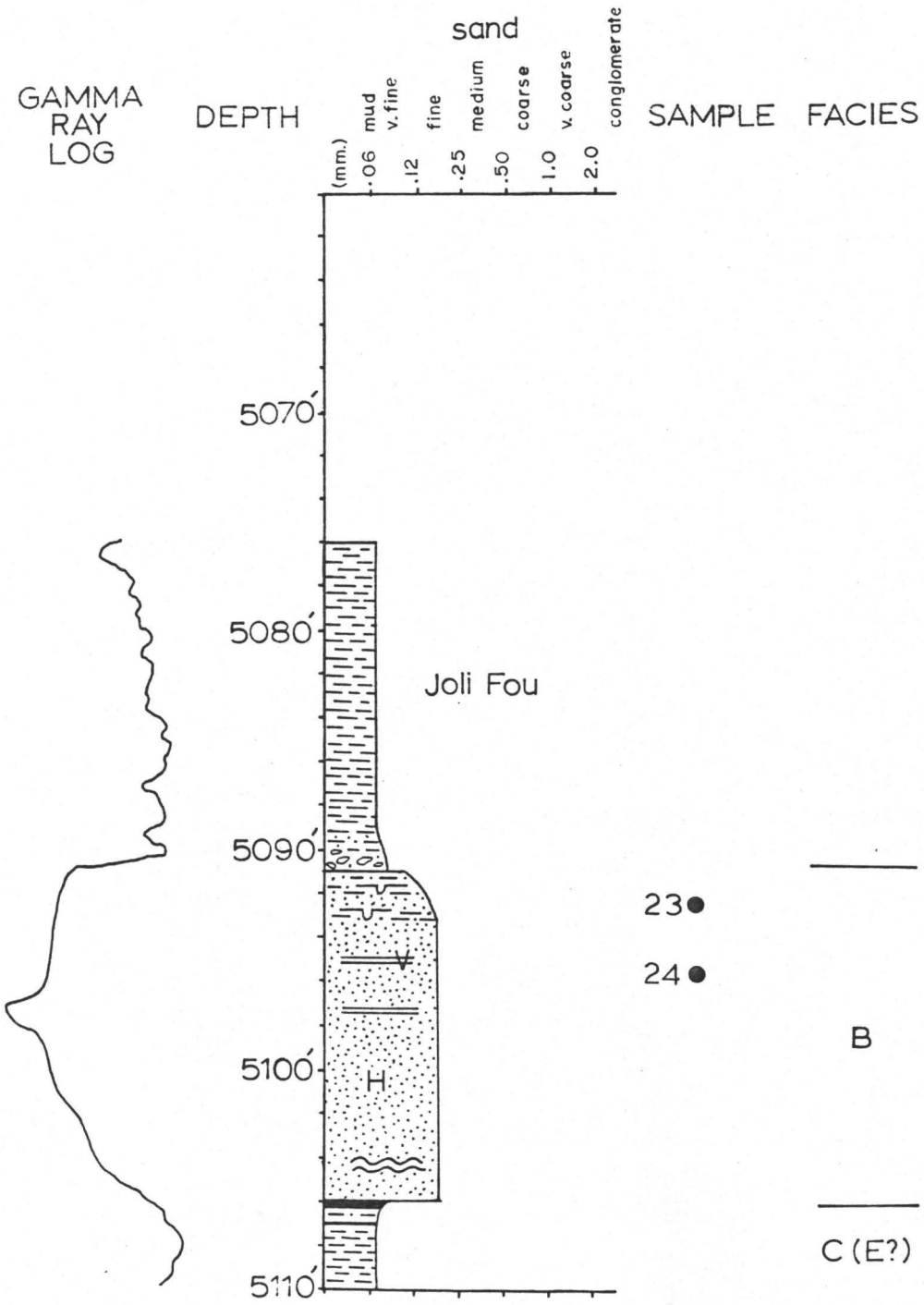
sand
GAMMA RAY LOG
DEPTH
(mm.)
.06
mud
v. fine
.12
fine
.25
medium
.50
coarse
1.0
v. coarse
2.0
conglomerate
SAMPLE
FACIES
5070'
5080'
5090'
5100'
5110'
Joli Fou
H
23
24
B
C (E?)

10-27-63-19 W5

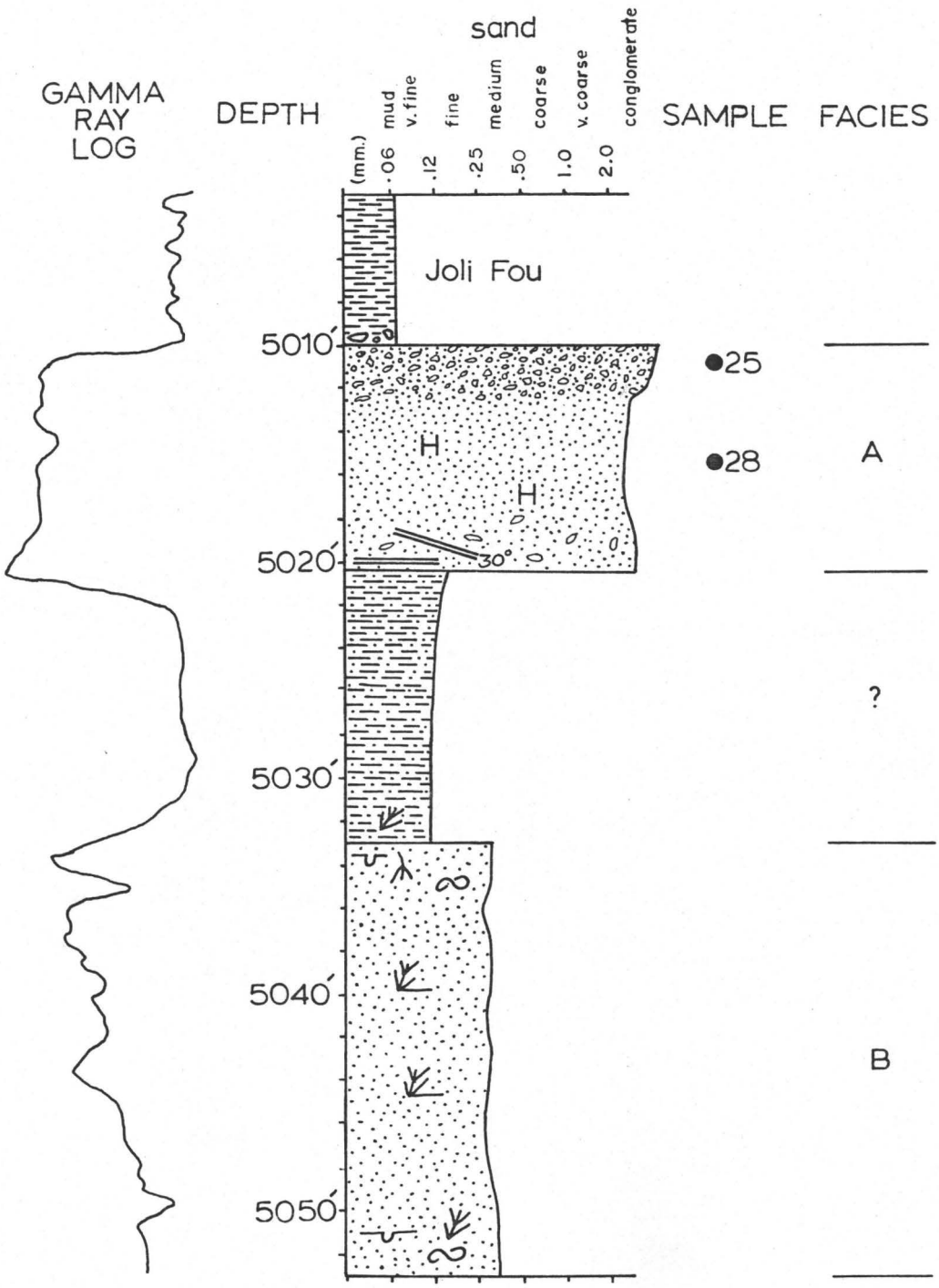
GAMMA RAY LOG
DEPTH
sand
mud
v. fine
fine
medium
coarse
v. coarse
conglomerate
(mm.)
.06
.12
.25
.50
1.0
2.0
SAMPLE
FACIES
Joli Fou
5010'
5020'
5030'
5040'
5050'
H
H
30°
●25
●28
A
?
B

6-18-59-14 W5

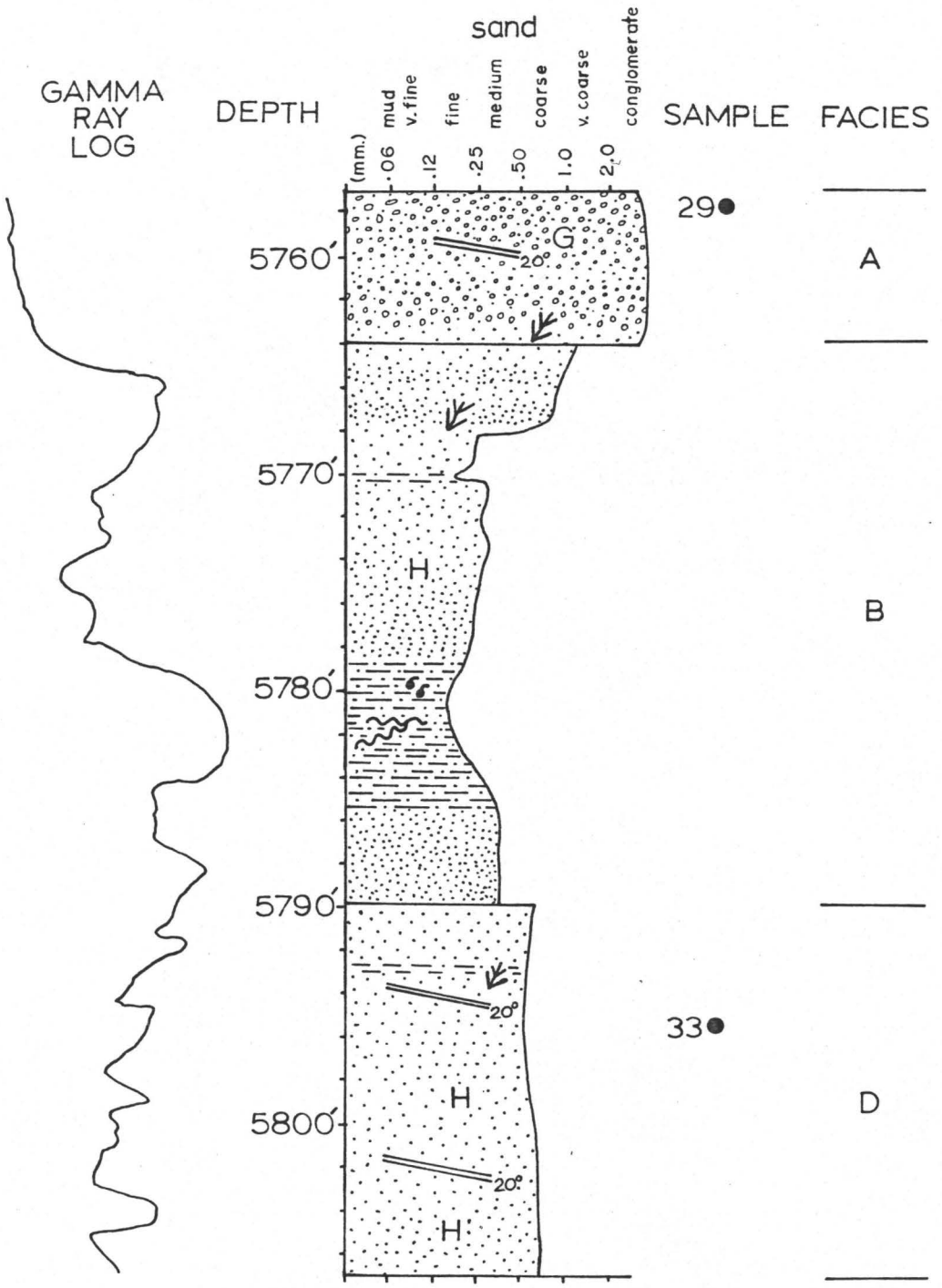
sand
GAMMA RAY LOG
DEPTH
mud
v. fine
fine
medium
coarse
v. coarse
conglomerate
(mm.)
.06
.12
.25
.50
1.0
2.0
SAMPLE
FACIES
29
33
5760'
5770'
5780'
5790'
5800'
G
H
H
H
20°
20°
A
B
D

10-31-64-17 W5

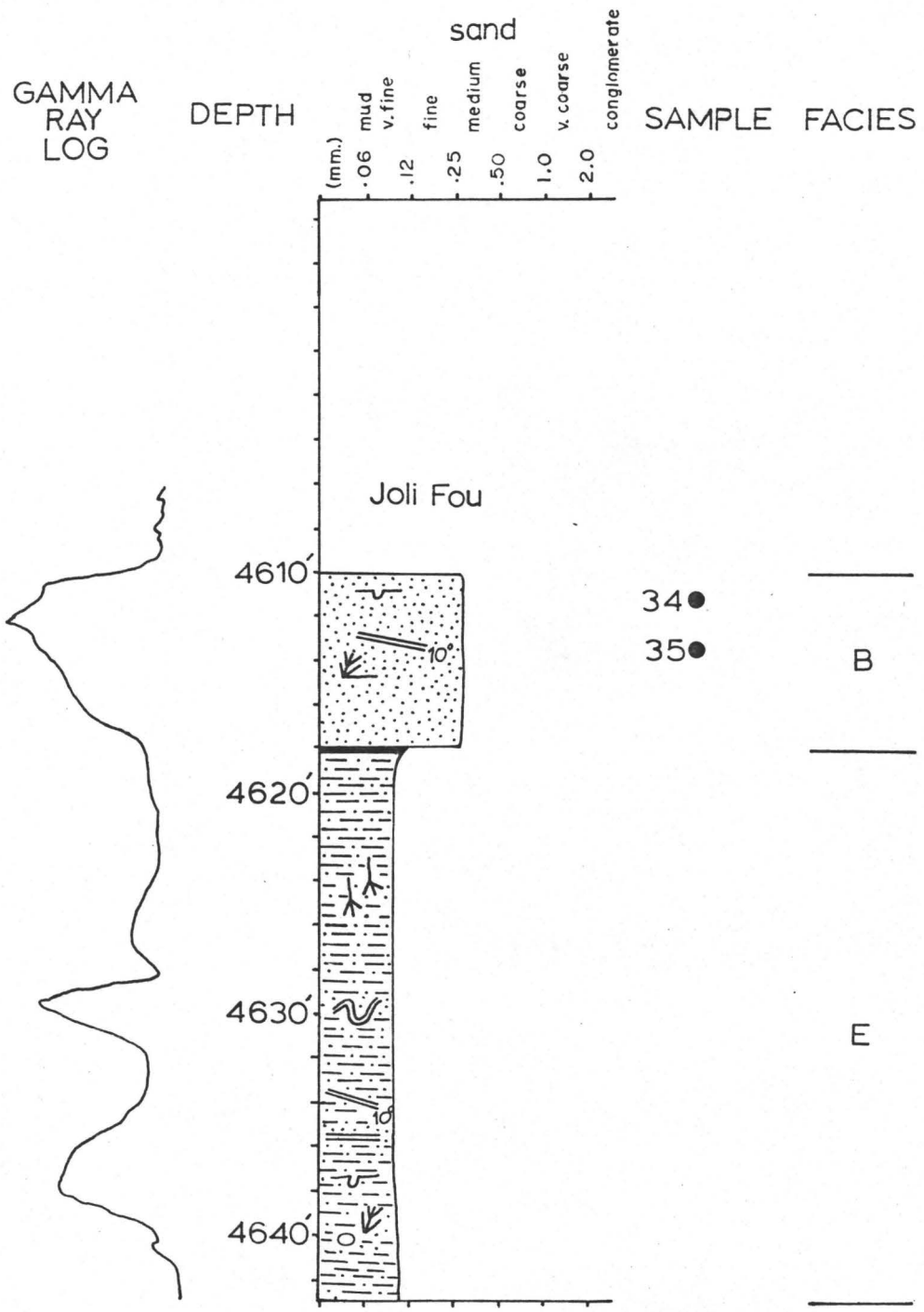
sand
GAMMA RAY LOG
DEPTH
(mm.)
.06
mud
v. fine
.12
fine
.25
medium
.50
coarse
1.0
v. coarse
2.0
conglomerate
SAMPLE
FACIES
Joli Fou
4610'
4620'
4630'
4640'
10°
10°
10°
34
35
B
E

22 21 20 19 18 17 Rge. 16

Twp. 67

66

65

64

63

62

NOTIKEWIN A SAND ISOLITH MAP

5 kilometres

0 3 miles

contour interval = 5 feet